Fakultät für Medizin

Name der promotionsführenden Einrichtung

Characterization and Cloning of Ewing Sarcoma Selective HLA-A*02:01 Restricted T Cell Receptors Directed Against ADRB3 and PAPPA

Titel der wissenschaftlichen Abhandlung

Andreas Manfred Kirschner

Vorname und Name

Vollständiger Abdruck der von der promotionsführenden Einrichtung
Fakultät für Medizin
der Technischen Universität München zur Erlangung des akademischen Grades
eines Doktors der Naturwissenschaften
genehmigten Dissertation.

Vorsitzende/-r: Prof. Dr. D. Busch

Prüfende/-r der Dissertation:

1. Prof. Dr. S. Burdach

2. Prof. Dr. M. Hrabé de Angelis

3. Prof. Dr. E. Nößner

Die Dissertation wurde am 02.11.2016 bei der Technischen Universität München
eingereicht und durch die Fakultät für Medizin am 12.07.2017 angenommen.

Für Christina und meine Familie

Table of contents

List of abbreviations

7-AAD	7-aminoactinomycin D
AA	Amino acid
AB	Antibody
ADRB3	Beta-3 adrenergic receptor
AES	Advanced ewing sarcoma
Allo-SCT	Allogeneic stem cell transplantation
Amp	Ampicillin
APC	Allophycocyanin
β2MG	β2 microglobulin
BM	Bone marrow
BSA	Bovine serum albumin
CAR	Chimeric antigen receptor
CCR7	C-C chemokine receptor type 7
cDNA	Complementary desoxyribonucleic acid
CDR	Complementary-determing regions
CHM1	Leukocyte cell-derived chemotaxin 1
CI	Cellular index
CML	Chronic myeloid leukemia
CRS	Cytokine release syndrome
CTLA4	Cytotoxic T-lymphocyte-associated protein 4
DC	Dendritic cell
DEPC-H2O	Diethylpyrocarbonate
DLI	Donor lymphocyte infusion
DMEM	Dulbecco's Modified Eagle's medium
DMSO	Dimethyl sulfoxide
DNA	Deoxyribonucleic acid
dNTPs	Deoxyribose nucleoside triphosphate
EDTA	Ethylenediaminetetraacetic acid

EGR	Early growth response
EISpot	Enzyme-Linked ImmunoSpot
ERG	Transcriptional regulator ERG
EryLysis	Erythrocyte lysing
ES	Ewing sarcoma
EtBr	Ethidium bromide
ETS	E-twenty-six
EWS	Ewing sarcoma breakpoint region 1
FACS	Fluorescence activated cell sorter
FCS	Fetal calf serum
FITC	Fluorescein isothiocyanate
FLU	Influenza
GAPDH	Glyceraldehyde 3-phosphate dehydrogenase
GM-CSF	Granulocyte-macrophage colony-stimulating factor
grB	Granzyme B
GvES	Graft versus Ewing sarcoma
GvHD	Graft versus Host disease
GvT	Graft versus Tumor
HBSS	Hank's balanced salt solution
HCl	Hydrogen chloride
HECW1/2	E3 ubiquitin-protein ligase HECW1/2
HLA	Human leukocyte antigen
HPLC-MS	High-pressure liquid chromatography–mass spectrometry
HRP	Horseradish peroxidase
IFNγ	Interferon gamma
IGF	Insulin-like growth factor
IGFBP	Insulin-like growth factor-binding protein
IGFR	Insulin-like growth factor receptor
IL	Interleukin
IMGT	International ImMunoGeneTics

LAMP1	Lysosomal-associated membrane protein 1
LB	Lysogeny broth
LCL	Lymphoblastoid cell lines
MAGE-A3	Melanoma-associated antigen 3
MHC	Major histocompatibility complex
mm	Minimal murinization
mSats	Microsatellite
MSC	Mesenchymal stem cells
MT-ND2	Mitochondrially encoded NADH dehydrogenase 2
NEAA	Non-essential amino acids
NK cell	Natural killer cell
OAT	Ornithine aminotransferase
OKT3	Muromonab-CD3
$p16^{INK4A}$	Cyclin-dependent kinase inhibitor 2A
$p19^{ARF}$	ARF tumor suppressor
p53	Tumor protein p53
PAPPA	Pappalysin
PBMC	Peripheral blood mononuclear cell
PBS	Phosphate-buffered saline
PCR	Polymerase chain reaction
PD-L1	Programmed death-ligand 1
PE	Phycoerythrin
PFA	Paraformaldehyde
PGE2	Prostaglandin E2
pMHC	Peptide/MHC complex
qRT-PCR	Real-time quantitative PCR
RNA	Ribonucleic acid
RNase	Ribonuclease
RPMI	Roswell Park Memorial Institute medium
RT	Room temperature

SD	Standard deviation
SEM	Standard error of the mean
SNP	Single nucleotide polymorphism
STAT4	Signal transducer and activator of transcription 4
TAA	Tumor associated antigen
TAE	Tris-acetate-EDTA
TAP	Transporter associated with antigen processing
TCM	T cell medium
TCR	T cell receptor
TIL	Tumor infiltrating lymphocytes
TNF	Tumor necrosis factor
TRAV /Vα	T cell receptor alpha variable
TRBV / Vβ	T cell receptor beta variable
wt	Wild type

1. Introduction

1.1 Bone Cancers and Ewing sarcoma

James Ewing first described in 1921 the Ewing sarcoma (ES) as a “round cell sarcoma” of unknown origin and nature (Ewing 1972). Under the microscope these tumors appear as small round blue cells. In 85% of all cases ES is associated with a chromosomal translocation t(11;22)(q24:q12) resulting in the EWS-FLI1 fusion protein. It is composed of the 5’ *EWS* gene with the 3’ segment of the ETS family gene *FLI-1* (Delattre et al. 1992). The second most common fusion partner of *EWS* in ES is the *ERG* (10%) gene. Other fusion partners for EWS are less common (Burchill 2003). The resulting fusion protein EWS-FLI1 encodes an aberrant transcription factor that binds DNA at GGAA-microsatellites (mSats), which are converted by this protein to active enhancers (Riggi et al. 2014). EWS-FLI1 binding to GGAA-mSats drives the expression of oncogenic key downstream effectors and therefore contributes to the tumor transformation (Janknecht 2005, Luo et al. 2009, Grunewald et al. 2015). The origin of ES is believed to be mesenchymal stem cells (MSC). It was also shown that ES has similarities to both endothelial and neural crest-derived cells (Schmidt et al. 1985, Staege et al. 2004, Richter et al. 2009). EWS-FLI1 expression silencing via shRNA demonstrate that ES expression profiles become similar to those of mesenchymal stem cells (Tirode et al. 2007). Vice versa, expression of the EWS-FLI1 oncogene in primary bone marrow derived mesenchymal progenitor cells (MPC) transformed these cells that display an ES expression signature. Furthermore, these cells are able to generate tumors in vivo. However, EWS-FLI1 expression in primary human fibroblasts or mouse embryonic fibroblasts results in p53 dependent growth arrest. Deletion of p53, $p19^{ARF}$, and $p16^{INK4A}$ can rescue these transformed cells from apoptosis. Interestingly, only 10% of Ewing sarcomas show a genetic lesion in p53. Yet MPCs are able to transform/grow under EWS-FLI1 without an altered p53 expression or mutation highlighting the importance of the ES uprising cell type for the tumor development (Lessnick et al. 2002, Riggi et al. 2005, Takashima et al. 2007, Tirode et al. 2007, Miyagawa et al. 2008, Potikyan et al. 2008, Neilsen et al. 2011).

Bone sarcomas are rare and only constitute 0.2% of all tumors in adults. In children however, they account for about 5% of all cancer. As for bone tumors in adults chondrosarcomas predominate with 40%, followed by osteosarcomas (28%), chondromas (10%), and ES (8%). For

childhood bone tumors however, osteosarcomas (56%) and ES (34%) are much more common than chondorsarcomas (6%) (2016). Further ES seems to be more frequent in the Caucasian population than in Asian or African populations implicating a genetic predisposition (Glass et al. 1970, Burchill 2003, Bernstein et al. 2006). One reason for the predisposition relies on the increased numbers of GGAT motives in the EGR region. These are actively converted towards GGAA thus increasing the number of consecutive GGAA motifs and the EWS-FLI1 enhancer activity (Grunewald et al. 2015).

Ewing sarcoma is a very infrequent type of cancer with only approximately 225 new cases per year in patients under the age of 20 years in north America (Bernstein et al. 2006). It is slightly more common in boys than in girls and in 70% – 80% of all cases diagnosed between the ages of 10 and 20 years (Burchill 2003, Bernstein et al. 2006).

Frequent sites for primary Ewing's sarcoma are the pelvic bones (26%), followed by the long bones of the lower extremities (femur, 20%). However, soft tissue expansions are common in osseous Ewing's sarcoma. Typical symptoms for bone tumors are pain, swelling, and problems with movement. Often the pain does not completely disappear during the night. For children however, as the majorities are in the second decade of their life these symptoms often are being misinterpreted as pain caused by bone growth. Therefore Ewing's sarcoma is often diagnosed late after first symptoms (Burchill 2003, Bernstein et al. 2006, cancerresearchuk.org 2016).

At diagnosis about 20% to 30% of patients have metastases in lung, bone, and/or bone marrow (Bernstein et al. 2006). Before the implementation of chemotherapy less than 10% of Ewing sarcoma patients survived more than 2 years due to metastasis. Now, with a combined treatment of chemotherapy, radiation and surgery approximately 70% of patients without metastatic spread can be cured (Gasparini et al. 1977, Jurgens et al. 1988, Laws et al. 1999). However, the presence of metastasis at diagnosis is a most unfavorable prognostic feature and the outcome is highly dependent on the site of metastasis. Patients that have pulmonary metastases have a 50% event-free survival rate at 3 years. Despite of complete response to treatment, 30 – 40% of patients with no metastatic spread show relapse after treatment. This risk is even increased if the initial diagnosis was held with primary metastasis. For these high-risk patients the long term survival in less than 25% (Schleiermacher et al. 2003, Bernstein et al. 2006, Burdach et al. 2010, Uwe Thiel 2016). Moreover, the outcome for patients that were initially diagnosed with bone

marrow metastasis is fatal despite high dose radio-chemistry and allogeneic stem cell transplantation (Uwe Thiel 2016). An additional treatment option for patients with recurrent or advanced Ewing sarcoma (AES) is the allogeneic stem cell transplantation (Burdach et al. 2000, Koscielniak et al. 2005, Lucas et al. 2008).

1.2 Adoptive immunotherapy in cancer treatment

Allogeneic stem cell transplantation (allo-SCT) is a widely used treatment in cancer therapy for multiple myeloma or certain types of leukemia. It is the most effective form of adoptive immunotherapy and often the only treatment option for patients with high-risk hematological malignancies (Nicholson et al. 2012, Cieri et al. 2014). The effect of this treatment option relies on a presumed graft-vs-tumor (GvT) effect. In this kind of response the administered allogeneic lymphocytes are capable of reducing the tumor burden in the patients. This effect is mediated by natural killer cells, $CD4^+$ and $CD8^+$ T cells in the transplanted graft or by later additionally applied donor lymphocyte infusions (DLI) (Ringden et al. 2009, Cieri et al. 2014). Allogeneic T cells have the potential to cause a GvT effect to induce complete remissions in patients with relapsed disease after allo-SCT or in patients with chronic myeloid leukemia (CML) (Kolb 2008). On the other side this T cell mediated curative effect after allo-SCT may result in a life threatening graft-vs-host disease (GvHD) (Goldman et al. 1988, Horowitz et al. 1990, Marmont et al. 1991). In this case the alloreactive lymphocytes are not only reactive against the patient's malignant disease but also against healthy tissues. GvHD is a major complication of the allo-SCT treatment observed in up to 60% of all cases. Also, it is the major cause of non-relapse mediated death after allo-SCT even though chronic GvHD is less common in children than it is in adults (Baker et al. 2008, Ferrara et al. 2009, Baird et al. 2010, Saillard et al. 2014). However, partially this effect is also desired as a GvHD may be accompanied by a GvT effect, which remains a matter of debate (Mathe et al. 1965, Weiden et al. 1981, Nicholson et al. 2012, Negrin 2015).

Most potent mediators of both effects are T lymphocytes. $CD8^+$ T cell mediate cytotoxicity via its T cell receptor (TCR), which consists of a α- and β-chain. These two chains are composed of variable (V), diversity (D), joining (J), and constant (C) gene fragments through a process of somatic gene arrangement via nucleotide insertions and deletions. The diversity of the TCRs is based on six complementary-determining regions (CDRs), which engage the peptide and the

MHC. This TCR is presented on the cell surface of a T cell and capable of recognizing peptides bound to MHC class I molecules (pMHC) on cells (Davis et al. 1988, Davis 1990, Rudolph et al. 2006). Healthy as well as infected or transformed cells present expressed cellular proteins on its cell surface to $CD8^+$ T cells after proteasomal degradation in the form of 9-mer peptides bound to MHC I (Eggensperger et al. 2015). T cells are capable of recognizing and lysing infected or mutated cells. The major mechanism of T cell mediated killing is accomplished via the delivery of secreted lysosomes into the immunological synapse between the effector cell and the target cell (Shresta et al. 1998). The main components of these granules are perforin and granzymes (Shresta et al. 1998). Perforin plays a major role in delivering granzyme B (grB) into the target cell. However, it is yet not fully clear whether perforin forms pores into the target cell membrane through which the granzymes pass directly into the cytosol or whether they are taken up together into target cell endosomes and perforin is required there for the granzyme release (Catalfamo et al. 2003, Voskoboinik et al. 2006). Once grB, the most common granzyme in humans, has entered the target cell its apoptosis is either induced via direct process of the effector caspases-3 and -7, or through BID-dependent mitochondrial permeabilization, followed by cytochrome c release and the formation of the apoptosome (Darmon et al. 1995, Alimonti et al. 2001).

A widely studied solid tumor type for T cell mediated immunotherapy is malignant melanoma. Exome sequencing data indicate that melanomas harbor more mutations than any other type of cancer in contrast to pediatric tumors where a low mutation rate is a general feature (Walia et al. 2012, Agelopoulos et al. 2015). These types of neo-antigens in melanomas represent potential targets for T cells that have not been negatively selected in the thymus (Robbins et al. 1996). Observations often perceived in patients with melanomas are tumor-infiltrating lymphocytes (TIL). These TILs can be isolated from the tumors and cultured *ex vivo* before re-infusion into the patient (Restifo et al. 2012). In melanoma patients, even complete remission of established cancer after re-administration of patient derived TILs was observed (Rosenberg et al. 2011). However, TILs are only detectable in a minority of cancers, e.g. mostly melanoma and renal cancer (Ruella et al. 2014). Auto-reactive T cells with high affinity receptors against healthy peptides are previously eliminated via negative selection in the thymus. Due to this fact T cells reactive against non-mutated but over expressed antigens in cancers are rare. Comparative analyses have also shown that natural occurring tumor reactive T cells have a lower antigen

affinity compared with TCRs directed against virus-derived antigens (Cole et al. 2007, Aleksic et al. 2012). This places them in a disadvantage in controlling the disease. But TCRs can be further modified to improve their affinity and thus their clinical efficacy. Most efficient is the affinity maturation via mutating the peptide-binding CD3 regions of the TCR of tumor reactive T cells (Goldrath et al. 1999, Nicholson et al. 2012). Although this approach gives promising results *in vitro* and *in vivo* still the characteristics of the TCR are altered. The artificially modified TCR is not a naturally occurring TCR that underwent negative selection by the thymus for its auto-reactivity. Due to that it also has the potential for severe off-tumor/off-target reactivity. A conducted study of a former MAGE-A3 specific TCR showed reactivity against titin in cardiomyocytes after TCR affinity maturation. This off-tumor/off-target reactivity resulted in life threatening GvHD and the death of two patients showing the potential threat of this treatment (Cameron et al. 2013, Linette et al. 2013).

As already mentioned before, pediatric tumors only show a very low mutation rate (Walia et al. 2012, Agelopoulos et al. 2015). This fact makes it very difficult to generate T cells directed against mutated proteins or to isolate patient derived tumor reactive T cells. Further, as tumor associated antigens (TAA) do not harbor mutations but represent normal, healthy proteins, T cells against these targets are negatively selected by the thymus. Therefore in a different strategy for the generation of tumor reactive T cells the alloreactive potential of the TCR is being used (Sadovnikova et al. 1996, Sadovnikova et al. 1998). Alloreactivity is the ability of T cells to recognize peptide-allogeneic MHC structures without a previous negative selection by the thymus (Felix et al. 2007, Burdach et al. 2013). Feasibility of allo-SCT in the treatment of ES was reported by Koscielniak et. al and Lucas et. al on AES patients who experienced tumor regression (Koscielniak et al. 2005, Lucas et al. 2008). As the allogeneic T cells in DLI lack specificity and also normal tissue is being attacked further improvement in the application of DLIs are necessary to further exploit this effect (Clay et al. 1999, Falkenburg et al. 1999). By selecting allorestricted TCRs against tumor associated antigens the potential life threatening GvHD reaction should be reduced whereas the desired GvT reaction is still taking place (Falkenburg et al. 1999). This approach is based on the alloreactive potential of TCRs to recognize foreign pMHC structures with high affinity (Sewell 2012, Burdach et al. 2013). In contrast to autologous T cells, which are less effective in tumor control, allogeneic TCRs should be able to kill tumors *in vivo* without further

affinity enhancement. The goal is the production of high amounts of tumor reactive TCR transgenic T cells to establish an *in vivo* immune response.

In the past years many protocols have been established to isolate, culture and characterize allorestricted-peptide specific T cells (Moris et al. 2001, Dutoit et al. 2002, Mutis et al. 2002, Amrolia et al. 2003, Whitelegg et al. 2005, Schuster et al. 2007). Also agents activating the immune system have been introduced into the clinic as the anti-CTLA4 and anti-PD-L1 antibodies to further augment T cell reactivity *in vivo* and consequently increase patient survival (Mellman et al. 2011). Even more insight into T cell biology and efficacy was gained with the differentiation process of T cells from the naïve precursor to fully differentiated T_{EFF} and their differential *in vitro* efficiency / *in vivo* efficacy. This understanding of T cell biology has lead to the conclusion that the ability of T cells to engraft, proliferate and persist *in vivo* is required for clinical tumor responses. Its long-term persistency further highlights the great potential in immunotherapy (Gattinoni et al. 2005, Huang et al. 2005, Powell et al. 2005, Gattinoni et al. 2012).

2. Research objectives

As illustrated above allogeneic T cell therapy can play a central role in future treatment of patients with AES. A schematic illustration of the workflow for generating TCR transgenic T cells for clinical application is shown in Figure 1.

The aim of this doctoral thesis was the generation of TCR transgenic T cells directed against ES TAAs. The TAAs Pappalysin-1 (PAPPA) and beta-3 adrenergic receptor (ADRB3) were previously identified and considered as potential targets for T cell mediated cancer immunotherapy. To generate T cells with a high avidity against their targets allogeneic T cell priming from HLA-A2^{-} healthy donors was considered as a suitable approach. Specific T cells directed against the TAAs were isolated via multimer assisted cell sorting. For the characterization of isolated and monoclonally cultured T cells interferon gamma (IFNγ) and grB ELISpot or xCELLigence assays were used.

For the identification of the TCR sequence of selected T cells a set of PCR primers for the various Vα- and Vβ-chains were used. Further a Vβ FACS antibody panel was used to ensure monoclonality of the T cells and the expression of the Vβ-chain previously identified via PCR. Finally, new primers were designed for the amplification of the whole TCR sequence. Sequence modifications were performed to improve expression and to prevent mispairing before cloning the sequences into the MP71 vector system.

The transgenic TCR was introduced into donor T cells via retroviral transduction and tested for its reactivity towards ES target cell lines. Cross reactivity was tested using various LCL cell lines and an amino acid exchange assay. *In vivo* experiments were carried out in immune-deficient Rag2$^{-/-}$γc$^{-/-}$ mice. Next to anti tumor reactivity, tumor infiltration and persistence, the lytic potential of TCR transgenic T cells was of interest.

In summary, this work gains to substitute a possible DLI with TCR transgenic T cells specifically direct against in ES over expressed TAAs. Thereby the potentially life threatening GvHD could be reduced while maintaining the tumor reactive GvT effect.

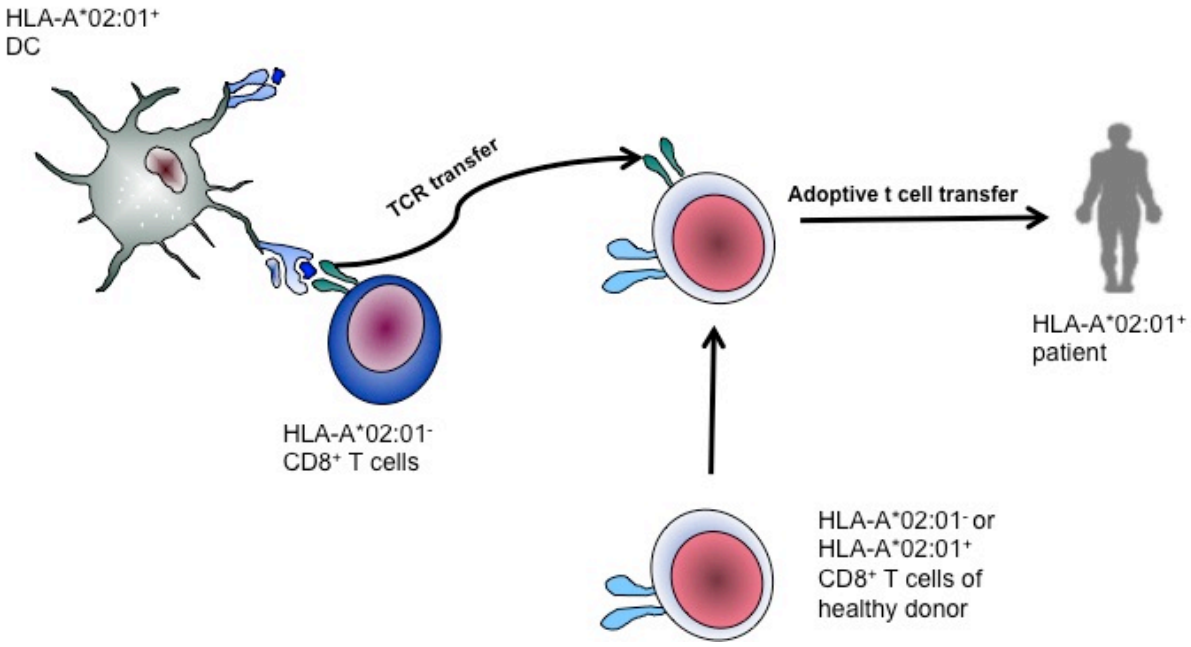

Figure 1: Illustration of application for TCR transgenic T cells in the clinic. Peptide pulsed DCs are used to stimulate HLA-A*02:01$^-$ T cells from healthy donors. After identification of HLA/peptide restricted T cells the TCR is retrovirally transferred into donor T cells and transfused into the patient.

3. Materials

3.1 List of manufacturers

Manufacturers	Locations
Abcam	Cambridge, UK
Abbott	Wiesbaden, Germany
Abnova	Taipei, Taiwan
AEG	Nürnberg, Germany
Affimetrix	High Wycombe, UK
Ambion	Austin, TX, USA
Amersham	Biosciences Piscataway, NJ, USA
Applied Biosystems	Darmstadt, Germany
ATCC	Rockyville, MD, USA
B. Braun Biotech Int.	Melsungen, Germany
BD Biosciences Europe	Heidelberg, Germany
Becton Dickinson (BD)	Heidelberg, Germany
Berthold detection systems	Pforzheim, Germany
Biochrom	Berlin, Germany
Biometra	Göttingen, Germany
BioRad	Richmond, CA, USA
Biozym	Hess. Olendorf, Germany
Brand	Wertheim, Germany
Calbiochem	Darmstadt, Germany
Carestream Health, Inc.	Stuttgart, Germany
Cell Signaling Technology	Frankfurt a. M., Germany
Charles River Laboratories	Wilmington, MA, USA
Clontech-Takara Bio Europe	Saint-Germain-en-Laye, France
DSMZ	Braunschweig, Germany
Eppendorf	Hamburg, Germany
Eurofins MWG GmbH	Ebersberg, Germany
Falcon	Oxnard, CA, USA
Feather	Osaka, Japan
Fermentas	St. Leon-Rot, Germany
GE Healthcare	Uppsala, Sweden
Genomed	St. Louis, MO, USA
Genzyme	Neu-Isenburg, Germany
GFL	Segnitz, Germany

Gibco	Darmstadt, Germany
GLW	Würzburg, Germany
Greiner Bio one	Nürtingen, Germany
Hamilton	Bonaduz, Switzerland
Heidolph Instruments	Schwabach, Germany
Heraeus	Hanau, Germany
Invitrogen	Karlsruhe, Germany
Jackson ImmunoResearch Laboratories	Baltimore, MD, USA
Kern	Balingen-Frommern, Germany
Köttermann	Uetze/Hänigsen
Laborservice	Harthausen, Germany
Leica	Wetzlar, Germany
LMS	Brigachtal, Germany
Lonza	Basel, Switzerland
Macherey-Nagel	Düren, Germany
Memmert	Schwabach, Germany
Merck	Darmstadt, Germany
Metabion	Martinsried, Germany
Millipore	Billerica, MA, USA
Molecular BioProducts,	MbP San Diego, CA, USA
Nalgene	Rochester, NY, USA
Nikon	Düsseldorf, Germany
Nunc	Naperville, IL, USA
PAA	Cölbe, Germany
Pechiney Plastic Packaging	Menasha, WI, USA
Peptides&Elephants	Berlin, Germany
Peqlab	Erlangen, Germany
Peske OHG	München, Germany
Philips	Hamburg, Germany
Promega	Madison, WI, USA
Qiagen	Chatsworth, CA, USA
R&D Systems	Minneapolis, MN, USA
Ratiopharm	Ulm, Germany
Roche	Mannheim, Germany
Roche/ACEA Biosciences	San Diego, CA, USA
(Carl) Roth	Karlsruhe, Germany
Santa Cruz Biotechnology	Heidelberg, Germany
Sartorius	Göttingen, Germany
Scientific Industries	Bohemia, NY, USA

Scotsman	Milan, Italy
Sempermed	Wien, Austria
Sequiserve	Vaterstetten, Germany
Sigma	St. Louis, MO, USA
Siemens	München, Germany
Stratagene	Cedar Creek, TX, USA
Syngene	Cambridge, UK
Systec	Wettenberg, Germany
Taylor-Wharton	Husum, Germany
Techlab	Braunschweig, Germany
Thermo Scientific	Braunschweig, Germany
TKA GmbH	Niederelbert, Germany
TPP	Trasadingen, Switzerland
Thermo Fisher Scientific	Ulm, Germany
Whatman	Dassel, Germany
Zeiss	Jena, Germany

3.2 Consumable material

Materials	**Manufacturers**
Cryovials	Nunc
E-plates (96-well)	Roche
Filters for cells, Cell Strainer	Falcon
Filters for solutions (0.2 µm and 0.45 µm)	Sartorius
Flasks for cell culture (25 cm^2, 75 cm^2 and 175 cm^2)	TPP
Gloves (nitrile, latex)	Sempermed
Hypodermic needle (23 G, 30 G)	B. Braun
MACS Separation Columns (MS; LS)	Miltenyi Biotec
Parafilm	Pechiney Plastic Packaging
Pasteur pipettes	Peske OHG
Petri dishes	Falcon
Pipettes (2, 5, 10 and 25 ml)	Falcon
Pipette tips (10, 200 and 1000 µl)	MbP
Pipette tips (10, 200 and 1000 µl with a filter)	Biozym
Plates for cell culture (6-well, 24-well and 96-well)	TPP
Plates for qRT-PCR (96-well)	Applied Biosystems

Scalpels (Nr. 12, 15, 20)	Feather
Tubes for cell culture (polypropylene, 15 ml and 50 ml)	Falcon
Tubes for molecular biology, Safelock (1.5 ml and 2 ml)	Eppendorf
Tubes for FACS™ (5 ml)	Falcon
Twin.tec real-time PCR plate 96	Eppendorf

3.3 Instruments and equipment

Type of device	Specification	Manufacturer
Airflow		Köttermann
Autoclave	2540EL	Systec
Autoclave	V95	Systec
Bacteria shaker	Certomat BS-T	Sartorius
Centrifuge	Multifuge 3 S-R	Heraeus
Centrifuge	Biofuge fresco	Heraeus
Controlled-freezing box		Nalgene
Flow cytometer	FACSCalibur™	Becton Dickinson
Freezer (-80 °C)	Hera freeze	Heraeus
Freezer (-20 °C)	cool vario	Siemens
Fridge (+4 °C)	cool vario	Siemens
Gel documentation	Gene Genius	Syngene
Ice machine	AF 100	Scotsman
Incubator	B20	Heraeus
Incubator	Hera cell 150	Heraeus
Liquid Nitrogen Tank	L-240 K series	Taylor-Wharton
Multichannel pipette	(10-100 µl)	Eppendorf
Heating block	Thermomixer Comfort	Eppendorf
Hemocytometer	Neubauer	Brand
Micropipettes	(0.5-10 µl, 10-100 µl, 20-200 µl, 100-1000 µl	Eppendorf
Microscope	DMIL	Leica
Microwave oven		Siemens, AEG
Mini centrifuge	MCF-2360	LMS
PCR cycler	iCycler	BioRad
Pipetting assistant	Easypet	Eppendorf
Power supplier	Standard Power Pack P25	Biometra
qRT- PCR cycler	7300 Real-Time PCR	Applied Biosystems

Rotator		GLW
Scales	770	Kern
Scales	EW3000-2M	Kern
Sterile Bench		Heraeus
Water bath		GFL
Vortexer	Vortex-Genie 2	Scientific Industries
Water purification system	TKA GenPure	TKA GmbH

3.4 Chemical and biological reagents

Reagents	Manufacturer
Agar	Sigma
Agarose	Invitrogen
Ampicillin	Merck
AmpliTaq DNA Polymerase	Invitrogen
BCP (1-bromo-3-chloropropane)	Sigma
1kb DNA Ladder	Invitrogen
dNTPs	Roche
DMEM medium	Invitrogen
DMSO (dimethyl sulfoxide)	Merck
EtBr (Ethidium bromide)	BioRad
Ethanol	Merck
FBS (fetal bovine serum)	Biochrom
37% Formaldehyde	Merck
Gentamycin	Biochrom
Glycerol	Merck
Glycine	Merck
G418	PAA
HBSS (Hank's buffered salt solution)	Invitrogen
HCl (hydrochloric acid)	Merck
HEPES	Sigma
Isoflurane	Abbott
Isopropanol	Sigma
L-glutamine	Invitrogen
MACS BSA Stock Solution	Miltenyi Biotec
MACS Buffer autoMACS™ Rinsing Solution	Miltenyi Biotec
Maxima™ Probe / ROX qPCR Master Mix (2x)	Fermentas

Methanol	Roth
PBS 10x (phosphate buffered saline)	Invitrogen
PCR Buffer (10x)	Invitrogen
Peptone	Invitrogen
Penicillin / streptomycin	Invitrogen
PFA (paraformaldehyde)	Merck
Polybrene (hexadimethrine bromide)	Sigma
Propidium iodide	Sigma
Puromycin	PAA
Ready-Load 1 Kb DNA Ladder	Invitrogen
RNase A (Ribonuclease A)	Roche
RPMI 1640 medium	Invitrogen
SYBR Green Master Mix	Applied Biosystems
Tris	Merck
Trypan blue	Sigma
Trypsin / EDTA	Invitrogen
Tween 20	Sigma

3.5 Chemicals, Enzymes and Cytokines

3.6 Commercial reagent kits

Table 1: Commercially obtained kits

Name	**Manufacturer**
Annexin V-PE Apoptose Detection Kit I	BD Biosciences
Anti-PE MicroBeads	Miltenyi Biotec
Anti-FITC MicroBeads	Miltenyi Biotec
BD IMag™ Anti-Human CD14 Magnetic Particles	BD Biosciences
CD8 MicroBeads	Miltenyi Biotec
$CD8^+$ T Cell Isolation Kit	Miltenyi Biotec
Dynal® CD4 Positive Isolation Kit	Invitrogen
EndoFree® Plasmid Maxi Kit	Quiagen
High-Capacity cDNA Reverse Transcription Kit	Applied Biosystems
JETSTAR 2.0 Plasmid Maxiprep Kit	Genomed
MycoAlert Mycoplasma Detection Kit	Lonza
TaqMan® Gene Expression Assays	Applied Biosystems

3.7 Buffer and Solutions

Table 2: Buffer solutions

Buffer / Solution	Properties
FACS Buffer	D-PBS, 2% FCS
i.v. Injection solution	D-PBS, 0,1% huAB Serum
i.p./s.c. Injection solution	D-PBS, 0,1% FCS
2.5% HEPES Buffer	HEPES in HBSS
Protaminsulfate	
Acetate Buffer	37.5 ml H_2O 3.75 ml 0.2 N acetic acid 8.8 ml 0.2 N sodium acetate
ACE solution	1 ACE tablet in 2.5 ml DMF + 47.5 ml acetate buffer
Developing solution	10 ml ACE solution + 25 µl H_2O_2
BSA 2%	2% BSA in PBS
BSA 5%	5% BSA in PBS
50x TAE running buffer	2 M Tris, 10% EDTA (0.5 M), 5.71% HCl

3.8 Cell Culture Media

Table 3: Cell culture media

Medium	Supplements	Final Concentration
LCL Medium	RPMI-1640	
	FCS	10%
	L-Glutamine	2 mM
	Pen Strep	1x
	Sodium-Pyruvate	1 mM
	Non essential amino acids	1x
Standard Medium	RPMI-1640	
	FCS	10%
	L-Glutamine	2 mM
	Pen Strep	1x
NSO / 293T Medium	DMEM	
	FCS	10%
	L-Glutamine	2 mM
	Pen Strep	1x
	Sodium-Pyruvate	1 mM
	Non essential amino acids	1x

TCM	AIM-V Human AB Serum L-Glutamine Pen Strep	 5% 2 mM 1x
X-Vivo	X-Vivo Human AB Serum	 1%
LB Medium	10 g peptone, 5 g yeast extract, 10 g NaCl, in 1000 ml distilled water	
Agar	LB medium, 2% Select agar	
Freezing medium (tumor cells)	FCS, 10% DMSO	
Freezing medium (human cells)	Human AB serum, 10% DMSO	

3.9 Cell lines, bacteria, and primary cell lines

3.9.1 Cell lines

Table 4: Description of utilized human cell lines

Cell line	Description	Medium	Source
A673	ES cell line (type 1 translocation), established from the primary tumor of a 15-year-old girl, p53 mutation	Standard Medium	
TC-71	ES cell line (type 1 translocation), established in 1981 from a biopsy of recurrent tumor at the primary of a 22-year-old man with metastatic ES (humerus)	Standard Medium	
EW7	ES cell line established from a shoulder-blade tumor	Standard Medium	Olivier Delattre, Institut Curie, Paris

SK-N-MC	ES cell line (type 1 translocation), established from the supraorbital metastases of a 14-year-old girl (Askin's tumor, related to ES)	Standard Medium	
SB-KMS-KS1	ES cell line (type 1 translocation), established from an extra osseous inguinal metastasis of a 17-year old girl (new nomenclature, originally designated as SBSR-AKS)	Standard Medium	
T2	TAP-deficient hybrid of a T and B lymphoblastic cell line; HLA-A*02:01^{+}, (ATCC CRL-1992)	LCL Medium	
LCL	EBV-immortalized B lymphoblastic cell line	LCL Medium	generated in the laboratory
K562	Established from the pleural effusion of a 53-year-old woman with chronic myelogenous leukemia.	Standard Medium	
293T GalV	GalV envelope plasmid transfected GP21C cells (293SF-derived clone expressing MLV Gag- Pol).	LCL Medium	

Table 5: Description of utilized LCL cell lines

Nr.	Cell line	HLA-A	HLA-B	HLA-C
1	RML	A*02:04	B*51:01	Cw*15:02
2	KLO	A*02:08	B*8/B*50	Cw*7/Cw*6
3	OZB	A*02:09/A3	B*39/B*35	Cw*4
4	AMALA	A*02:17	B*15:01	Cw*03:03
5	HOM2	A*03:01	B*27.052	Cw*01:02
6	SWEIG007	A*29:02	B*40.02	Cw*020:22
7	RSH	A*68:02/A*30:01	B*42:01	Cw*17:01
8	DUCAF	A*30:02	B*18:01	Cw*05:01
9	LWAGS	A*33:01	B*14:02	Cw*08:02
10	BM21	A*01:01	B*41:01	Cw*17:01

3.9.2 Bacteria

Table 6: Description of utilized bacterial strains

Bacteria	Description	Source
TOP10	F- *mcr*A Δ(*mrr-hsd*RMS-*mcr*BC) φ80*lac*ZΔM15 Δ*lac*X74 *rec*A1 *ara*D139 Δ(*araleu*) 7697 *gal*U *gal*K *rps*L (StrR) *end*A1 *nup*G	Invitrogen
Stabl2	F^- *mcr*A Δ(*mcr*BC-hsdRMS-*mrr*) *rec*A1 *end*A1*lon gyr*A96 *thi sup*E44 *rel*A1 λ^- Δ(*lac-pro*AB)	Invitrogen

3.9.3 Primary cell lines

Primary cells were isolated from Buffy Coats purchased from the Deutsches Rotes Kreuz (DRK), Ulm. PBMCs were isolated via Ficoll® gradient centrifugation.

Table 7: Description of utilized cell lines isolated from Buffy Coats

Cells	Description	Medium	Source
PBMCs	Peripheral blood mononuclear cells obtained via Ficoll-Paque	TCM	Buffy Coat
$CD8^+$ T cells	$CD8^+$ T cells isolated from PBMCs via negative selection	TCM	PBMC

$CD14^+$ Monocytes	Cells were isolated from PBMCs via BD IMag™ Anti-Human CD14 Magnetic Particles	X-Vivo	PBMC
Pool-PBMC	Mixture of 5 PBMCs from different donors in equal ratio	TCM	Buffy Coat

3.10 Mouse model

The mouse model on a BALB/c background used in the experiments has knockouts in the *Rag2* as well as in the *gamma(c)* locus. Deletion of the *Rag2* locus leads to a complete loss of functional peripheral B-lymphocytes as well as thymus-derived T-lymphocytes. The common cytokine receptor gamma chain (γc) is a functional subunit of a variety of cytokine receptors including the IL-2, IL-7 and IL-15 receptor. Loss of this gene leads to an impaired development of NK cells and hampers survival of NK cells and T lymphocytes. As a result the $Rag2^{-/-}\gamma c^{-/-}$ mouse model is completely abolished from B- and T-lymphocytes as well as nearly completely from NK cells. Therefore this mouse strain can be declared as immunodeficient (Goldman et al. 1998). The animals were obtained from the Central Institute for Experimental Animals (Kawasaki, Japan) and kept in the Zentrum für Präklinische Forschung (Klinikum rechts der Isar, München) under pathogen free conditions.

3.10 Peptides

Most peptides were ordered at ThermoFischer™ or peptides&elephant. Purity of peptides was > 90% for *in vitro* priming. Peptides for alanine/serine/threonine scan had a purity of > 70%. Purity was determined via mass spectrometry. Peptides were dissolved in DMSO. Stock concentration was 10 µg/µl.

Table 8: List of ordered peptides (purity > 90%).

Peptide	Sequence
Influenza	GILGFVFTL
CHM1^{319}	VIMPCSWWV
ADRB3^{38}	ALAGALLAL
ADRB3^{295}	GLIMGTFTL
ADRB3^{309}	FLANVLRAL
ADRB3^{321}	SLVPGPAFL
ADRB3^{44}	LALAVLATV
PAPPA^{1064}	IILPMNVTV
PAPPA^{1434}	CLDHNSESI
PAPPA^{111}	GTWNGSFHV
PAPPA^{157}	SIILPMNVT
PAPPA^{601}	PMNVTVRDI
CHM1^{319}	VIMPCSWWV

Table 9: List of ordered peptides for alanine/serine scans. Substituted peptides are highlighted (bold).

Peptide	Sequence
ADRB3_295-A1	**A**LIMGTFTL
ADRB3_295-A2	G**A**IMGTFTL
ADRB3_295-A3	GL**A**MGTFTL
ADRB3_295-A4	GLI**A**GTFTL
ADRB3_295-A5	GLIM**A**TFTL
ADRB3_295-A6	GLIMG**A**FTL
ADRB3_295-A7	GLIMGT**A**TL
ADRB3_295-A8	GLIMGTF**A**L
ADRB3_295-A9	GLIMGTFT**A**
ADRB3_295-S1	**S**LIMGTFTL
ADRB3_295-S2	G**S**IMGTFTL
ADRB3_295-S3	GL**S**MGTFTL
ADRB3_295-S4	GLI**S**GTFTL
ADRB3_295-S5	GLIM**S**TFTL
ADRB3_295-S6	GLIMG**S**FTL
ADRB3_295-S7	GLIMGT**S**TL
ADRB3_295-S8	GLIMGTF**S**L
ADRB3_295-S9	GLIMGTFT**S**
CHM1_319-A1	**A**IMPCSWWV
CHM1_319-A2	V**A**MPCSWWV

CHM1_319-A3	VI**A**PCSWWV
CHM1_319-A4	VIM**A**CSWWV
CHM1_319-A5	VIMP**A**SWWV
CHM1_319-A6	VIMPC**A**WWV
CHM1_319-A7	VIMPCS**A**WV
CHM1_319-A8	VIMPCSW**A**V
CHM1_319-A9	VIMPCSWW**A**
CHM1_319-T1	**T**IMPCSWWV
CHM1_319-T2	V**T**MPCSWWV
CHM1_319-T3	VI**T**PCSWWV
CHM1_319-T4	VIM**T**CSWWV
CHM1_319-T5	VIMP**T**SWWV
CHM1_319-T6	VIMPC**T**WWV
CHM1_319-T7	VIMPCS**T**WV
CHM1_319-T8	VIMPCSW**T**V
CHM1_319-T9	VIMPCSWW**T**
PAPPA_1064-A1	**A**ILPMNVTV
PAPPA_1064-A2	I**A**LPMNVTV
PAPPA_1064-A3	II**A**PMNVTV
PAPPA_1064-A4	IIL**A**MNVTV
PAPPA_1064-A5	IILP**A**NVTV
PAPPA_1064-A6	IILPM**A**VTV
PAPPA_1064-A7	IILPMN**A**TV
PAPPA_1064-A8	IILPMNV**A**V
PAPPA_1064-A9	IILPMNVT**A**
PAPPA_1064-S1	**S**ILPMNVTV
PAPPA_1064-S2	I**S**LPMNVTV
PAPPA_1064-S3	II**S**PMNVTV
PAPPA_1064-S4	IIL**S**MNVTV
PAPPA_1064-S5	IILP**S**NVTV
PAPPA_1064-S6	IILPM**S**VTV
PAPPA_1064-S7	IILPMN**S**TV
PAPPA_1064-S8	IILPMNV**S**V
PAPPA_1064-S9	IILPMNVT**S**

Table 10: List of peptides for PAPPA-2G6 putative cross reactivity exclusion

Gene name	Sequence	Description
CREBBP	AASPMNHSV	CREB-binding protein
C16orf62	ATLAMSEKV	UPF0505 protein C16orf62
EPSIN2	LALAMSREV	Epsin-2
HECW1/2	QISPMSAFV	E3 ubiquitin-protein ligase HECW1/2
MT-ND2	TLLPMSNNV	NADH-ubiquinone oxidoreductase chain 2
OAT	KVLPMNTGV	Ornithine aminotransferase, mitochondrial
STAT4	DLLPMSPSV	Signal transducer and activator of transcription 4

3.11 Antibodies

3.11.1 ELISpot assay antibodies

Table 11: List of ELISpot assay antibodies

Name	Specification	Manufacturer
Anti-human Granzyme B mAB	GB10, purified	Mabtech
Anti-human Granzyme B mAB	GB11, biotinylated	Mabtech
Anti-human IFNγ mAB	1-D1K, purified	Mabtech
Anti-human IFNγ mAB	7-B6-1, biotinylated	Mabtech

3.11.2 FACS antibodies

Table 12: FACS antibodies and fluorescent conjugation

Antibody	Clone	Conjugation	Manufacturer
Anti-HAL-DR	L243	PE	BD
CD4	SK3	PE	BD
CD8	RPA-T8	APC	BD
CD8	SK1	FITC	BD
CD45-RA		PE	MACS
CD45RO		PE	MACS
CD56	NCAM16.2	APC	BD
CD62L	DREG-56	APC	BD
CD83	HB15e	FITC	BD

CD86	2331	FITC	BD
CD107a	H4A3	FITC	BD
CD107a	H4A3	PE	BD
CD197/CCR7		PE	BD
Mouse Anti-Human HLA-A2	BB7.2	FITC	BD
Mouse IgG2a k Isotype	G155-178	FITC	BD
Mouse γ1	X40	APC	BD
Mouse γ1	X40	FITC	BD
Mouse γ1	X40	PE	BD

Table 13: List of specific multimer

Multimer	Sequence	Fluorescent conjugation	Source
Multimer PAPPA^{1434}	IILPMNVTV	PE	Dirk Busch, TU München
Multimer ADRB3^{295}	GLIMGTFTL	PE	Dirk Busch, TU München
Multimer CHM1^{319}	VIMPCSWWV	PE	Dirk Busch, TU München

Table 14: Reagent composition of the IOTest® Beta Mark TCR V β Repertoire Kit

Tube	Fluorochrome	Vβ
A	PE PE + FITC FITC	Vb 5.3 Vb 7.1 Vb 3
B	PE PE + FITC FITC	Vb 9 Vb 17 Vb 16
C	PE PE + FITC FITC	Vb 18 Vb 5.1 Vb 20

D	PE PE + FITC FITC	Vb 13.1 Vb 13.6 Vb 8
E	PE PE + FITC FITC	Vb 5.2 Vb 2 Vb 12
F	PE PE + FITC FITC	Vb 23 Vb 1 Vb 21.3
G	PE PE + FITC FITC	Vb 11 Vb 22 Vb 14
H	PE PE + FITC FITC	Vb 13.2 Vb 4 Vb 7.2

Table 15: List of used antibodies for immunohistochemistry

Antibody	Source	Dilution/Amount	Product Number	Manufacturer
Anti-CD8	mouse	1:100	SP16	DCS
Anti-PAPPA	mouse	1:50	HPA001667	Sigma Aldrich

3.12 Vectors and Primer

3.12.1 Vectors of retroviral transduction

Table 16: Vector description for TCR transgenic T cells

Vector	Description	Resistance	Source
MP71-ADRB3-1F4mm	Beta and Alpha chain of the ADRB3-1F4 TCR linked by a P2A sequence. Minimal murinization and codon optimization.	Amp	GeneArt, Regensburg
MP71-PAPPA-2G6mm	Beta and Alpha chain of zhe PAPPA-2G6 TCR linked by a P2A sequence. Minimal murinization and codon optimization.	Amp	GeneArt, Regensburg

MP71-CHM1-4B4mu	Beta and Alpha chain of the CHM1-4B4 TCR linked by a P2A sequence. Human constant chain exchanged for the murine constant chain and codon optimization.	Amp	GeneArt, Regensburg

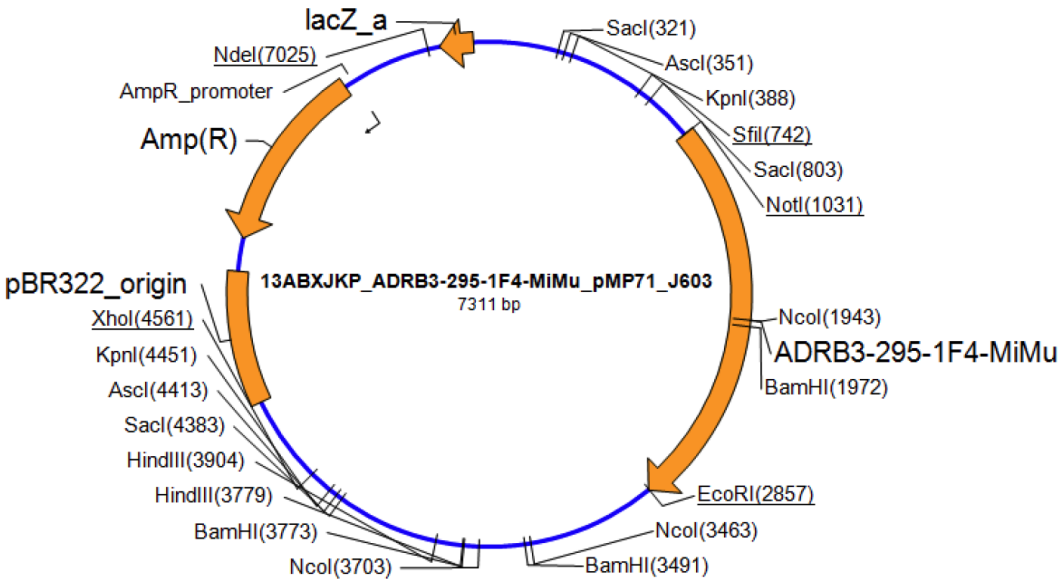

Figure 2: Vector map of the MP71 vector system carrying the ADRB3-1F4mm TCR construct

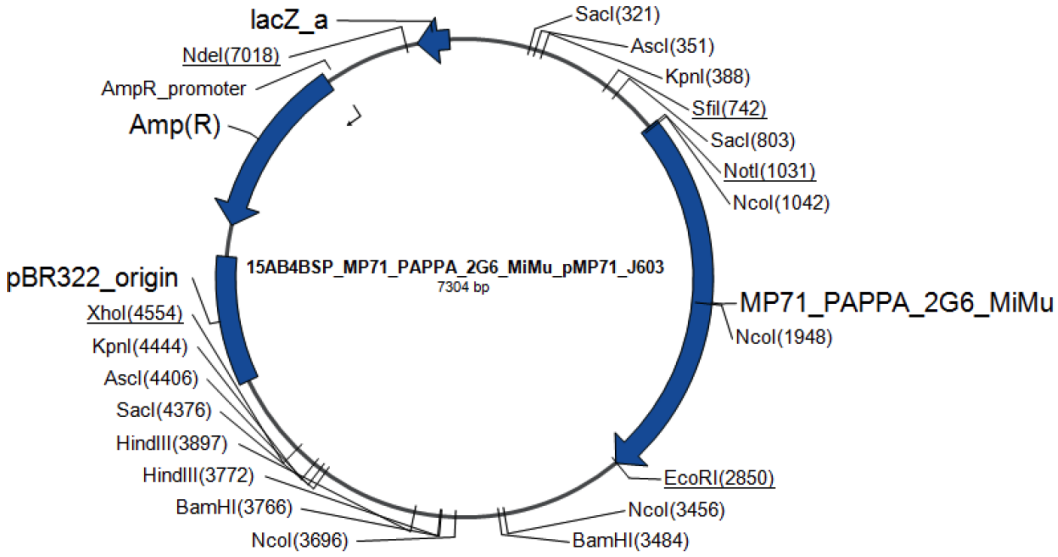

Figure 3: Vector map of the MP71 vector system carrying the PAPPA-2G6mm TCR construct

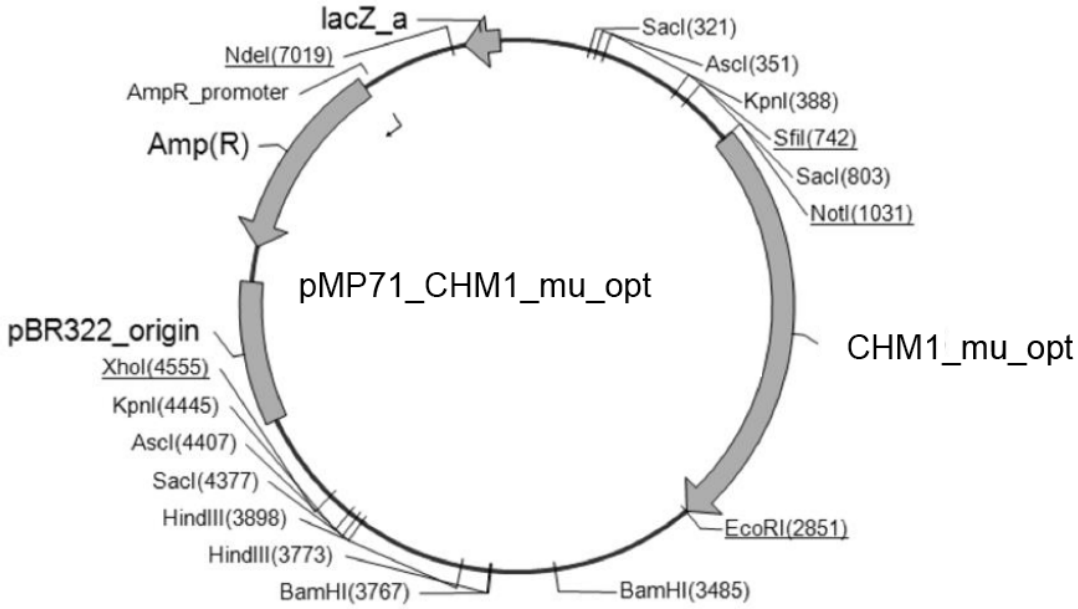

Figure 4: Vector map of the MP71 vector system carrying the CHM1-4B4mu TCR construct

3.12.2 Primers

Primers were synthesized by Metabion International AG, Planegg/Steinkirchen. All primers are listed in 5'-3' direction. All TaqMan Gene Expression qRT-PCR primers were obtained from Applied Biosystems.

3.12.2.1 Primer for the Identification of TCRs

Nomenclature is according to B. Arden (Arden et al. 1995)

T cell α-chain repertoire (Steinle et al. 1995)

Table 17: T cell α-chain PCR primers

P-5'αST	ST CTG TGC TAG ACA TGA GGT CT	
P-3'αST	ST CTT GCC TCT GCC GTG AAT GT	
3'T-Cα	GGT GAA TAG GCA GAC AGA CTT GTC ACT GGA	
PANVα1	AGA GCC CAG TCT GTG ASC CAG	S = C/G
PANVα1.1	AGA GCC CAG TCR GTG ACC CAG	R = A/G
Vα2	GTT TGG AGC CAA CRG AAG GAG	
Vα3	GGT GAA CAG TCA ACA GGG AGA	
Vα4	TGA TGC TAA GAC CAC MCA GC	
Vα5	GGC CCT GAA CAT TCA GGA	
Vα6	GGT CAC AGC TTC ACT GTG GCT A	
Vα7	ATG TTT CCA TGA AGA TGG GAG	
Vα8	TGT GGC TGC AGG TGG ACT	
Vα9	ATC TCA GTG CTT GTG ATA ATA	
Vα10	ACC CAG CTG CTG GAG CAG AGC CCT	
Vα11	AGA AAG CAA GGA CCA AGT GTT	
Vα12	CAG AAG GTA ACT CAA GCG CAG ACT	
Vα13	GAG CCA ATT CCA CGC TGC G	
Vα14.1	CAG TCC CAG CCA GAG ATG TC	
Vα14	CAG TCT CAA CCA GAG ATG TC	
Vα15	GAT GTG GAG CAG AGT CTT TTC	
Vα16	TCA GCG GAA GAT CAG GTC AAC	
Vα17	GCT TAT GAG AAC ACT GCG T	
Vα18	GCA GCT TCC CTT CCA GCA AT	
Vα19	AGA ACC TGA CTG CCC AGG AA	
Vα20	CAT CTC CAT GGA CTC ATA TGA	

Vα21	GTG ACT ATA CTA ACA GCA TGT	
Vα22	TAC ACA GCC ACA GGA TAC CCT TCC	
Vα23	TGA CAC AGA TTC CTG CAG CTC	
Vα24	GAA CTG CAC TCT TCA ATG C	
Vα25	ATC AGA GTC CTC AAT CTA TGT TTA	
Vα26	AGA GGG AAA GAA TCT CAC CAT AA	
Vα27	ACC CTC TGT TCC TGA GCA TG	
Vα28	CAA AGC CCT CTA TCT CTG GTT	
Vα29	AGG GGA AGA TGC TGT CAC CA	
Vα30	GAG GGA GAG AGT AGC AGT	
Vα31NEU	TCG GAG GGA GCA TCT GTG ACT A	
Vα32	CAA ATT CCT CAG TAC CAG CA	

T cell β-chain repertoire (Steinle et al. 1995)

Table 18: T cell β-chain PCR primers

P-5βST	AAG CAG AGA TCT CCC ACA C	
P-3βST	GAG GTA AAG CCA CAG TCT GCT	
P-3CβII	GAT GGC TCA AAC ACA GCG ACC TC	
Vβ1	GCA CAA CAG TTC CCT GAC TTG GCA C	
Vβ2	TCA TCA ACC ATG CAA GCC TGA CCT	
Vβ3	GTC TCT ACA TAT GAG AGT GGA TTT GTC ATT	
Vβ5.1	ATA CTT CAG TGA GAC ACA GAG AAA C	
Vβ5.2	TTC CCT AAC TAT AGC TCT GAG CTG	
Vβ6.1	GCC CAG AGT TTC TGA CTT ACT TC	
Vβ6.2	ACT CTG ASG ATC CAG CGC ACA	S=C/G
Vβ6.3	ACT CTG AAG ATC CAG CGC ACA	
Vβ7	CCT GAA TGC CCC AAC AGC TCT C	
Vβ8	ATT TAC TTT AAC AAC AAC GTT CCG	
Vβ8S3	GCT TAC TTC CGC AAC CGG GCT CCT	
Vβ9	CCT AAA TCT CCA GAC AAA GCT	
Vβ10	CTC CAA AAA CTC ATC CTG TAC CTT	
Vβ11	TCA ACA GTC TCC AGA ATA AGG ACG	
Vβ12	AAA GGA GAA GTC TCA GAT	
Vβ12S3	GCA GCT GCT GAT ATT ACA GAT	
Vβ13	TCG ACA AGA CCC AGG CAT GG	
Vβ13.1	CAA GGA GAA GTC CCC AAT	

Vβ13.2	GGT GAG GGT ACA ACT GCC	
Vβ13S5	ATA CTG CAG GTA CCA CTG GCA	
Vβ14	GTC TCT CGA AAA GAG AAG AGG AAT	
Vβ15	AGT GTC TCT CGA CAG GCA CAG GCT	
Vβ16	AAA GAG TCT AAA CAG GAT GAG TCC	
Vβ17	CAG ATA GTA AAT GAC TTT CAG	
Vβ18	GAT GAG TCA GGA ATG CCA AAG GAA	
Vβ19	CAA TGC CCC AAG AAC GCA CCC TGC	
Vβ20	AGC TCT GAG GTG CCC CAG AAT CTC	
Vβß21	AAA GGA GTA GAC TCC ACT CTC	
Vβ22.1	CAT CTC TAA TCA CTT ATA CT	
Vβ22.2	AAG TGA TCT TGC GCT GTG TCC CCA	
Vβ22.3	CTC AGA GAA GTC TGA AAT ATT CG	
Vβ23	GCA GGG TCC AGG TCA GGA CCC CCA	
Vβ24	ATC CAG GAG GCC GAA CAC TTC T	
Vβ25	TGA AAA TGT CTT TGA TGA AAC AG	
Vβ26	CCT AAC GGA ACG TCT TCC AC	
Vβ27	ATA CTG GAA TTA CCC AGA CAC	
Vβ28	TAC ACA ATT CCC AAG ACA CAG	

3.12.2.2 Primer for specific TCRs

Specific primers for the ADRB3-1F4 TCR:

Table 19: Specific PCR primers for ADRB3-1F4

TRAV12-2*02	ATG ATG AAA TCC TTG AGA GTT TTA C
TRBV19*03	CAA CCA GGT GCT CTG CTG T

Specific primers for the PAPPA-2G6 TCR:

Table 20: Specific PCR Primers for PAPPA-2G6

TRAV5*01	ATG AGG CAA GTG GCG AGA GTG AT
TRBV4-2*01	ATG GGC TGC AGG CTG CTC T

3.12.3.3 qRT-PCR primers

Table 21: qRT-PCR primer assays

Gene	Assay
ADRB3	Hs00609046_m1
GAPDH	Hs99999905_m1
OAT	Hs00236852_m1
PAPPA	Hs01032307_m1

3.13 Software and Online Services

Analysis of flow cytometric data:

BD CellQuest™ Pro,

Analysis of DNA sequences and construction of transgenic TCRs:

SerialCloner, Version 2.6.1

Analysis of TCR sequences:

IMGT (http://imgt.cines.fr)

Statistics:

GraphPad Prism®, Version 5.0b

HLA-A2 binding strength prediction:

www.syfpeithi.de

4. Methods

4.1 Cell culture conditions

All cells were cultured at 37 °C, 5% CO_2, and a relative humidity of 95% in an incubator. All work was performed under sterile conditions using a laminar-airflow bench. Retroviral transductions were done under a S2 sterile working bench.

4.2 Culture of tumor cell lines

Tumor cells cultured in suspension were given fresh medium every 2 to 3 days and split if required. Adherent cells were splitted and cultured in new flasks every 3 to 4 days or at 80% confluence. For this, cells were washed once with cold PBS. 1 ml, 2 ml, or 4 ml of Trypsin was added according to flask size and incubated at 37 °C until the adherent cells were present as single cells. Cells were re-suspended in fresh media and split depending on cell type and cultured in new flasks.

4.3 Cryoconservation

Single cells were frozen at a desired cell count in 500 µl freezing medium containing 90% FBS and 10% DMSO. T cells were frozen in 90% huAB serum plus 10% DMSO. Cells were stored at -80 °C for up to two weeks. For longer storage cells were transferred into liquid nitrogen tanks.
When thawed, cells were washed once in their according medium and then cultured under standard conditions in their corresponding medium and cytokines depending on the cell line.

4.4 Determination of cell count

For the determination of the cell count single cells were diluted in Trypan Blue to distinguish between dead or live cells. Trypan Blue only enters dead cells staining them blue. Under the microscope using a Neubauer Chamber only unstained bright viable cells were counted and cell count was calculated according to the following formula:

$c[cells/ml] = number\ of\ cells / number\ of\ quadrants * dilution * 10^4$

4.5 Peptide binding assay using TAP deficient T2 cells

T2 cells were washed twice in LCL medium and set to a concentration of 1×10^6 cells/ml. 250 µl of cell suspension was used per well in round-bottom 96-well plates. Peptides were added to the wells in increasing amounts to measure concentration dependency of MHC I binding. Unpulsed cells were used as a negative control.

After incubation over night cells were washed twice with FACS Buffer and stained with HLA-A2-FITC for 30 min at 4 °C. Afterwards cells were washed twice with FACS Buffer before being resuspended in PBS and measured using a FACSCalibur™. To determine the relative binding of a peptide at a defined concentration the measured fluorescent intensity was divided by the intensity of unpulsed T2 cells. A high binding affinity peptide should have similar values as the influenza control.

4.6 Isolation of PBMCs from Buffy coats

Buffy coats were obtained from the Deutsches Rotes Kreuz (DRK) in Ulm and PBMCs were isolated via density centrifugation. Briefly, Buffy coats were diluted 3:1 in PBS. 30 ml of blood was carefully placed on top of 20 ml Ficoll® and centrifuged at 400 g for 30 min without breaks. Afterwards the PBMC interphase was collected and washed once with PBS. Remaining erythrocytes were lysed using 12 ml EryLysis Buffer. Lysis was stopped after 5 min with cold PBS. After an additional centrifugation the cell count was determined.

4.7 Isolation of CD14$^+$ monocytes

For the isolation of CD14$^+$ Monocytes from PBMCs the BD IMag™ Anti-Human CD14 Magnetic Particles^{TM} were used according to the manufacturers protocol. 1 x 10^7 PBMCs were washed once with BD IMag Buffer and incubated with 50 µl magnetic particles for 30 min at RT. Afterwards, cells were washed with 3 ml Buffer and transferred into a BD FACS Tube before being set into a BD IMagnet™. Cells were separated once for 10 min, before supernatant was discarded, and then washed 3 times for 4 min with 4 ml of BD IMag Buffer. After the last washing step cells were taken up in X-Vivo 15 Medium and the cell count was determined.

4.8 Differentiation of CD14$^+$ monocytes to dendritic cells

Isolated CD14$^+$ cells were cultured for 7 days in X-Vivo 15 Medium at a concentration of 5 x 10^5 cells/ml with additional 10 µl/ml humanAB serum, 10 µl/ml IL-4 and 1 µl/ml GM-CSF. Cytokines were replaced on day 3 and day 5. On day 7 the maturation cocktail was added consisting of 1000 U/ml IL-6, 10 ng/ml IL-1β, 10 ng/ml TNF alpha, and 10 µl/ml PGE2. After 48 h cells were checked for maturation.

4.9 Analysis of dendritic cell maturation

48 h after addition of the maturation cocktail isolated CD14$^+$ cells were checked for their maturation towards dendritic cells (DCs). Cells were stained for CD86, CD83, and HLA-DR and analyzed via FACSCalibur^{TM}. DCs were further used when they were > 90% positive for all three markers.

4.10 Peptide pulsing of mature DCs

Mature DCs were artificially loaded with previously selected 9-mer peptides. 1 x 10^7 DCs / ml in TCM were incubated with 50 – 70 µg of peptide plus 5 µg/ml β2MG. Cells were incubated at 37 °C for 4 h and shortly vortexed every 15 min. Subsequently, cells were washed twice with TCM.

4.11 Isolation of $CD8^+$ T cells

Isolated PBMCs from Buffy Coats were washed once with ice cold MACS Buffer and resuspended in 40 µl of MACS Buffer per 1 x 10^7 cells. 10 µl of $CD8^+$ T Cell Biotin-Antibody Cocktail was added and the cells were incubated at 4 °C. After 10 min additional 30 µl of MACS Buffer were added plus 20 µl of $CD8^+$ T Cell MicroBeads Cocktail. Cells were mixed well and incubated for additional 15 min at 4 °C. After a washing step with 4 ml of MACS Buffer and centrifugation at 500 g for 15 min, labeled cells were placed on a previously equilibrated column at a concentration of up to 1 x 10^8 cells in 500 µl. After rinsing the column 3 times with 3 ml of MACS Buffer, cell count was determined in the collected flow-through.

4.12 Generation of Pool-PBMCs as feeder cells

T cells were cultured using freshly irradiated LCLs (100 Gy) and Pool-PBMCs (30 Gy) as feeder cells. PBMCs were isolated from five different Buffy coats. The amount of isolated PBMCs was determined after erythrocyte lysis and cell count from all Buffy coats was adjusted equally. Pool-PBMCs were then frozen in 5 x 10^7 aliquots in 500 µl freezing medium and stored in liquid nitrogen. Cells were thawed and irradiated when needed.

4.13 FACS sorting of multimer specific T cells

For the isolation of pMHC specific T cells peptide loaded multimers were used (Knabel et al. 2002). T cell reactivity is directed against peptides bound to the MHC I complex. Such pMHCs, linked together with a fluorescent dye were used to stain specific T cells and to isolate them after priming them with peptide pulsed dendritic cells.

Primed T cells were pooled, washed with FACS Buffer and stained with specific PE-labeled multimer and CD8-FITC for 30 min at 4 °C. Subsequently, cells were washed twice with FACS Buffer and resuspended in PBS. Cells were gated for $CD8^+$/$multimer^+$ T cells and sorted using a BD FACSAria™. Isolated T cells were cultured via single cell dilution before functional evaluation of their specificity.

4.14 Single cell dilution

After FACS sorting for multimer positive T cells the isolated cells were cultured in single cell dilution to generate cultures of monoclonal T cells. Cells were cultured in 96-well plates in 200 µl TCM with previously irradiated 1 x 10^5 LCLs (100 Gy) and 5 x 10^4 PBMCs (30 Gy) per well with additional 100 U/ml IL-2, 2 ng/ml IL-15, and 30 ng/ml of OKT3. Once a week 100 µl of TCM was replaced with fresh medium plus cytokines. After three weeks growing single cell clones were selected for specificity testing in IFNγ EISpot assays.

4.15 T cell culture in flasks

T cells were cultured upright in a T25 flask with 25 ml of TCM plus 2.5 x 10^7 irradiated PBMCs (30 Gy) and 5 x 10^6 irradiated LCLs (100 Gy). Additionally, T cells were stimulated with 30 ng/ml OKT3. After 24 h 100 U/ml IL-2 and 2 ng/ml IL-15 was added. Cytokines were replaced every second day. Up to 13 ml of TCM was replaced when depleted.

4.16 FACS staining of cell surface proteins

For surface staining of single cell suspension 2 x 10^5 cells were washed twice with FACS buffer. Cells were stained in 100 µl FACS buffer plus 1 µl of corresponding antibody for 30 min at 4 °C in the dark. Before measurement, cells were washed twice with FACS buffer, resuspended in PBS and measured with a BD FACSCalibur™. As an isotype control IgG antibodies were used for each measurement. Measurements were then analyzed with the CellQuest™ Pro (BD) software.

4.17 Annexin-V-PE staining of apoptotic cells

Measurement of apoptotic cells was done using the PE Annexin V Apoptosis Detection Kit 1 by BD. Staining with annexin-V-PE and 7-AAD was done according to the manufacturers manual. The 1X annexin V Binding Buffer was freshly diluted with water from a 10X stock before staining the cells. Cells were washed twice with ice cold PBS and resuspended in 1X Binding Buffer at a concentration of 1 x 10^6 cells/ml. 100 µl of the cell suspension was stained with 5 µl annexin-V-PE and 5 µl 7-AAD. After staining the cells for 15 min at RT, cells were directly diluted with 400 µl of

Binding Buffer and measured immediately using a BD FACSCalibur. Early apoptotic cells were annexin-V-PE positive, 7-AAD negative. Cells in late stage of apoptosis were characteristically stained annexin-V-PE and 7-AAD positive.

4.18 ELISpot Assay

96-well mixed cellulose ester plates (MultiScreen-HA Filter Plate, 0,45 µm, Millipore, Eschborn, Germany) were coated over night at 4 °C with a 50 µl capture antibody solution at a concentration of 10 µg/ml per well in PBS. The next day the antibody was discarded, plates were washed 4 times with 200 µl PBS and incubated 10 min at 4 °C. Afterwards wells were blocked with 150 µl of TCM for 1 h at 37 °C.

T cells were counted and the required amount of cells for two wells was placed onto 96-well V-bottom plates. The cells were washed 3 times with 100 µl of TCM and were resuspended in 110 µl of TCM. After blocking the ELISpot plate for 1 h at 37 °C the medium in the wells was discarded and 50 µl of the T cell suspension was added onto the wells.

Targets cells were incubated with IFNγ 48 h before adding them onto the T cells. Cells were harvested, washed, and set to a concentration of 4 x 10^5 cells per ml in TCM. 50 µl of target cell suspension was added dropwise onto the corresponding wells of the ELISpot plate. For peptide loaded T2 cells 1 x 10^7 T2 cells per ml were pulsed with 3,5 µl of corresponding peptide. Cells were incubated at 37 °C and pulsed every 15 min for 2 h. Afterwards, cells were washed twice and set to a concentration of 4 x 10^5 cells per ml. 50 µl were added dropwise onto the wells. After the target cell suspensions were added to the T cells, plates were incubated for 20 h at 37 °C.

The next day plates were washed 6 times with PBS/0,05% Tween and dried briefly. The wells were incubated for 2 h with 100 µl of detection antibody solution (2 µg/ml) in PBS/0.5% BSA per well at 37 °C. Afterwards, wells were again washed 6 times with PBS/0,05% Tween. Briefly dried plates were incubated with 100 µl of a 1/100 dilution of Streptavidin-HRP in PBS/0.5% BSA for 1 h at RT shielded from light. Before developing the ELISpot plate wells were washed thrice with PBS/0.05% Tween and 3 times with PBS, and afterwards were dried briefly.

Developing solution was freshly prepared by adding 25 µl of H_2O_2 per 10 ml of developing solution. 100 µl were added per well, afterwards plates were developed for up to 8 min before the reaction was stopped with running tap water.

ELISpot plates were airdried thoroughly and spots were counted on an AID-ELIRIFL04 ELISpot reader.

4.19 xCELLigence

Cell proliferation of A673 and SK-N-MC cells was measured with an impedance-based instrument system (xCELLigence, Roche/ACEA Biosciences) enabling label-free real time cell analysis. Briefly, 1-3 x 10^4 cells were seeded into 96-well E-plates with 200 µl media containing 10% FBS, and were allowed to grow up to 72 - 100 h. Cellular impedance was measured periodically every 15 min across gold micro-electrodes on the bottom of tissue culture E-plates. The presence of the cells on top of the electrodes affects the local ionic environment at the electrode/solution interface, leading to an increase in the electrode impedance, which is displayed as cell index (CI) values. The more cells are attached on the electrodes, the larger the increase in electrode impedance.

When the target cells reached the exponential growth phase 100 µl of media were replaced by 100 µl of T cell suspension. T cell activity could be observed by detachment of targets cells and therefore a decrease in the electrode impedance and reduced CI values.

4.20 Vesicle release of T cells after target stimulation

To measure T cell activity via FACS a LAMP1 (CD107a) antibody was used (Betts et al. 2003). Briefly, 2 x 10^5 T cells were washed twice with TCM and re-suspended in 100 µl TCM. T cells were then incubated with up to 4 x 10^5 target cells in a total volume of 200 µl for up to 2 h at 37 °C in round bottom 96-well plates. Afterwards, cells were washed twice with FACS buffer and stained for CD107a-FITC and CD8-APC for 30 min at 4 °C. Before measurement with the FACSCalibur™, the cells were washed twice with FACS buffer before being taken up in PBS.

4.21 RNA isolation

Isolation of RNA from tumor cell lines or T cells was done using TRI Reagent. Pelleted cells were homogenized in 1 ml TRI Reagent. After adding 100 µl BCP per ml of TRI Reagent the solution was vortexed and incubated at RT for 10 min. To separate RNA from DNA and protein fractions, the solution was centrifuged at 12.000 g, for 10 min, at 4 °C. The aqueous phase was transferred into a new tube. To precipitate the RNA 500 µl of isopropanol was added. After vortexing for 10 sec and incubation at RT for 10 min the RNA was centrifuged at 12.000 g at RT for 8 min. Supernatant was discarded and pellet was washed once with 75% ethanol. After a centrifugation step at 7.500 g for 5 min the supernatant was discarded and the pellet was air dried briefly before the RNA was dissolved in DEPC-H_2O. RNA concentration was measured using a NanoPhotometer™ (Pearl, Implemen).

4.22 cDNA synthesis

For further analysis RNA was reverse transcribed using the High Capacity cDNA Reverse Transcription Kit by Applied Bioscience. Shortly, 1 µg of RNA was used for the transcription towards cDNA with 50 U of MultiScribe© Reverse Transcriptase. Master Mix was prepared as follows:

Master Mix 1:

Buffer	2 µl
Primer	2 µl
dNTPs	0,8 µl
MultiScribe© Reverse Transcriptase	1 µl

	5,8 µl

Master Mix 2:

RNA	1 μg
DEPC-H_2O	X μl

	14,2 μl

Both Master Mixes were adjusted to a total volume of 20 μl. Thermo Cycler settings were as follows:

Step	Temperature [°C]	Duration [min]
1	25	10
2	37	60
3	37	60
4	85	5
5	4	∞

cDNA samples were then used for gene expression analysis in qRT-PCR reactions or for the identification of TCR sequences via PCR and sequencing.

4.23 Quantitative Real-Time PCR (qRT-PCR)

Quantification of synthesized cDNA via qRT-PCR was used to examine differential gene expression. qRT-PCR was performed using Maxima™ Probe/ROX qPCR Master Mix (2x) (containing Hot Start Taq DNA Polymerase, PCR buffer and dNTPs) and specific TaqMan® Gene Expression Assays (Applied Biosystems), which consist of two unlabeled PCR primers and a FAM™ dye-labeled TaqMan® MGB probe. Analyses were performed in 96-well plates and the reaction mix was prepared according to the manufacturer's instructions.

qRT-PCR Master Mix:

Maxima™ Probe/ROX qPCR Master Mix	10 µl
TaqMan® Gene Expression Assay	1 µl
cDNA template	0.5 µl
RNase-free water	8.5 µl

Fluorescence was detected and measured in an AB 7300 Real-time PCR system using a three step cycling protocol: 1 s 50 °C; 10 min 95 °C; (15 s 95 °C; 1 min 60 °C) 40x.
Gene expression profiles were normalized to the mRNA levels of the housekeeping gene *glyceraldehyde 3-phosphate dehydrogenase* (GAPDH) and calculated using the 2^{-ddCt} method.

4.24 PCR for identification of specific TCR-alpha and -beta chains

The TCR sequence of selected T cell clones was identified via PCR and sequencing. A total of 34 different 5'-Vα-primers and 38 different 5'-Vβ-primers were available for the variable regions of the TCR (Steinle et al. 1995). The corresponding 3' primers (3'T-Cα and P-3'βII) bound in the constant region of the corresponding α- or β-chain. As an internal control a primer pair was used amplifying parts of the constant region.

PCR Master Mix for the detection of the TCR β-chain:

DEPC-H_2O	18,5 µl
Puffer (10x)	2,5 µl
P-5'βST (2,5 pmol/µl)	0,5 µl
P-3'bST (2,5 pmol/µl)	0,5 µl
3'CβII (5 pmol/µl)	1,0 µl
cDNA	0,5 µl
Polymerase	0,5 µl

PCR Master Mix for the detection of the TCR α-chain:

DEPC-H_2O	18,5 µl
Puffer (10x)	2,5 µl
P-5'αST (2,5 pmol/µl)	0,5 µl
P-3'αST (2,5 pmol/µl)	0,5 µl
3'T-Cα (5 pmol/µl)	1,0 µl
cDNA	0,5 µl
Polymerase	0,5 µl

23.5 µl of either master mix were pipetted into 96-well Eppendorf-PCR plates and 1.5 µl of a specific Vα/Vβ TCR PCR primer was added.

The thermocycler was programmed as follows:

Step	Description	Temperature [°C]	Duration [min]
1	Initial denaturation	94	6
2	Denaturation	94	1
3	Annealing	54	1
4	Elongation	68	1
5	Final elongation	68	7
6	Cooling	4	∞

Steps 2 to 4 were repeated 40 times.

4.25 Gel electrophoresis and -extraction of PCR products

PCR products were diluted in 6x loading buffer and loaded on a 1,5% agarose gel with supplemented 0,7 µg/ml ethidiumbromide. DNA probes were separated at a voltage of 110 mV for about 50 min. For size determination a 1 Kb Plus DNA Ladder was used. Amplified DNA products

were visualized under UV light and documented. PCR products of expected size were cut out with a scalpel and DNA was extracted using the NucleoSpin Gel-Extraction-Kit (Macherey-Nagel). To do so, 300 µl of gel extraction buffer was added to the gel piece and incubated at 50 °C until it was dissolved. The dissolved gel was transferred to a microspin cup seated in a 2 ml recaptable tube and spun for 30 sec at maximum speed in a table-top centrifuge. Flow-through was discarded and fiber matrix was washed once with 750 µl of 1x wash buffer for 30 sec at maximum speed. The wash buffer was discarded and the microspin cup was dried at maximum speed for 30 sec. For elution of bound DNA the microspin cup was transferred into a fresh 1.5 ml tube and 50 µl DEPC-H_2O was placed directly on top of the fiber matrix. After 5 min of incubation at RT the tube was again centrifuged at maximum speed for 30 seconds. Concentration of recovered DNA was measured using a NanoPhotometer™.

4.26 Sequencing and analysis of TCRs

All sequencing samples were sent for analysis to Sequiserve (Vaterstetten) with the according primers. Sequencing results were analyzed using IMGT, the international ImMunoGeneTics information system® http://www.imgt.org (founder and director: Marie-Paule Lefranc, Montpellier, France) (Brochet et al. 2008, Giudicelli et al. 2011). Productive TCR sequences without stop codons or in-frame junctions were followed up and new primers covering the whole sequence of the TCR chain were ordered. PCR products from these new primers were again sequenced. This sequence was subsequently used to construct the transgenic TCR.

4.27 Construction of transgenic MP71 vector system

In 5'-3' direction the TCR β-chain was placed in front of the α-chain. Both were linked via a P2A sequence to ensure an equal expression (Leisegang et al. 2008). To prevent mispairing with the endogenous TCR in donor T cells, after transduction specific AAs in the human constant chain were replaced with the corresponding AAs from the constant murine TCR chains (Sommermeyer et al. 2010). According to Sommermeyer et. al five substitutions in the TCR beta chain (Q18K, S22A, F133I, E136A, and Q139H) and four substitutions in the TCR alpha chain (P90S, E91D, S92V, and S93P) are necessary to ensure correct dimerization. Using the GeneArt™ Project

Configurator a Kozak sequence was added. A codon optimization further increases the expression of the transgenic construct. NotI and EcoRI restriction sites were added 5' and 3' of the sequence for cloning into the MP71 vector system (Engels et al. 2003). Synthesis of the modified transgenic TCR and subcloning into the MP71 vector was performed by GeneArt™, Regensburg.

4.28 Transformation of competent bacteria

Transformation of MAX Efficiency® Stbl2™ Competent Cells (Invitrogen) was carried out according to the manufacturer. Cells were thawed on ice and 1 – 10 ng of MP71 plasmid DNA with the inserted sequence of the codon optimized transgenic TCR was added. After incubating the cells for 30 min on ice they were heat-shocked for 25 sec in a water bath at 42 °C. Afterwards they were placed again on ice for 2 min before adding RT S.O.C. Medium. Cells were put on a shaker for 90 min at 225 rpm and 37 °C. Afterwards, cells were spread on LB plates containing 100 µg/ml ampicillin and incubated over night at 37 °C.

4.29 Mini- and Maxi-preparation of plasmid DNA

Isolation of plasmid DNA from transformed E. coli cells was performed with the EndoFree Plasmid Maxi Kit from Quiagen according to the manufacturer's manual. DNA concentration was measured using a NanoPhotometer™. The insert was controlled via restriction enzymes and agarose gel electrophoresis.

4.30 Production of retroviral particles

Transfection of the packaging cell line GalV was done using the *Trans*IT®-293 Reagent by Mirus according to the manufacturer's protocol. GalV cells were seeded in 6 well plates at a concentration of 2 x 10^5 per well in a total of 3 ml medium. After 24 h the medium of the packaging cells was replaced and the cells were transfected with the MP71 Plasmid DNA for the transgenic TCR. Per well 9 µl of TransIT was added to 200 µl of serum free DMEM in 5 ml round bottom tubes, vortexed and incubated at RT for 20 min. 1 µg of plasmid DNA was added to the

TransIT/DMEM solution, carefully mixed and incubated for additional 30 min at RT. Afterwards the solution was pipetted dropwise onto the GalV cells and incubated at 37 °C for 48 h.

The virus in the supernatant was removed after 48 h and 72 h, respectively, centrifuged and filtered through a 45 μm filter before being added to the PBMCs. Virus was used fresh or stored at -80 °C.

4.31 Transduction of PBMCs

PBMCs were isolated from HLA-A*02:01 negative Buffy coats via density gradient centrifugation. T cells were resuspended in TCM at a concentration of 1 x 10^6 cells per ml. After addition of 100 U/ml IL-2 and 30 ng/ml OKT3 cells were rested for 48 h at 37 °C in cell culture treated 24 well plates.

Non-treated 24 well plates were coated with 400 μl of a 12,5 μg/ml retronectin solution over night at 4 °C. Before spin infection wells were blocked with a 5% BSA in HBSS solution for 30 min at 37 °C and washed twice with 2,5% HEPES in HBSS. Previously isolated and activated PBMCs were counted and set to a concentration of 1 x 10^6 per ml TCM.

1 ml of virus supernatant and PBMCs, respectively, were added into retronectin-coated 24 well plates, respectively, and protamine-sulfate (c_{end} = 4 μg/ml), HEPES (c_{end} = 0,5%), and IL-2 (c_{end} = 100 U/ml) was added. Plates were centrifuged for 90 min at 820 g in a centrifuge preheated at 32 °C and stored at 37 °C over night afterwards. The next day cells were harvested and split 1:1. Cells were again placed on coated 24 well plates with fresh virus plus additives and centrifuged at 820 g / 90 min / 32 °C. Medium was replaced after 48 h and transduction efficiency was checked 24 h later via FACS multimer staining.

4.32 Isolation of transduced T cells via anti-PE magnetic microbeads

TCR transgenic T cells were isolated from non-transduced T cells via magnetic Anti-PE MicroBeads (Miltenyi Biotec) according to the manufacturer's protocol. Transduced T cells were pooled, washed twice with FACS buffer, and stained with specific multimer-PE for 30 min at 4 °C. For the magnetic labeling T cells were washed once in FACS buffer and MACS buffer, respectively. 1 x 10^7 cells were then diluted in 80 µl of MACS buffer. 20 µl of Anti-PE MicroBeads

were added and cells were incubated at 4 °C for 15 min before being washed once with 2 ml MACS buffer. Labeled cells were placed on a previously equilibrated column at a concentration of up to 1 x 10^8 cells in 500 µl. After 3 washing steps with 3 ml of MACS Buffer each, cell count was determined after removing the column from the separator and flushing out the magnetically labeled cells with 5 ml of MACS Buffer by firmly pushing the plunger into the column.

Efficiency of magnetic separation was then confirmed via multimer FACS and isolated TCR transgenic T cells were taken into culture in 25 ml TCM with irradiated feeder cells.

4.33 *In vivo* validation of TCR transgenic T cell efficacy

To analyze local tumor growth *in vivo*, 2 x 10^6 A673 cells were re-suspended in a final volume of 0.2 ml PBS/0.2% FCS. 2 x 10^6 A673 tumor cells were inoculated subcutaneously at the lower back of immunodeficient $Rag2^{-/-}\gamma c^{-/-}$ mice. After 3 days mice received a full body irradiation with 3.5 Gy to facilitate engraftment of human T cells. 5 x 10^6 TCR transgenic T cells together with 5 x 10^6 $CD8^+$ depleted PBMCs were injected i.p. the following day. Control groups received either no T cells, $CD8^+$ depleted PBMCs, or $CD8^+$ depleted PBMCs plus 5 x 10^6 unspecific T cells. 1.5 x 10^7 IL-15 secreting NSO cells (previously irradiated with 80 Gy) were injected i.p. twice per week. Mice were sacrificed after 17 days of tumor growth or at a maximum tumor size of > 10 mm (Fig. 5). Tumor size was determined. Also blood, bone marrow, and tumor samples were collected and analyzed for T cell persistence.

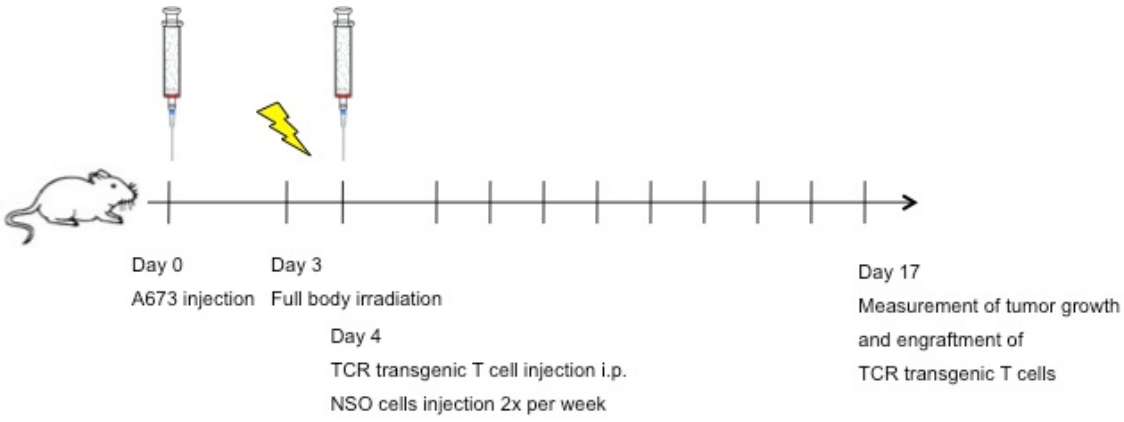

Figure 5: Time scale for validation of transgenic TCR *in vivo* efficacy. Mice were inoculated with 2 x 10^6 s.c. A673 ES cells at the lower back. On day 3 mice received a fully body irradiation with 3.5 Gy before receiving the TCR transgenic T cells on day 4. IL-15 secreting NSO cells were administered twice per week. Mice were sacrificed on day 17 and analyzed for tumor growth and T cell persistence.

4.34 Immunohistochemistry

Histological analyses were performed in cooperation with Dr. Thomas Grünewald (Institute of Pathology, Medical Department, Ludwig-Maximilians-Universität München). Immunohistochemistry (IHC) analyses of tumors were performed on formalin fixed, paraffin-embedded samples. All tissue slides were collected at the Department of Pathology of the Ludwig-Maximilians-Universität München. The following primary antibodies were used: CD8 (1:100, SP16, DCS) and PAPPA (1:50, HPA001667, Sigma Aldrich)

4.36 Statistical analyses

Descriptive statistics was used to determine mean, standard deviation (SD) and standard error of the mean (SEM). Differences were analyzed by unpaired two-tailed student's t-test as indicated using Excel (Microsoft) or Prism 5 (GraphPad Software); p values < 0.05 were considered statistically significant ($*p < 0.05$; $**p < 0.005$; $***p < 0.0005$).

5. Results

5.1 ADRB3 and PAPPA are over expressed in Ewing Sarcoma

In a previous publication we identified different over-expressed genes in ES (Staege et al. 2004). Among them was the Beta-3 adrenergic receptor (ADRB3) and Pappalysin-1 (PAPPA), which were shown to be over-expressed in biopsies of primary ES and metastases. We determined expression of ADRB3 and PAPPA in ES samples compared to a normal body map using the R2: Genomics Analysis and Visualization Platform (http://r2.amc.nl) (Fig. 6 A). Further we assessed ADRB3 and PAPPA expression in different ES cell lines (Fig. 6 B). Expression analysis showed increased expression of both antigens in comparison to the normal body map. Only for PAPPA very high expression levels in placenta were detected. Regarding the different ES cell lines ADRB3 and PAPPA expression could be confirmed.

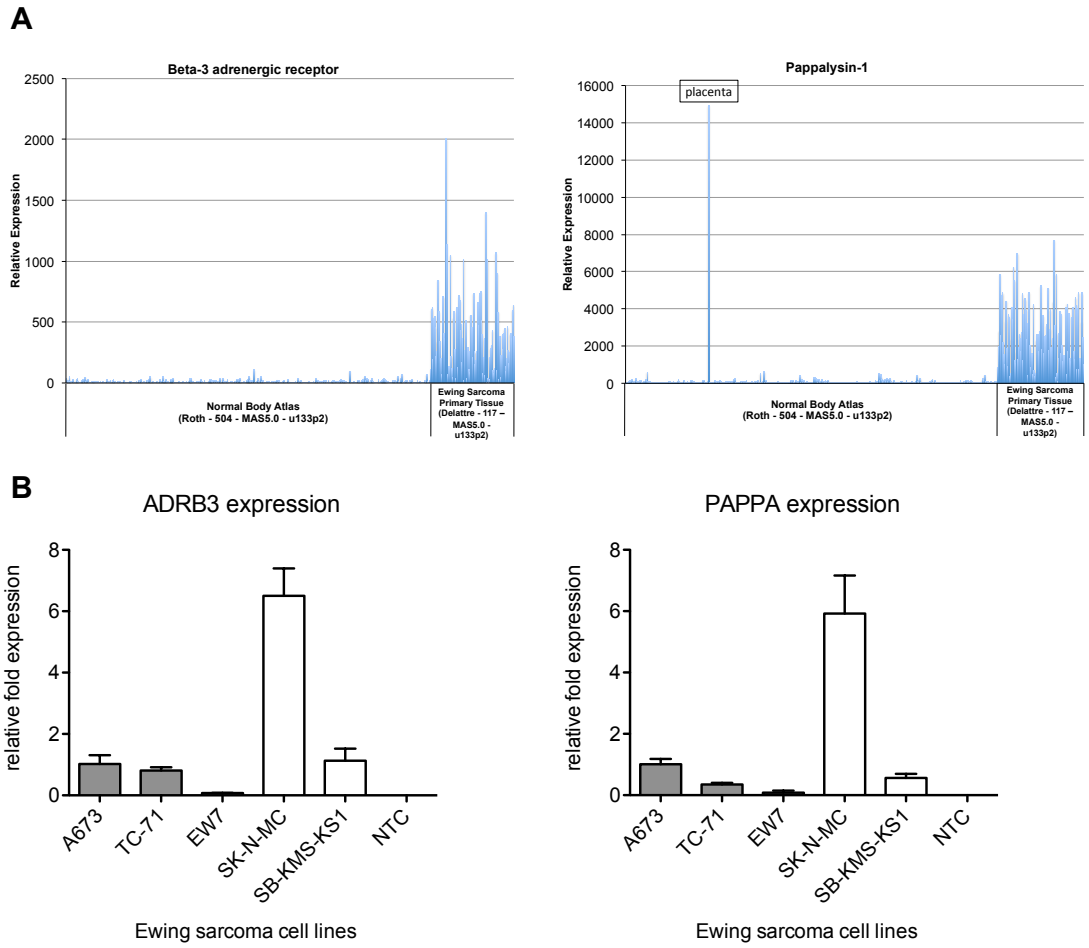

Figure 6: ADRB3 and PAPPA are ES associated target antigen. (A) ADRB3 and PAPPA are over-expressed in Ewing Sarcoma compared to a Normal Body Atlas. **(B)** Expression of both TAAs was detected via qRT-PCR in different ES cell lines. Results are shown relative to A673. Error bars represent standard deviation of duplicate experiments.

5.2 Selection of suitable ADRB3 and PAPPA 9-mer peptides for allogeneic T cell priming

For the selection of suitable 9-mer peptides for allogeneic T cell priming the "SYFPEITHI: database for MHC ligands and peptide motifs" (www.syfpeithy.com) was used (Rammensee et al. 1999). *In silico* analysis of the amino acid sequence of selected target genes resulted in a list of predicted ligation strength of possible 9-mer peptides to HLA-A*02:01. The peptide sequence for ADRB3 (Entry P13945) and PAPPA (Entry Q13219) was obtained from the UniProt web page (UniProt)(UniProt). A list of the peptides with the highest ligation strength according to SYFPEITHY is listed below (Tab. 20 + 21).

Table 22: List of predicted binding affinities for ADRB3 peptides for HLA-A*02:01 sorted by decreasing SYFPEITHY score

Protein Position	1 2 3 4 5 6 7 8 9	SYFPEITHY score
38	A L A G A L L A L	32
295	G L I M G T F T L	29
309	F L A N V L R A L	28
321	S L V P G P A F L	28
44	L A L A V L A T V	26

Table 23: List of predicted binding affinities for PAPPA peptides for HLA-A*02:01 sorted by decreasing SYFPEITHY score

Protein Position	1 2 3 4 5 6 7 8 9	SYFPEITHY score
1064	L I I P V V H D L	29
1434	I I L P M N V T V	28
111	Y L P G Q W V Y L	26
157	V L M L G G S A L	25
601	V L G H T T D S V	25
715	S L T I W V T F V	25

Peptides with the highest predicted binding strength were ordered. Tap deficient T2 cells were then incubated with increasing amounts of peptide over night. Measurement of surface HLA-A*02:01 stabilization was done via staining with a FITC labeled HLA-A*02:01 FACS antibody. Fluorescence intensity of measured samples was compared to the influenza matrix peptide (GILGFVFTL). Suitable peptides for allogeneic priming should show binding affinities comparable to the influenza positive control. For ADRB3 we chose the 9-mer peptide ADRB3^{295} (Fig. 7). Although we did not observe HLA stabilization over night we still could show increased peptide binding after 4 h.

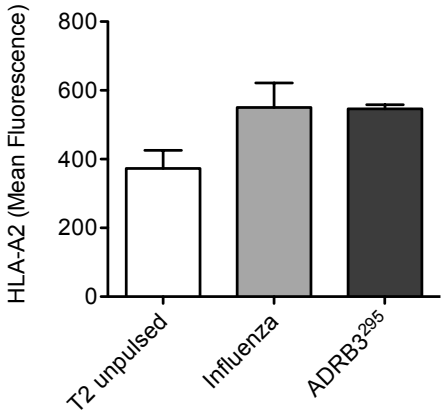

Figure 7: Flow-cytometry confirms ADRB3^{295}/HLA-A*02:01 binding on T2 cells. T2 cells loaded with ADRB3^{295} show HLA-A*02 positivity in FACS analysis comparable to the influenza positive control already after 4 hours of incubation. Data are presented as mean and SEM. All experiments were carried out in triplicates. Error bar represent standard deviation of triple experiments.

For the PAPPA antigen we could identify two different peptides PAPPA^{1434} and PAPPA^{601} with comparable binding properties (Fig. 10 A). Both were then further tested in titration assays and showed specific peptide concentration depended HLA-A*02:01 stabilization on T2 cells over night (Fig. 10 B). Although both peptides proofed to be suitable for allogeneic priming only the PAPPA^{1434} 9-mer peptide was chosen for further allogeneic priming due to its more efficient HLA-A*02:01 stabilization compared to PAPPA^{601}.

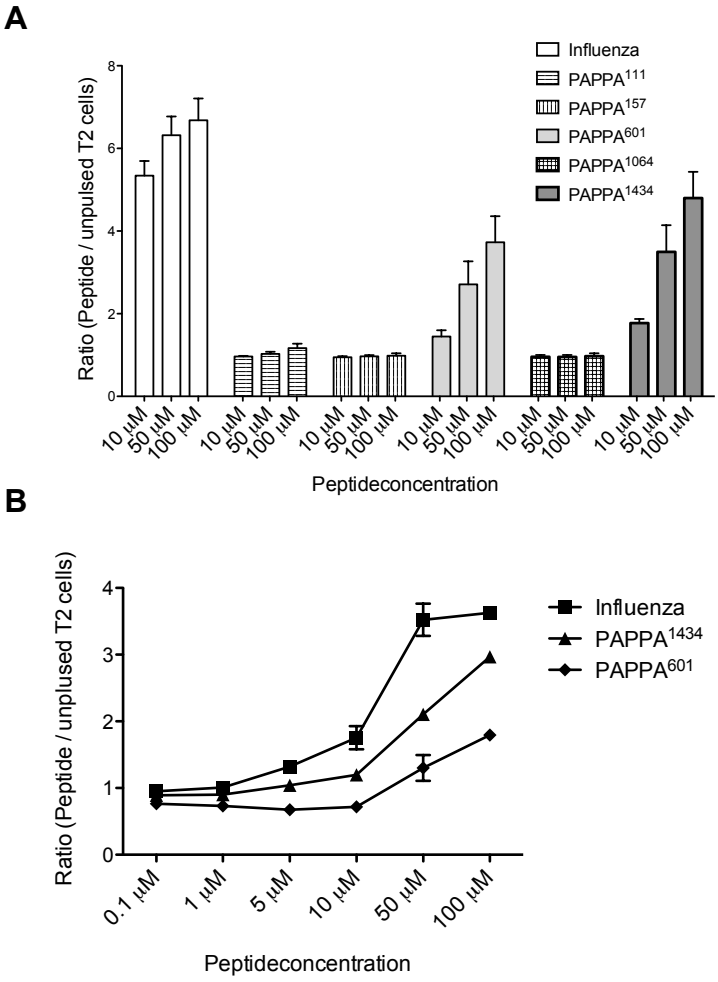

Figure 8: PAPPA^{1434} more efficiently stabilizes the MHC I complex on TAP deficient T2 cells. (A) Five different 9-mer peptides with high HLA-A*02:01 predicted binding affinities were loaded onto T2 cells. PAPPA^{1434} and PAPPA^{601} showed MHC I stabilization over night after FACS analysis. **(B)** Peptide titrations further revealed higher stabalizing capabilities for PAPPA^{1434} in comparison to PAPPA^{601}. Data are presented as mean. All experiments were carried out in triplicates. Error bars represent standard deviation of triple experiments.

5.3 Allogeneic T cell priming with peptide loaded dendritic cells and cell sort of multimer specific T cells.

DCs were generated from isolated CD14^{+} monocytes. After 7 days of culture DCs were controlled for their maturation. DCs were considered mature when at least 90% of the population was positive for CD83, CD86, and HLA-DR (Fig. 9 A). Allogeneic T cells were then incubated twice with peptide loaded DCs. Peptide specific T cells were isolated via FACS sorting. To isolate pMHC specific T cells directed against either ADRB3^{295} or PAPPA^{1434} the previously primed

T cells were pooled and stained for CD8 and its specific multimer, respectively. Using a FACS Aria cell sorter CD8-FITC and multimer-PE double positive T cells were isolated (Fig. 9 B). In total 796 double positive T cells were isolated from 2 x 10^7 T cells. This represents 0.04% of the T cell population. Afterwards isolated T cells were then further cultured using single cell dilution to generate clonal T cells populations for analysis.

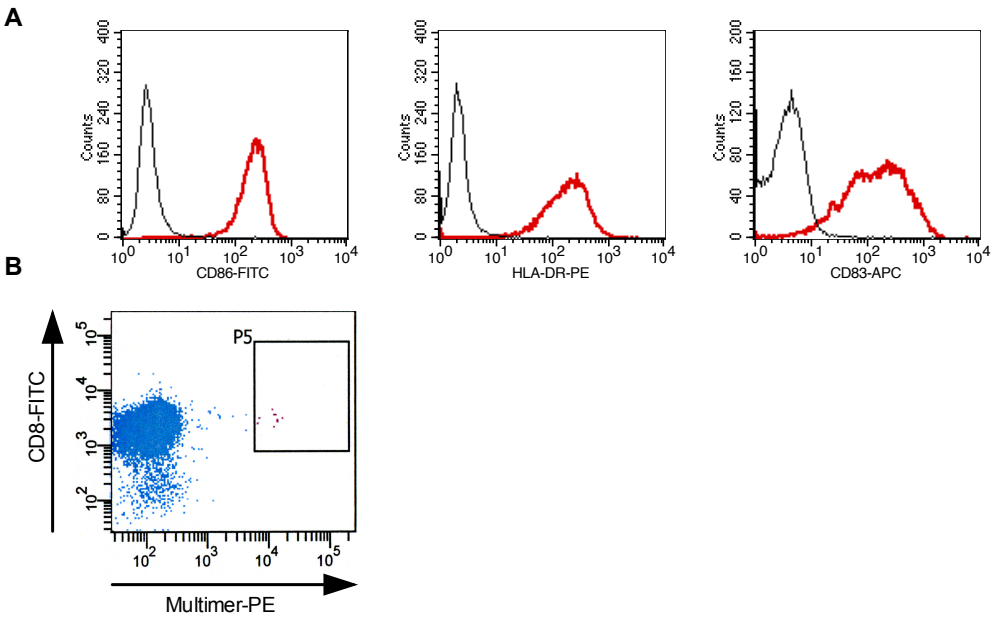

Figure 9: Maturation of dendritic cells and FACS sorting of multimer postive T cells after allogeneic T cell priming. (A) DCs were considered mature when positive for CD86, HLA-DR and CD83. **(B)** Multimer specific T cells in region P5 were isolated via specific multimer assisted FACS sort.

5.4 Generation of ADRB3 specific TCR transgenic T cells

5.4.1 Screening for ADRB3^{295} T cell specificity after single cell dilution

Cultured clones were first tested in IFNγ Screening ELISpot assays. Peptide loaded T2 cells with either unspecific influenza (T2 -) or specific ADRB3^{295} (T2 +) peptide were used to show peptide specificity. A673 (HLA-A*02:01$^+$) and SK-N-MC (HLA-A*02:01$^-$) were used for HLA restriction and ES specificity, respectively. In total 7 clones were tested (Fig. 10). Only the T cell clones 1F4, 1H12 and 4B4 only showed peptide specificity and HLA restriction.

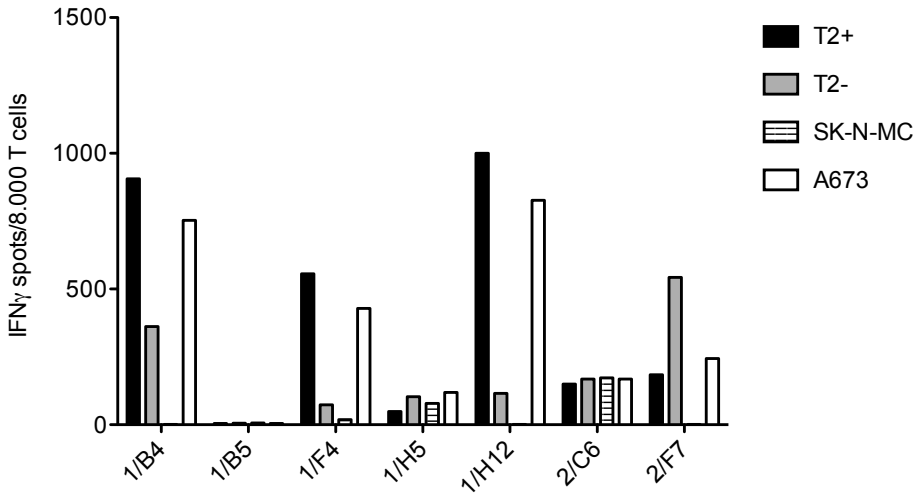

Figure 10: IFNγ Screening ELISpot assays to identify peptide specific and HLA-A*02:01 restricted T cell clones. Screeing for peptide specificity and HLA-A*02:01 restriction eliminated the unspecific T cell clones 1B5, 1H5, 2C6, and 2F7. Only the clones specifically recognizing T2 + (black bar) and A673 (white bar) but not T2 - and SK-N-MC (1B4, 1F4, and 1H12) were considered specific.

5.4.2 ES specificity of T cell clone ADRB3-1F4

Regarding the results from the initial IFNγ ELISpot assay three different clones were selected for further analysis. Among them was the T cell clone ADRB3-1F4 which showed a distinct recognition of ADRB3^{295} peptide pulsed T2 cells (Fig. 11 A). Sensitivity limit of the TCR for its peptide was up to a 10 nM peptide concentration in T2 peptide titrations (Fig. 11 B). Also, the HLA-A*02:01 positive ES cell lines A673, EW7, and TC-71 were recognized in IFNγ ELISpots in contrast to SK-N-MC (HLA-A*02:01$^-$). The MCH negative cell line K562 served as an additional NK cell control (Fig. 11 C). Lysis of ES cell lines was shown via grB release. ADRB3-1F4 T cells were titrated onto A673 or SK-N-MC target cells. For A673, specific grB release was shown whereas for SK-N-MC, the grB levels were in the range of the K562 and T cell controls with no target cell (Fig. 11 D). This shows specificity of the ADRB3-1F4 TCR towards HLA-A*02:01$^+$ ES cells. According to these results the corresponding TCR of this T cell clone 1F4 was chosen for the generation of TCR transgenic T cells.

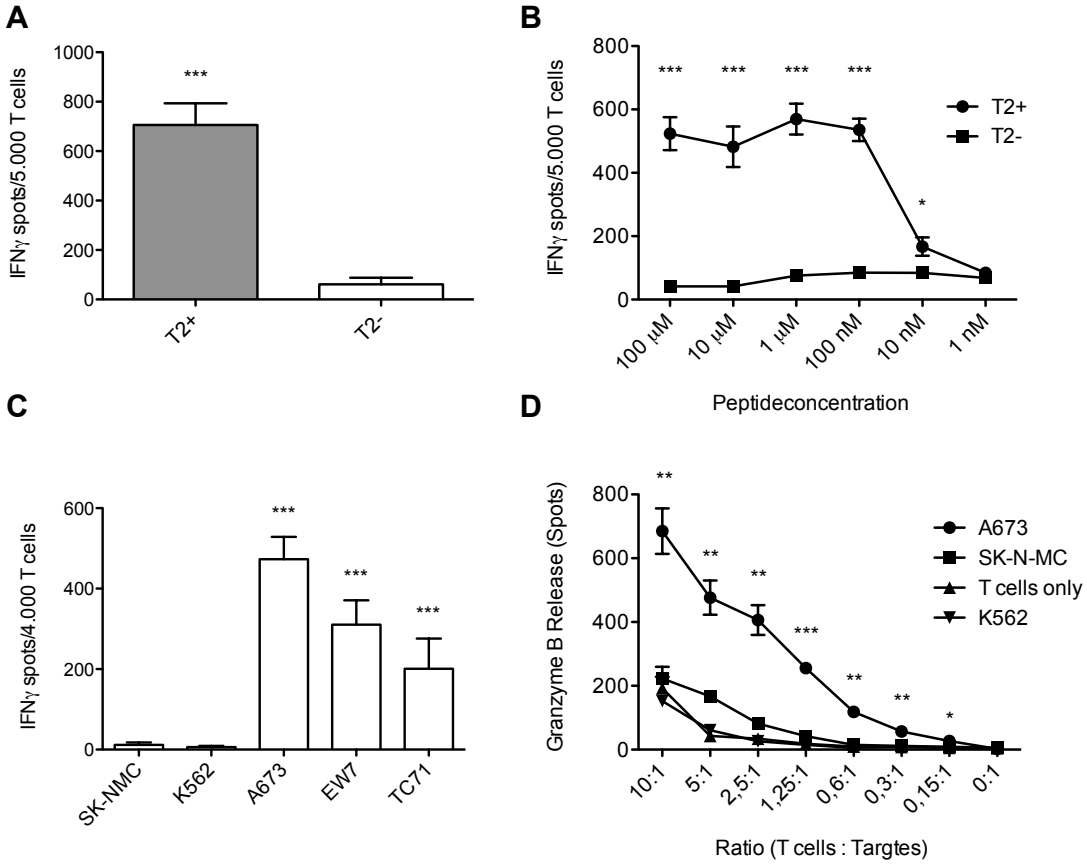

Figure 11: Wild type T cell clone ADRB3-1F4 specifically recognizes and kills HLA-A*02:01^{+}/ADRB3^{295} expressing ES cell lines. (A) ADRB3-1F4 shows peptide specificity against ADRB3^{295} (T2 +) peptide loaded T2 cells. **(B)** Recognition of T2 cells is dose dependent in peptide titration assay. IFNγ release diminishes at a threshold of < 10 nM. **(C)** ADRB3-1F4 T cells specifically recognize HLA-A*02:01^{+}/ADRB3^{+} ES cell lines compared to controls in IFNγ ELISpot assays. **(D)** Dose-dependent killing of HLA-A*02:01^{+}/ADRB3^{+} ES cell lines compared to controls was determined by ELISpot granzyme B release. A673, EW7 and TC-71; HLA-A*02:01^{+} ES, SK-N-MC: HLA-A*02:01^{-} ES, K562: MHC^{-} NK cell control. Error bars represent standard deviation of triplicate experiments. Data are presented as mean and SEM. Asterisks indicate significance levels. p values < 0.05 were considered statistically significant (*p < 0.05; **p < 0.005; ***p < 0.0005).

5.4.3 ADRB3-1F4 TCR PCR identifies Vα2 and Vβ17 chains

Isolated RNA of the ADRB3-1F4 clone was transcribed into cDNA. For the identification of the Vα chain a set of 34 different primers was used. In the agarose gel three PCR products within a range of 350 – 500 bp were identified next to the internal TCR constant chain control (550 bp). These three PCR products were cut out, isolated and sequenced (Fig 12). According to the IMGT/V-QUEST only the PCR product for the Vα2 resulted in a productive TCR sequence (TRAV12-2*02). The Vα12 sequence was an unproductive TCR (TRAV-19*01F). For Vα29 the sequence was unspecific and gave no result.

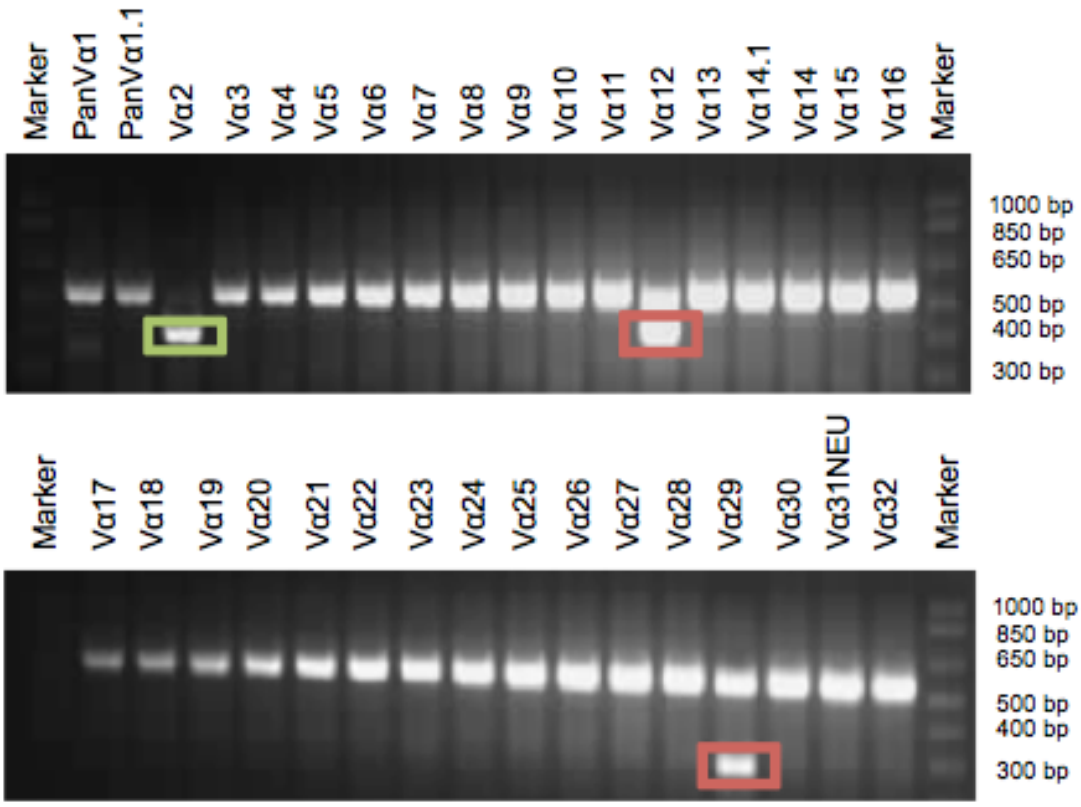

Figure 12: TCR PCR identifies Vα2 expression in ADRB3-1F4 T cells. ADRB3-1F4 only had one productive variable α-chain (TRAV12-2*02 detected by the Vα2 primer) marked by a green box. All other sequenced PCR products were unspecific or showed no open reading-frame (red bordered boxes). Internal constant alpha chain control: 550 pb; Expected PCR product sizes for Vα chains: 350 – 500 bp.

For the identification of the corresponding Vβ chain the IOTest® Beta Mark Kit was used to show expression of the Vβ chain via FACS analysis (see Table 14). This kit covers 70% of the human Vβ repertoire. The positivity of the T cells for FITC and PE in Tube B indicates the expression of a Vβ17 (TRBV19) TCR (Fig. 13 left). Additionally, this FACS analysis confirmed T cell clonality. A PCR for Vβ17 further confirmed the FACS results (Fig 13 right). Sequencing results and *in silico* IMGT/V-QUEST results for the sequenced PCR product identified the Vβ-chain TRBV19-01.

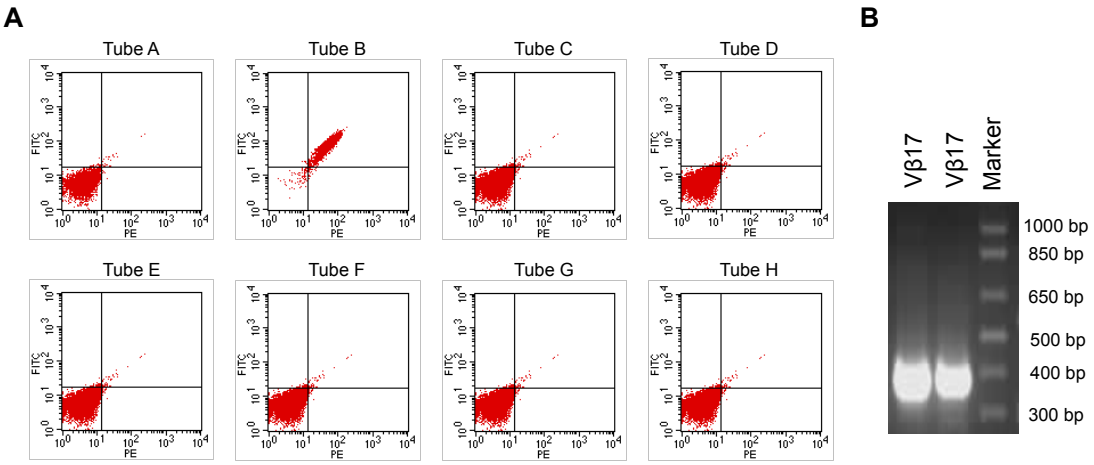

Figure 13: ADRB3-1F4 T cells express the Vβ17 chain and are clonal. (A) The IOTest® Beta Mark Kit showed the expression of the Vβ17 on the cell surface of the ADRB3-1F4 T cells detected by FITC and PE double positivity in Tube B. Absence of a second T cell populations further confirmed T cell clonality. **(B)** Expression of Vβ17 was further confirmed via PCR. PCR product was extracted from the gel and sequenced.

As these primers only cover the Vα- and Vβ-chain to some extent, new primers were chosen according to these results covering the whole sequences of the TRAV12-2*02 and TRBV19-01 TCR. The sequencing results of these PCRs were then used for the construction of the transgenic TCR (Tab. 25 + 26).

5.4.4 Generation of ADRB3-1F4 TCR transgenic T cells

The transgenic TCR was constructed as described in 4.27 and cloned into the pMP71 vector system. GalV 293T virus producing packaging cells were transfected with the plasmid DNA containing the transgenic ADRB3-1F4 TCR. After transduction the efficiency was controlled after additional 72 h. TCR transgenic T cells were identified by their capability to specifically bind its specific multimer. An unspecific multimer served as a control. Isolation of TCR transgenic T cells was carried out via magnetic labeling (Fig. 14). Multimer-PE stained T cells were labeled with anti-PE magnetic beads and purified using a magnetic column. These purified TCR transgenic T cells were then further cultured.

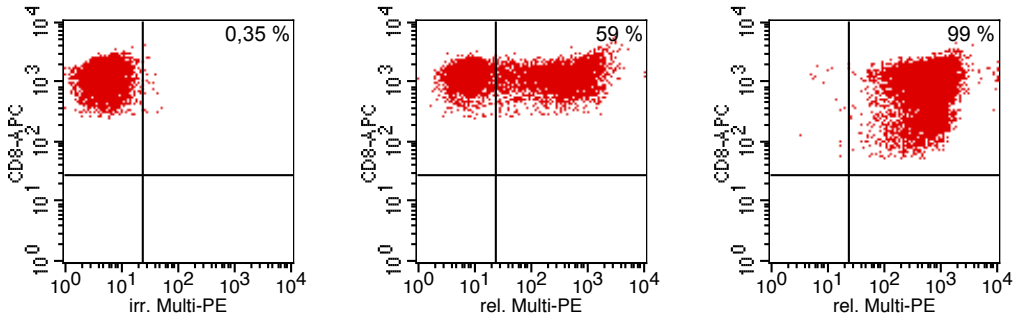

Figure 14: Transduction and isolation efficiency of ADRB3-1F4 TCR transgenic T cells. Flow cytometry revealed a transduction rate of 59% (middle) for ADRB3^{295} specific TCR transgenic T cells. An irrelevant multimer served as control (left). Purification using HLA-A*02:01-ADRB3^{295}-multimer staining revealed a 99% positive ADRB3-1F4 TCR transgenic T cell population after magnetic bead separation (right).

5.4.5 Functionality of ADRB3-1F4 TCR transgenic T cells

Donor PBMCs transduced with the transgenic TCR were tested for their peptide specificity towards ADRB3^{295} and influenza matrix protein peptide loaded T2 cells, as well as their ability to specifically recognize and kill HLA-A*02:01^{+} ES cell lines. The ADRB3-1F4 TCR transgenic T cells showed comparable results to the wild type TCR regarding recognition of pulsed T2 cells pulsed with the specific peptide (Fig. 15 A). Sensitivity of the transgenic TCR towards the ADRB3^{295} peptide was observed up to a peptide concentration of 1 nM (Fig. 15 B).

Regarding the recognition of ES cell lines the transgenic T cells showed a specific recognition of HLA-A*02:01^{+} ES cells lines A673, TC-71, and EW7 in contrast to the SK-N-MC (HLA-A*02:01^{-}) and K562 (MHC I^{-}) controls (Fig. 15 C). To show killing efficiency of the TCR transgenic T cells the xCELLigence assay was used. After addition of the transgenic T cells to the ES target cells only the A673 cells showed distinct reduction in adherence. In contrast, the controls were unaffected in their growth and showed no detachment over time (Fig. 15 D). This assay not only demonstrated in real-time the specificity of the transgenic TCR towards HLA-A*02:01^{+} ES cells but also showed the rapidity in which the reaction takes place.

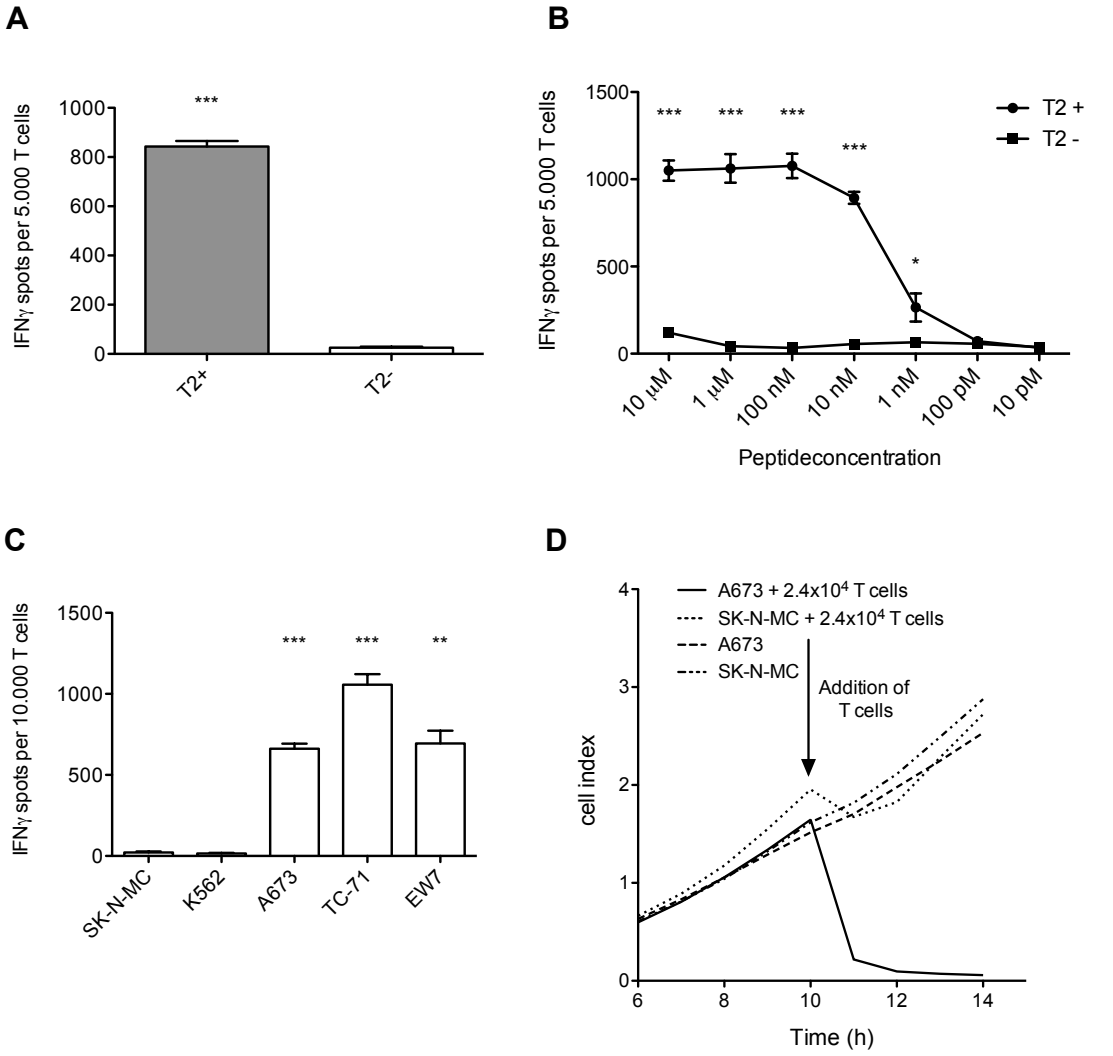

Figure 15: Functional evaluation of ADRB3-1F4 TCR transgenic T cells. (A) ADRB3-1F4 TCR transgenic T cells specifically recognize ADRB3^{295} (T2 +) pulsed T2 cells in contrast to the unspecific influenza (T2 -) control. **(B)** ADRB3-1F4 TCR transgenic T cells recognize ADRB3^{295} peptide pulsed T2 cells in an IFNγ ELISpot assay in a dose dependent manner. IFNγ release diminishes at a threshold of < 1 nM. **(C)** HLA-A*02:01^{+}/ADRB3^{+} ES cell lines are specifically recognized in contrast to its controls. **(D)** Killing/detachment of A673 ES cell line is shown in real time in xCELLigence assay. The control cell line SK-N-MC is not affected in its growth by the presence of the TCR transgenic T cells. Adherence/growth of target cells is shown via the cell index. An arrow indicates time of ADRB3-1F4 T cell addition. A673, EW7 and TC-71: HLA-A*02:01^{+} ES; SK-N-MC: HLA-A*02:01^{-} ES; E/T ratio for ELISpot assay: (A and B) 1:4, (C) 1:2. Error bars represent standard deviation of triplicate experiments. Asterisks indicate significance levels. *p < 0.05; **p < 0.005; ***p < 0.0005.

5.4.6 Impeded cell growth and increased apoptosis after TCR transduction

Although we were able to generate ADRB3-1F4 TCR transgenic T cells, the transduction of donor PBMCs often resulted in low cell count after isolation and further cultivation. Therefore we chose to simultaneously transduce 3 different donor PBMCs with different HLAs. As a control we additionally transduced donor T cells with a different, already established transgenic TCR directed

against CHM1. When we compared the cell counts of the ADRB3-1F4 transgenic T cells with the CHM1-4B4 TCR transgenic T cells, we observed a reduced cell count after 7 days for ADRB3 T cells in comparison to CHM1 in two of the donor PBMCs. Only donor #3 showed a normal growth rate for ADRB3 (Fig. 16 A).

Annexin-V staining revealed no increased apoptosis levels for CHM1-4B4 transduced T cells. The same results were observed for ADRB3-1F4 transgenic T cells with donor #3 as well as for donor #1. However, for donor #2 we saw highly increased levels of apoptosis already 24 h after transduction for the ADRB3-1F4 TCR. These levels increased even further over the next two days (Fig. 16 B).

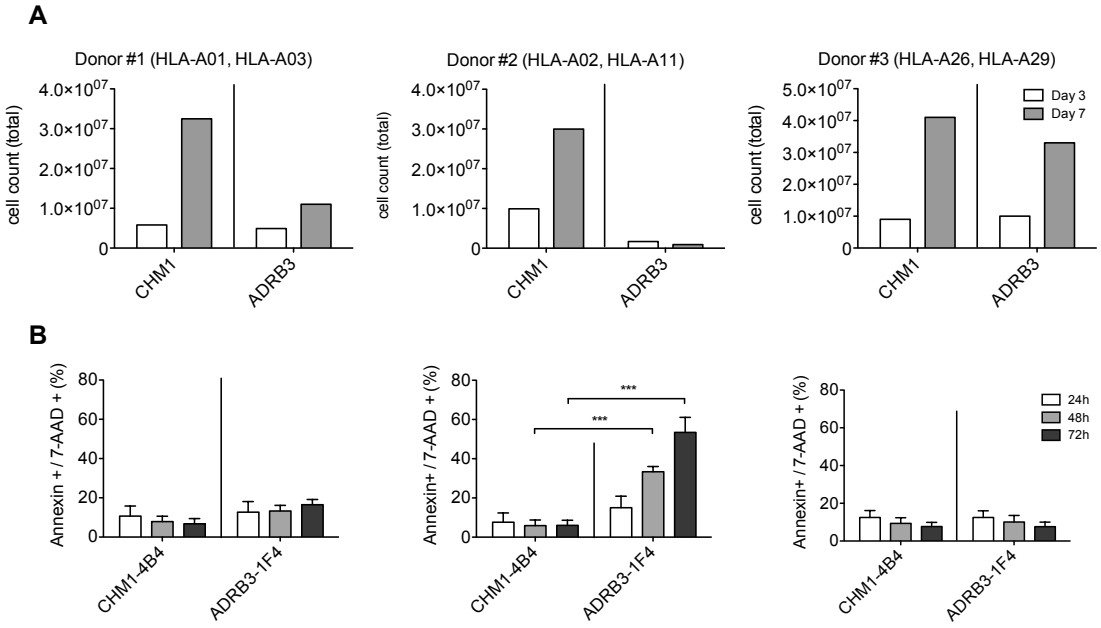

Figure 16: Impeded growth and annexin positivity were measured for ADRB3-1F4 TCR transgenic T cells (A) For donors #1 and #2 ADRB3-1F4 TCR transgenic T cell expansion is hampered compared to CHM1-4B4 TCR transgenic T cells as measured by total cell counts at expansion day 3 and day 7, respectively; **(B)** Flow cytometry only shows increased annexin-v positivity for donor #2 although growth impairment was also seen in donor #1 after ADRB3-1F4 TCR transduction in contrast to CHM1-4B4 TCR transgenic T cells. Error bars represent standard deviation of triplicate experiments. Asterisks indicate significance levels. *p < 0.05; **p < 0.005; ***p < 0.0005.

5.4.7 ADRB3 is not expressed in CD8$^+$ T cells

The group of Dolores Schendel has previously shown that target gene expression in T cells can lead to T cell mediated apoptosis in an autologous setting, a phenomenon termed fratricide (Leisegang et al. 2010). However, when we analyzed CD8$^+$ T cells for their ADRB3 expression via qRT-PCR we did not measure target gene expression (Fig. 17). Therefore we could exclude the

expression of our target gene as the target of fratricide responsible for the impeded cell growth for the HLA-A*02:01^{+} donor #2.

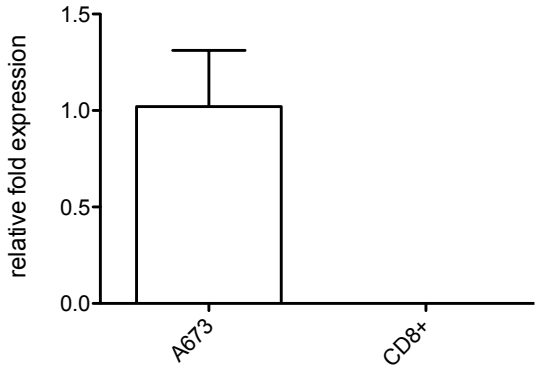

Figure 17: CD8+ T cells do not express ADRB3. ADRB3 expression was assessed in CD8+ T cells relative to A673.

5.4.8 TCR transduced T cells are positive for CD107a

Although we could detect increased apoptosis for ADRB3-1F4 TCR transgenic T cells we further aimed to directly measure T cell activity after the transduction. The Lysosome-associated membrane protein 1 (LAMP1/CD107a) is a transmembrane protein and has shown to be a specific marker for degranulation in active T cells upon target recognition (Betts et al. 2003). We analyzed our transductions for T cell activity via CD107a FACS staining. Again, CHM1-4B4 transduced donor T cells were negative for CD107a. However, in two donors (#1 and #2) PBMCs transduced with ADRB3-1F4 – in which impeded cell growth had been observed before - we also measured increased overall CD107a positivity. Moreover, in donor #1, which showed impeded cell growth but no signs of increased apoptosis, CD107a positivity was measurable (Fig. 18 A).

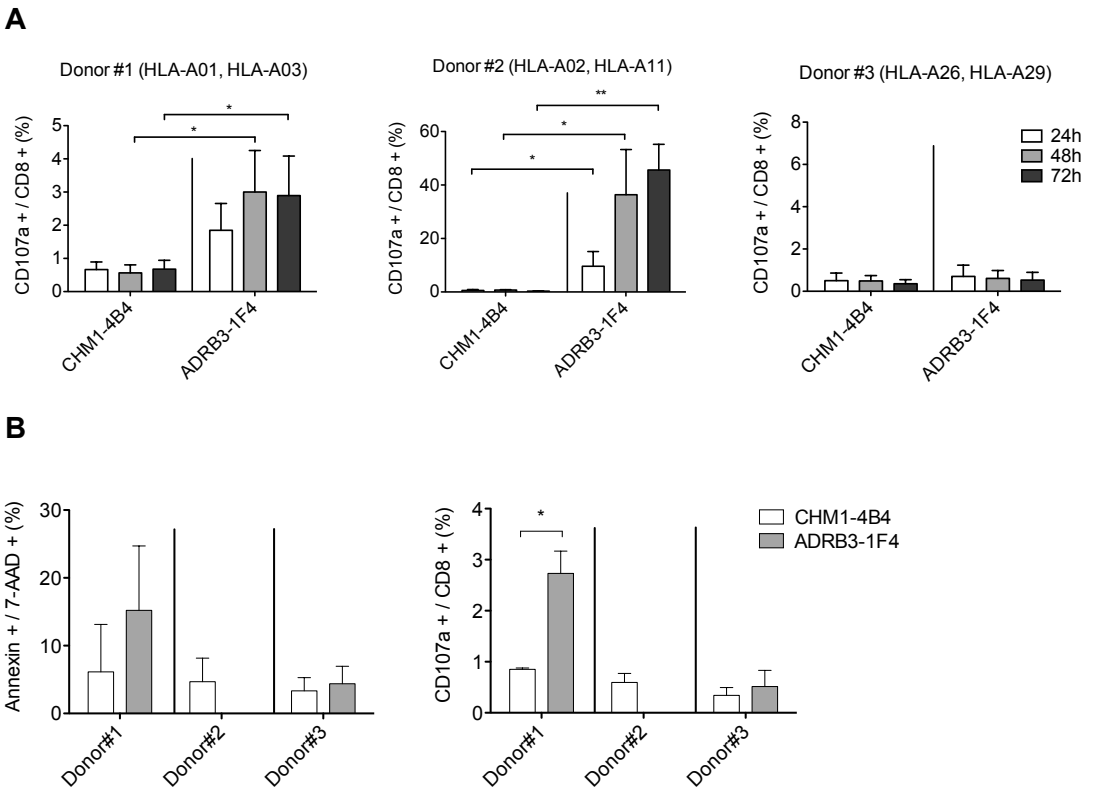

Figure 18: T cells activity was assessed via CD107a staining in FACS after transduction with the transgenic ADRB3-1F4 and CHM1-4B4 TCR. (A) Transduced T cells with the ADRB3-1F4 transgenic TCR show elevated T cell activity via CD107a staining already 24 h after transduction in comparison to CHM1-4B4 transduced T cells. CD107a positivity was only measurable in donors with impeded cell growth after 7 days. **(B)** CD107a T cell activity was still measurable after 7 days in donor #1 and correlate with impeded cell growth. Error bars represent standard deviation of triplicate experiments. Asterisks indicate significance levels. *p < 0.05; **p < 0.005; ***p < 0.0005.

Seven days after transduction again annexin and CD107a positivity was analyzed. In donor #1, increased annexin levels were measured (Fig. 18 B left). Also, CD107a positivity was measurable indicating ongoing T cell activity (Fig. 18 B right). Again, no increase in annexin and CD107a were detected in donor #3. In donor #2 no further measurements were possible as no living T cells for analysis were left after 7 days.

To finally examine whether the ADRB3-1F4 TCR transgenic T cells are active upon donor PBMC recognition we incubated previously generated ADRB3-1F4 TCR transgenic T cells with the three different donor PBMCs. After 2 h of incubation donor PBMCs and TCR transgenic T cells were measured for CD107a positivity. When gating for the multimer positive T cell fraction we observed CD107a positivity for those donor PBMCs in which impeded cell growth had previously been

observed (Fig. 19). Donor #3 for ADRB3 as well as all three samples for CHM1 remained negative.

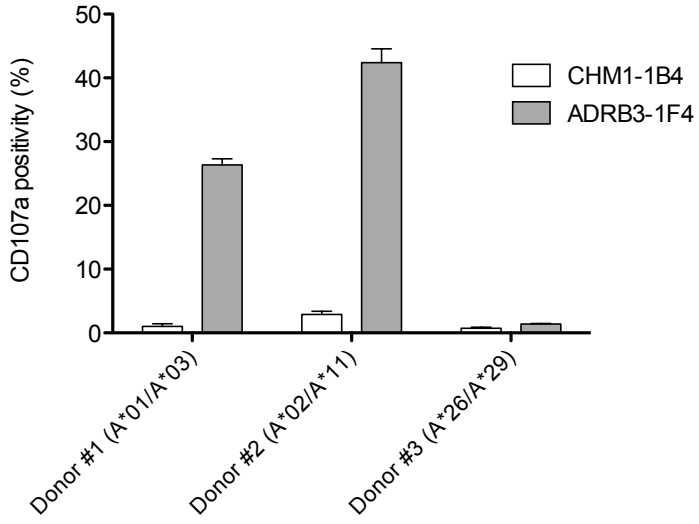

Figure 19: ADRB3-1F4 TCR transgenic T cells are positive for CD107a. After incubation of the ADRB3-1F4 or CHM1-4B4 TCR transgenic T cells with three different donor PBMCs CD107a positivity was only measurable for the ADRB3-1F4 T cells in which impeded cell growth had been previously observed. Live gate was set on $CD8^+$/$multimer^+$ double positive T cells. Error bars represent standard deviation of triplicate experiments.

This shows that the transgenic TCR is active upon recognition of certain donor PBMCs. Furthermore, CD107a positivity correlates with impeded cell growth.

5.4.9 Alanine/serine scan analysis confirms cross reactivity of the ADRB3-1F4 TCR

As TCRs are capable of recognizing more than one pMHC combination we determined the possible peptide cross reactivity potential of both transgenic TCRs, ADRB3-1F4 and CHM1-4B4, respectively. Alanine/serine or alanine/threonine substituted peptides at each position were ordered and loaded onto T2 cells. For both experiments, we used peptide concentrations close to the minimum detection limit to exclude unspecific reactivity due to overloaded T2 cells. For both TCRs results were similar, and both showed various positions at which amino acids could be exchanged (Fig. 20 A + B). Although this result indicates a major peptide cross-reactive potential, the amount of possible peptides with these motives differ significantly in humans. An X in the motive indicates peptides that were not essential for target recognition. For the ADRB3 motive X-L-X-X-X-X-F-X-[LA] 5068 different peptides with this motive were found. For CHM1 however,

the corresponding motive X-X-X-X-X-[ST]-W-W-[VT] resulted in only 38 hits (Fig. 20 C). When we further analyzed the *in silico* binding strength of these predicted peptides for HLA-A*01, HLA-A*02:01, and HLA-A*03 we observed an increased binding strength for the ADRB3 peptides for all three HLAs in comparison for the CHM1 peptides (Fig. 20 D).

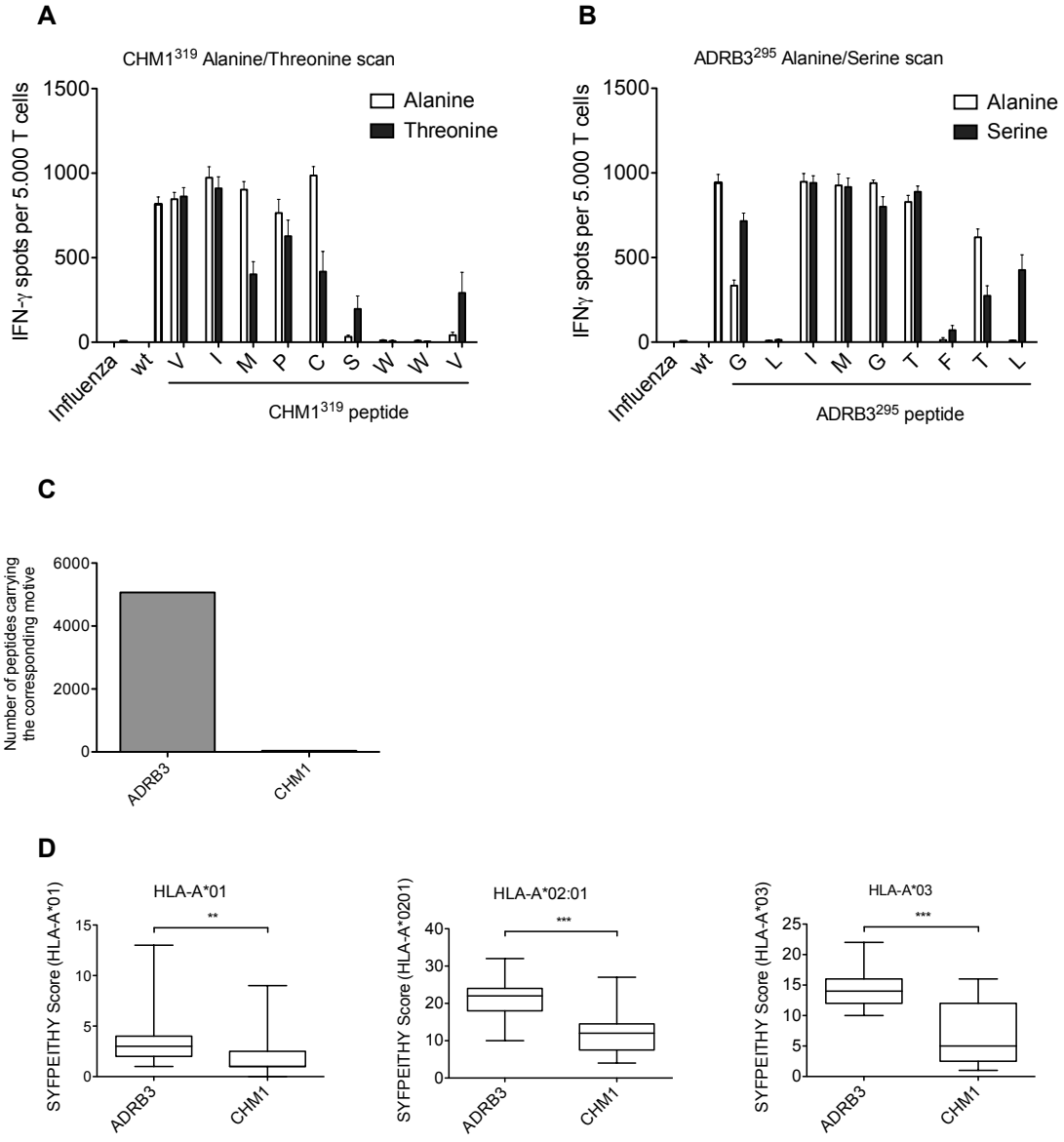

Figure 20 Amino-acid exchange scans yield only limited power to predict cross-reactivity of CD8$^+$ TCR transgenic T cells in contrast to *in silico* HLA-A*02:01 binding prediction. (A + B) ADRB3^{295}-TCR transgenic T cells (left) as well as CHM1^{319}-TCR transgenic T cells (right) reveal unspecific recognition upon selective amino-acid exchange of respective target antigens to **(A**) alanine/serine and **(B)** alanine/threonine in IFNγ ELISpot assays. **(C)** The number of peptides carrying the ADRB3 specific core motive is much higher in comparison to peptides carrying the CHM1 specific core motive. **(D)** Peptides with similar ADRB3^{295} motive patterns (n=780) show higher binding scores for HLA-A*02:01 in comparison to the peptides with similar CHM1^{316} motive (n=33) (middle). Also, binding affinities of peptides similar to ADRB3 (n=180) show higher binding affinities towards HLA-A*01 (left) and HLA-A*03 (right) in comparison to CHM1 (n=33). Error bars represent standard deviation of triplicate experiments if not indicated otherwise. Asterisks indicate significance levels. *p < 0.05; **p < 0.005; ***p < 0.0005.

5.4.10 HLA-A2 blocking of ES cells shows cross reactivity of ADRB3-1F4 TCR transgenic T cells in contrast to LCL scan

We further assessed the MHC I cross-reactive potential of the ADRB3-1F4 TCR using ADRB3^{295} pulsed and unpulsed LCL cell lines (Fig. 21 A). Interestingly this assay did not confirm the cross-reactive potential as mainly LCLs of the HLA-A2 superfamily were recognized. Further pulsing of the target cells only increased T cell reactivity against two LCL cell lines also expressing the HLA-A2 superfamily showing unspecific ADRB3^{295} binding. In a second approach we were blocking the accessibility of HLA-A*02 molecules on the ES cell lines (Fig. 21 B). Here, only minor reduction in reactivity of the T cells against the target cell lines could be observed. This further indicates that apart from HLA-A*02:01, other HLA types are also being recognized on the ES cell surface by the transgenic TCR.

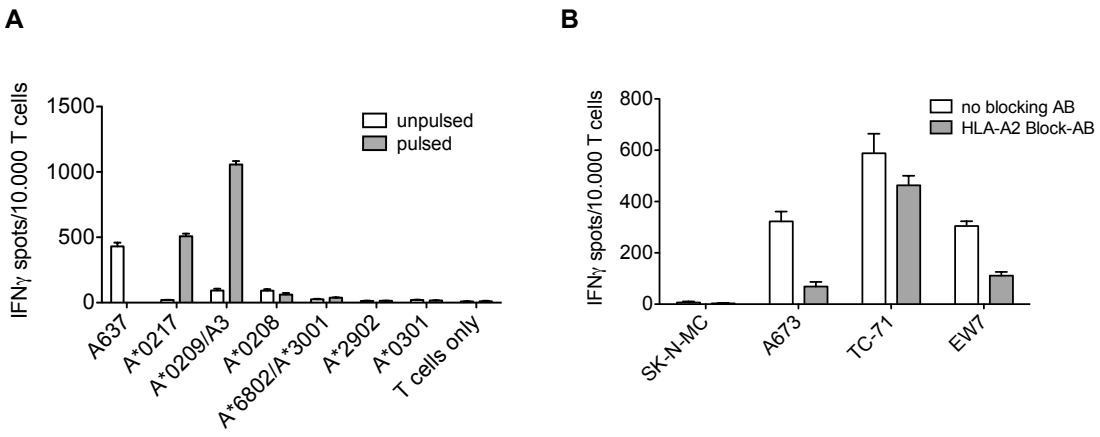

Figure 21: Various LCL cell lines and HLA-A*02 blocking of ES target cell lines to distinguish T cell cross-reactivity. (A) Recognition of LCLs was limited to two cell lines expressing the HLA-A2 superfamily. Further pulsing the cells with specific ADRB3^{295} peptide showed unspecific binding/T cell reactivity in two cases. ES cell line A673 served as a positive control. **(B)** Blocking of the HLA-A*02 molecules on ES cell lines shows reduced but still detecable IFNγ release in ELISpot assays. SK-N-MC: HLA-A01:01, 25:01; A673: HLA-A01:01, 02:01; TC-71: HLA-A*02:01, 68:01; EW7: HLA-A*02:01, 03:01. E/T ratio for ELISpot assay: 1:2. Error bars represent standard deviation of triplicate experiments.

5.4.11 CD107a can be used to predict viability of TCR transduced T cells

As shown before, CD107a positivity after transduction of the ADRB3-1F4 TCR is associated with impeded expansion rates. To predict future transduction outcome we tested possible donor PBMCs with ADRB3-1F4 TCR transgenic T cells and stained for CD107a positivity. Out of six different PBMCs, ADRB3-1F4 only showed for one donor no CD107a positivity. For CHM1-4B4 however no CD107a positivity was detected (Fig. 22). This shows that we have no limitations

regarding possible donors for the CHM1 transgenic TCR whereas for ADRB3 only one donor would have been suitable.

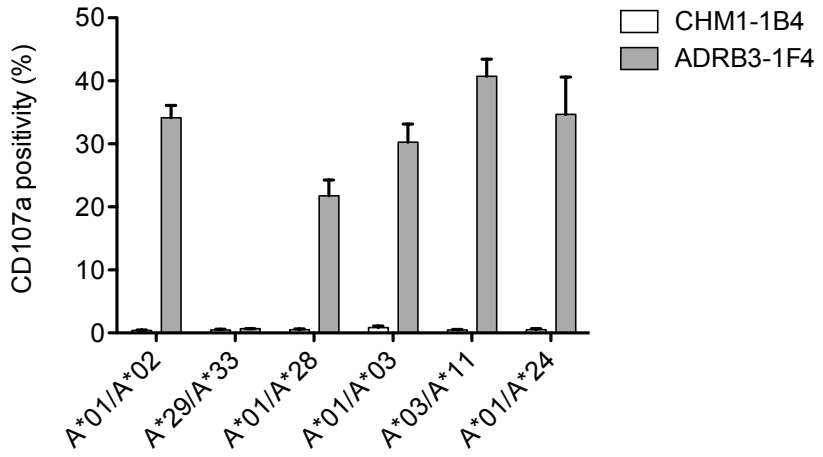

Figure 22: TCR transgenic T cells are negative for CD107a when incubated with a possible donor. ADRB3-1F4 TCR transgenic T cells are only negative for CD107a when incubated with the HLA-A*29/HLA-A*33 positive donor whereas for CHM1-1B4 no T cell reactivity via CD107a upon incubation was measurable. Error bars represent standard deviation of triplicate experiments.

5.5 Generation of PAPPA specific TCR transgenic T cells

5.5.1 ES specificity of PAPPA-2G6 T cells

In IFNγ ELISpot the PAPPA-2G6 T cell clone showed specificity towards $PAPPA^{1434}$ (T2 +) peptide pulsed T2 cells in contrast to the influenza (T2 -) negative control (Fig. 23 A). This peptide specificity is concentration dependent as shown in T2 peptide titration assay up to 1 nM (Fig. 23 B). Further, reactivity towards HLA-A*02:01^{+} ES cell lines A673, TC-71, and EW7 was observed whereas the ES HLA-A*02:01^{-} cell line SK-N-MC was not being recognized (Fig. 23 C). Specific lysis of A673 was shown for PAPPA-2G6 T cells in xCELLigence assay. SK-N-MC cells served as a negative control and were not affected by the addition of the T cells whereas A673 detached upon addition of PAPPA-2G6 T cells (Fig. 23 D).

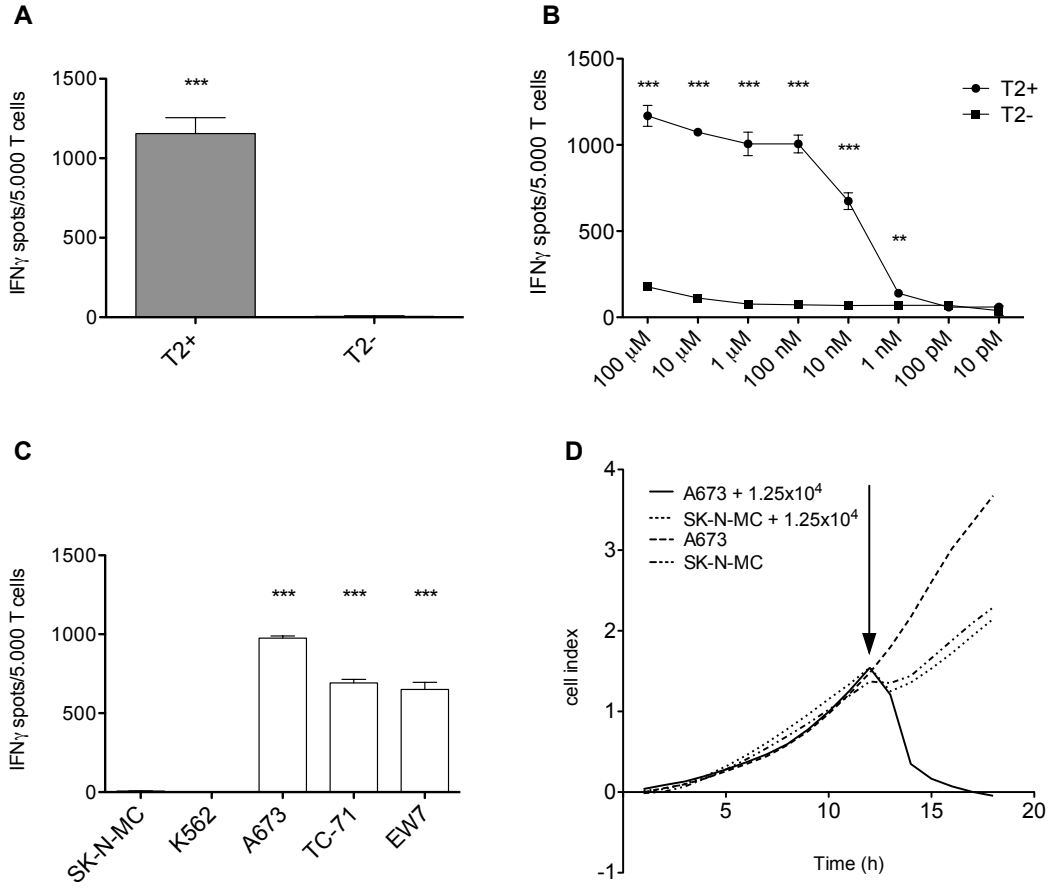

Figure 23: Wild type T cell clone PAPPA-2G6 specifically recognizes and kills HLA-A*02:01$^+$/PAPPA$^+$ ES cell lines. (A) PAPPA-2G6 shows peptide specificity against peptide loaded T2 cells. **(B)** Reactivity is dose dependent in IFNγ ELISpot T2 titration assays. IFNγ release diminishes at a threshold of < 1 nM. **(C)** HLA-A*02:01$^+$/PAPPA$^+$ ES cell lines are recognized specifically in contrast to the controls in IFNγ ELISpot assays. **(D)** Killing/detachment of A673 ES cell line is shown in real time in xCELLigence assay. The control cell line SK-N-MC is not affected in its growth by the presence of the TCR transgenic T cells. An arrow indicates addition time point of PAPPA-2G6 T cells. Data are presented as mean and SEM. E/T ratio for ELISpot assay: 1:4. A673, EW7 and TC-71: HLA-A*02:01$^+$ ES; SK-N-MC: HLA-A*02:01$^-$ ES; K562: MHC$^-$ NK cell control. Error bars represent standard deviation of triplicate experiments. Asterisks indicate significance levels. p values < 0.05 were considered statistically significant (*p < 0.05; **p < 0.005; ***p < 0.0005).

5.5.2 Identification of the PAPPA-2G6 TCR sequence

For the identification of the Vβ-chain the IOTest® Beta Mark Kit was used to identify the expressed Vβ TCR. A single FITC positivity in Tube H indicated the expression of a Vβ7.2 TCR (Fig. 24 A). FACS results were further confirmed via PCR (Fig. 24 B). Sequencing results and IMGT/V-Quest analysis identified this partial sequence as the TRBV4-2*01F TCR.

For the Vα-chain three different PCR products were isolated and sequenced (Fig. 24 C). The identified DNA sequences and IMGT/V-Quest analysis for the Vα29 sequence were inconclusive.

The Vα8 and Vα15 sequences were identical and *in silico* analysis predicted the TRVA5*01F as the identified TCR sequence.

New specific primers directed against both identified variable chains were ordered. For both, PCR products of the expected size were extracted from the gel and sequencing results were further used for the construction of the transgenic TCR (Fig. 24 D). For the construction of the transgenic TCR the same modifications were made as previously for the ADRB3-1F4 transgenic TCR (see 4.27 and Tab. 27 + 28).

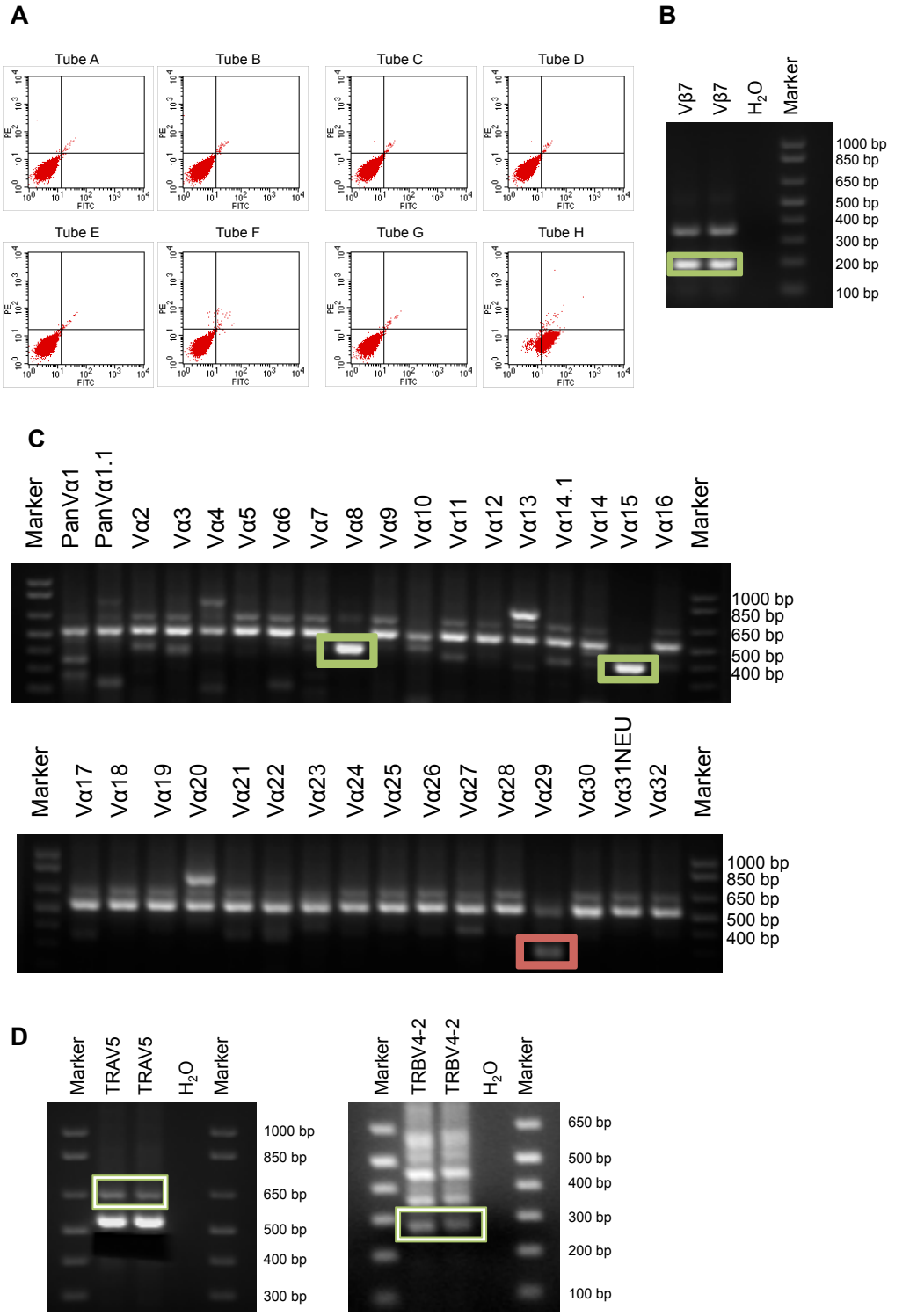

Figure 24: Identification of the PAPPA-2G6 TCR sequence. (A) FITC positivity in tube H of the IOTest® Beta Mark Kit indicates the expression of the Vβ7 TCR. **(B)** Vβ7 expression was confirmed via PCR (green box). **(C)** Different primers were used to amplify the expressed Vα chain in the PAPPA 2G6 T cells. TCR PCR products (green/red boxes) were sequenced and analysed. **(D)** Full TCR PCR with specific primers for TRAV5 and TRBV4-4. PCR products (green boxes) were sequenced and analysed.

5.5.3 ES reactivity of PAPPA-2G6 TCR transgenic T cells

The MP71 construct bearing the transgenic PAPPA-2G6 TCR was amplified using MAX Efficiency® Stbl2™ Competent Cells. After retroviral transduction multimer positive T cells were isolated via magnetic beads and further cultured (Fig. 25 A). In IFNγ ELISpot specificity of the TCR transgenic T cells towards T2 cells pulsed with the $PAPPA^{1434}$ peptide was maintained in contrast to the influenza control peptide (Fig. 25 B). Also, in T2 peptide titrations the sensitivity of the TCR towards the peptide pulsed T2 cells remained comparable to the wild type TCR (Fig. 25 C). Next to peptide reactivity also HLA-A*02:01^{+} ES cell lines A673, TC-71, and EW7 are still being recognized in contrast to the HLA-A*02:01^{-} ES cell lines SK-N-MC and SB-KMS-KS1 (Fig. 25 D). Furthermore, killing assay was repeated in the xCELLigence. Reactivity of the transgenic T cells directed against the HLA-A*02:01^{+} ES cells A673 in contrast to the SK-N-MC control was confirmed (Fig. 25 E).

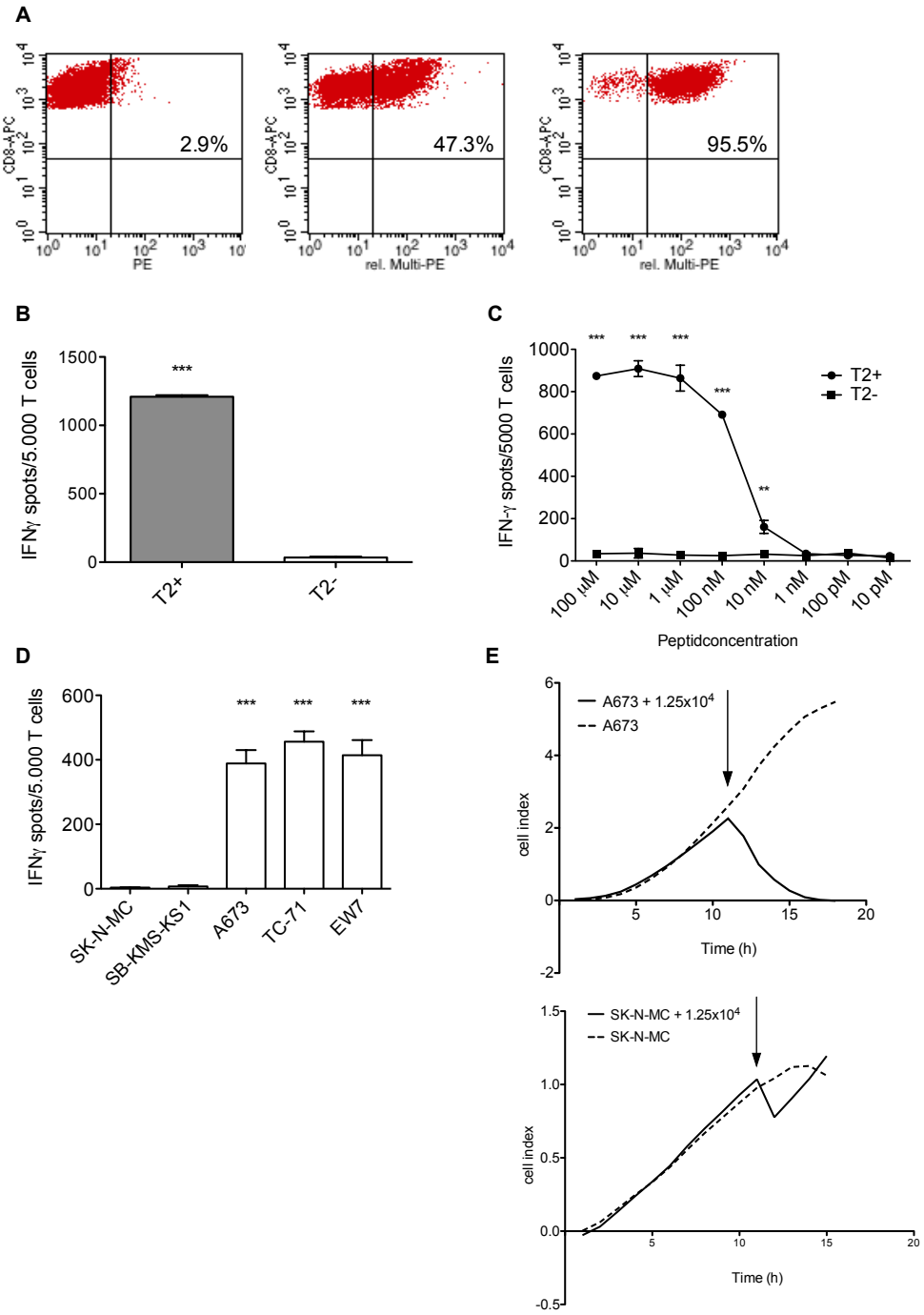

Figure 25: Generation and ES specificity of PAPPA-2G6 TCR transgenic T cells. (A) Transduction efficiency for PAPPA-2G6 TCR transgenic T cells of 47.3 % was determined via FACS multimer staining (middle). Multimer-PE stained transgenic T cells were isolated via magnetic beads (right) **(B)** PAPPA-2G6 transgenic T cells show peptide specificity against peptide loaded T2 cells. **(C)** Reactivity is dose dependent in IFNγ ELISpot T2 titration assays. IFNγ release diminishes at a threshold of < 10 nM. **(D)** HLA-A*02:01^{+}/PAPPA^{+} ES cell lines are recognized specifically compared to the controls in IFNγ ELISpot assays. **(E)** Killing/detachment of A673 ES cell line is shown in real time in xCELLigence assay (top). The control cell line SK-N-MC is not affected in its growth by the presence of the TCR transgenic T cells (bottom). An arrow indicates addition time point of PAPPA-2G6 T cells. Data are presented as mean and SEM. E/T ratio for ELISpot assay: 1:4. A673, EW7 and TC-71: HLA-A*02:01^{+} ES; SK-N-MC and SB-KMS-KS1: HLA-A*02:01^{-} ES; K562: MHC^{-} NK cell control. Error bars represent standard deviation of triplicate experiments. Asterisks indicate significance levels. p values < 0.05 were considered statistically significant (*p < 0.05; **p < 0.005; ***p < 0.0005).

5.5.4 Validation of PAPPA 2G6 cross reactivity potential

To determine cross reactivity of the transgenic TCR an IFNγ ELISpot assay with unpulsed and PAPPA^{1434} peptide pulsed LCL cells lines was performed. Recognition of target cell lines was not completely limited to the HLA-A2 superfamily. Also pulsing these cells with PAPPA^{1434} specific peptide increased T cell reactivity in one case (Fig. 26 A).

As for the TCRs directed against ADRB3 and CHM1, we performed an alanine/serine scan for the PAPPA^{1434} peptide to predict possible cross-reactive peptide targets (Fig. 26 B). Pulsing T2 cells with alanine/serine substituted amino acids peptides resulted in IFNγ ELISpot assay in the motive X-X-[LS]-[AP]-M-[NS]-X-X-[VS]. According to the ExPASy ScanProsite tool 71 peptide sequences including the PAPPA^{1434} were found carrying this motive. Among these candidates, 7 peptides had an affinity score for HLA-A*02:01 of 20 or greater in SYFPEITHY *in silico* binding prediction (Tab. 22). These 7 peptides were ordered for further evaluation of PAPPA-2G6 TCR peptide cross reactivity.

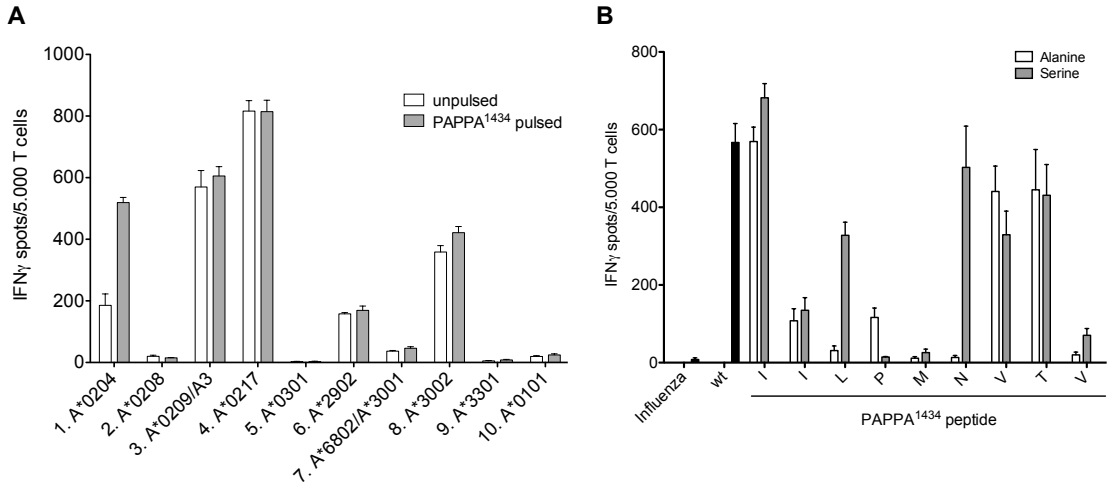

Figure 26: Various LCL cell lines and alanin/serin scan to validate MHC cross reactivity and pMHC specificity. (A) PAPPA-2G6 TCR transgenic T cells recognize LCLs expressing different HLAs next to the HLA*A02 superfamily. Binding of PAPPA^{1434} to A*0204 further increased T cell reactivity. **(B)** The alanin/serin scan identifies essentials peptides for the pMHC recognition of the PAPPA-2G6 TCR. Error bars represent standard deviation of triplicate experiments. E/T ratio for ELISpot assay: 1:4.

Table 24: List of potential cross reactive peptides recognized by PAPPA-2G6 TCR transgenic T cells sorted by SYFPEITHY binding affinity score. Identical peptides with PAPPA^{1434} are shown in capital letters.

Gene name	Description	Sequence	SYFPEITHY Score
STAT4	Signal transducer and activator of transcription 4	dlLPMspsV	26
MT-ND2	NADH-ubiquinone oxidoreductase chain 2	tlLPMsnnV	25
HECW1/2	E3 ubiquitin-protein ligase HECW1/2	qlsPMsafV	22
CREBBP	CREB-binding protein	aasPMNhsV	21
C16orf62	UPF0505 protein C16orf62	atLaMsekV	20
OAT	Ornithine aminotransferase, mitochondrial	kvLPMNtgV	20
EPSIN2	Epsin-2	laLaMsreV	20

5.5.5 Evaluation of putative PAPPA-2G6 peptide cross reactivity

The 7 peptides with an *in silico* binding affinity of ≥ 20 were ordered and loaded onto T2 cells in an IFNγ ELISpot assay. Among these 7 peptides only OAT was recognized by the transgenic TCR (Fig. 27 A). When we loaded OAT and PAPPA^{1434} on a T2 titration assay with decreasing concentrations we observed a 100 fold higher sensitivity of PAPPA-2G6 TCR transgenic T cells against the PAPPA^{1434} specific peptide in contrast to OAT (Fig. 27 B).

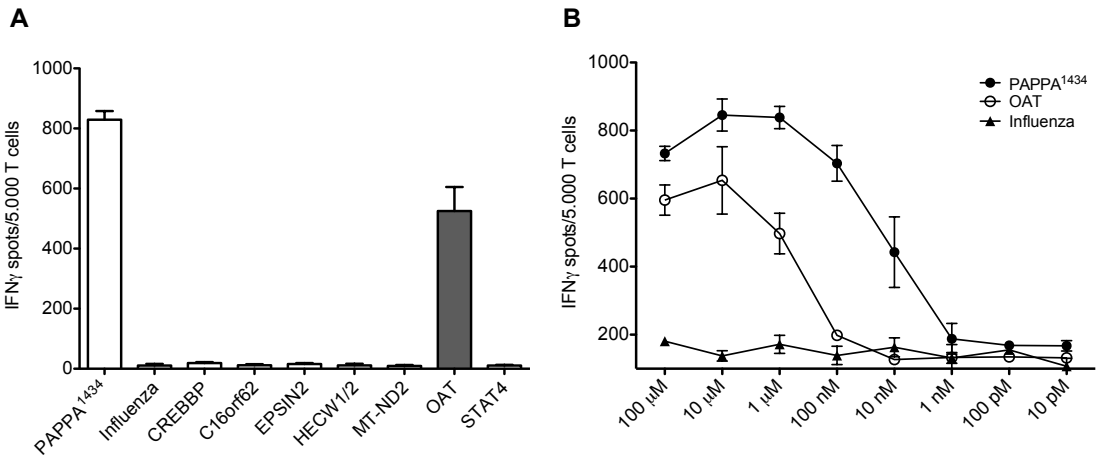

Figure 27: PAPPA-2G6 TCR transgenic T cells recognize T2 cells pulsed with an OAT derived peptide. (A) Different peptides identified via the alanine/serine scan have been loaded onto T2 cells. Next to the PAPPA^{1434} specific peptide only one more peptide is being recognized indicating a potential cross reactivity against OAT. **(B)** Peptide sensitivity for OAT and PAPPA^{1434} was assessed in T2 titration assays in IFNγ ELISpot. OAT recognition was measurable up to 100 nM. For PAPPA^{1434} the IFNγ signal was elevated up to 1 nM. Error bars represent standard deviation of triplicate experiments. E/T ratio for ELISpot assay: 1:4.

We further assessed the OAT and PAPPA expression in ES cell lines, the osteosarcoma cell line SaOS and HLA-A*02:01^{+} T cells. In contrast to the ES cell lines the SaOS cell line and CD8^{+} T cells are negative for PAPPA but show OAT expression (Fig. 28 A). When we assessed target cell reactivity in IFNγ ELISpot assay we observed reactivity of the PAPPA-2G6 T cells towards SaOS as well as against HLA-A*02:01^{+} PBMCs. HLA-A*02:01^{-} PBMCs are not being recognized (Fig. 28 B + C). Although the ELISpot results already indicated T cell reactivity towards HLA-A*02:01^{+} T cells we further assessed a transduction of HLA-A*02:01$^{+/-}$ PBMCs. Here, CD107a positivity after transduction of the HLA-A*02:01^{+} PBMCs could be observed, in contrast to the negative controls (Fig. 28 D). Further, we observed an impeded cell growth, which corresponds with the T cell activity measured via CD107a (Fig. 28 E).

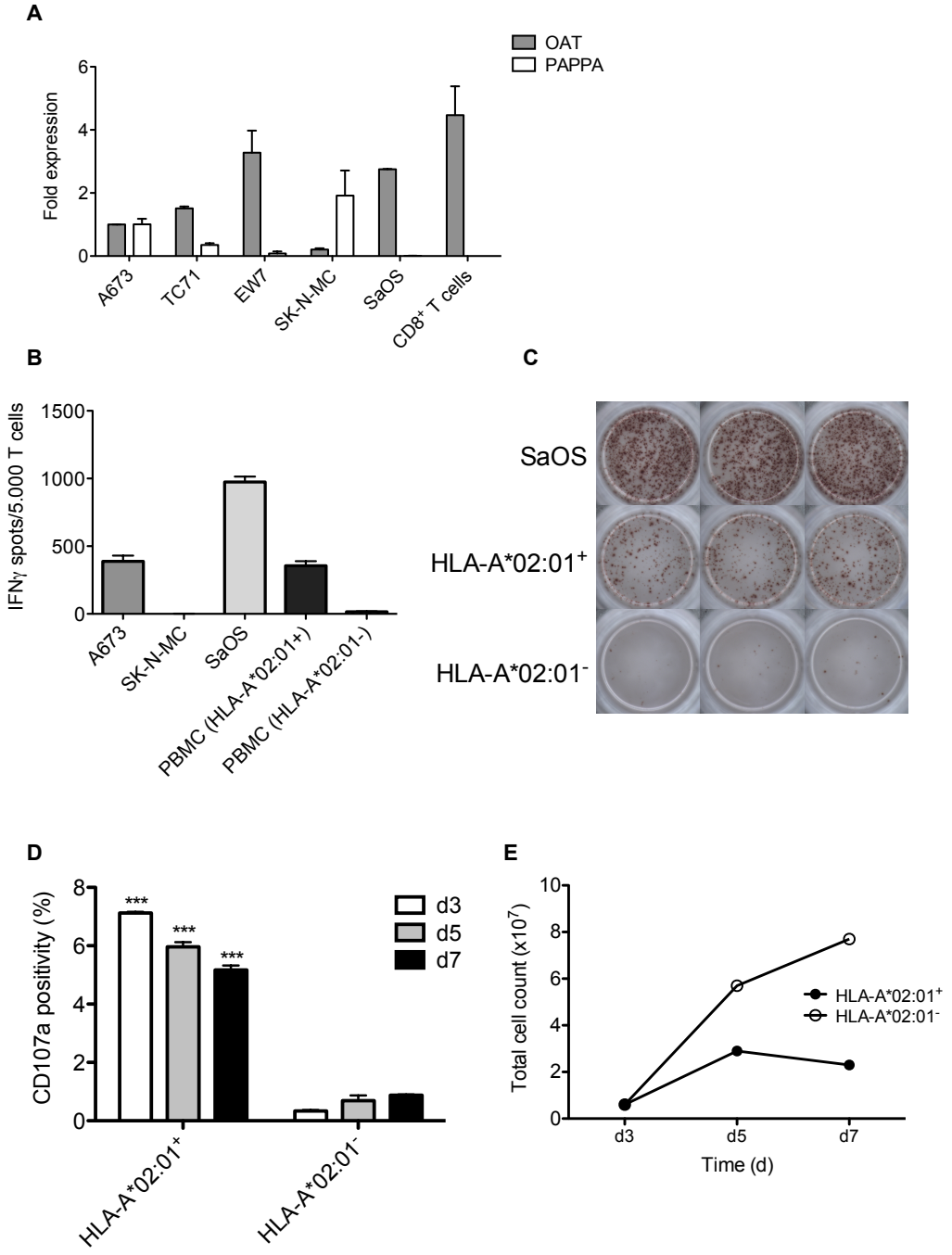

Figure 28: Putative recognition of OAT by PAPPA-2G6 TCR transgenic T cells. (A) OAT (grey bars) is expressed in all tested cell lines. The osteosarcoma cell line SaOS and $CD8^+$ T cells are negative for PAPPA (white bars) expression. Expression of OAT and PAPPA was evaluated in relation to the ES cell line A673. **(B+C)** PAPPA-2G6 T cells show IFNγ release upon recognition of A673, SaOS, and HLA-A*02:01$^+$ PBMCs in IFNγ ELISpot assays. The HLA-A*02:01$^-$ control cells (SK-N-MC and PBMCs) are not being recognized. **(D)** Upon transduction in HLA-A*02:01$^+$ T cells, the PAPPA-2G6 TCR transgenic T cells show vesicle release measured via CD107a positivity. **(E)** Cell growth is impeded in HLA-A*02:01$^+$ transduced T cells. Data are presented as mean and SEM. E/T ratio for ELISpot assay: 1:4. A673: HLA-A*02:01$^+$ ES; SK-N-MC: HLA-A*02:01$^-$ ES. Error bars represent standard deviation of triplicate experiments. Asterisks indicate significance levels. p values < 0.05 were considered statistically significant (*p < 0.05; **p < 0.005; ***p < 0.0005).

5.5.6 Reduced tumor burden after application of PAPPA-2G6 TCR transgenic T cells

Before application, the transgenic T cells were checked for phenotypic markers. Positivity for CD45RO+++, CD62L++, and CD45RA+ was characteristic for an effector memory (T_{EM}) phenotype except for the weak CCR7 expression (Fig. 29 A).

To study the *in vivo* efficacy and the immunotherapeutic potential of the PAPPA-2G6 TCR transgenic T cells in $Rag2^{-/-}\gamma c^{-/-}$ mice 3 control groups and 1 study group were chosen. Mice in all groups were inoculated with A673 s.c. on day 1. The mice received a full body irradiation on day 3. Additionally 1.5 x 10^7 irradiated IL-15 secreting NSO cells were injected twice per week i.p. The control groups were either untreated (n=6), received 5 x 10^6 $CD8^+$ depleted PBMCs (n=6) or 5 x 10^6 $CD8^+$ depleted PBMCs substituted with 5 x 10^6 unspecific T cells (n=5). The study group received 5 x 10^6 $CD8^+$ depleted PBMCs substituted with 5 x 10^6 specific PAPPA-2G6 TCR transgenic T cells (n=14).

On day 17 xenografted A673 tumors were resected and their weight was determined. Among the three different control groups no significant difference in tumor weight was measurable. However, the study group that was treated with the TCR transgenic T cells showed a significant tumor weight reduction in contrast to the controls (Fig. 29 B).

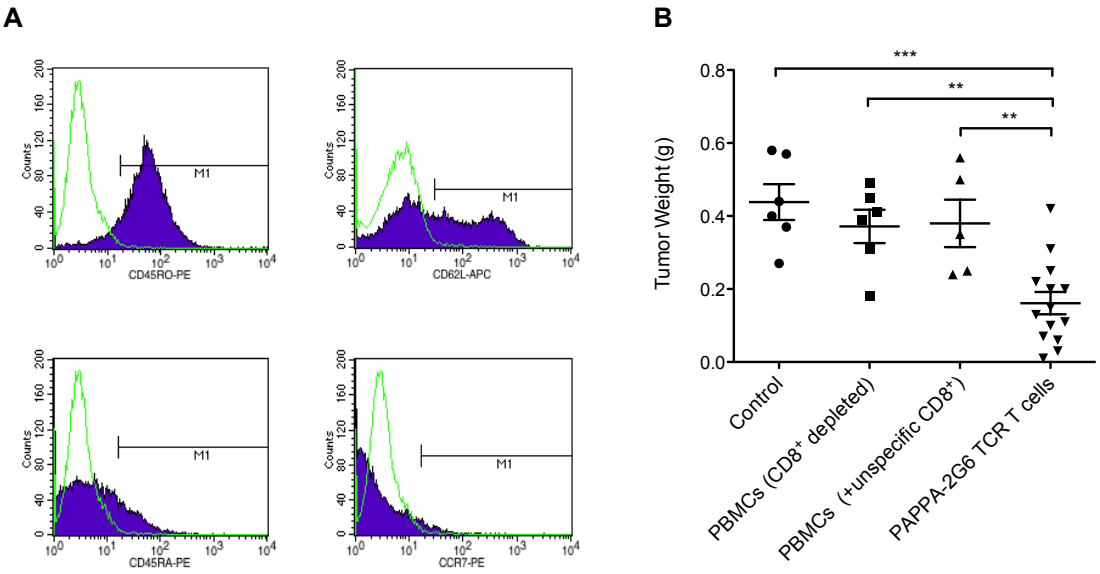

Figure 29: PAPPA-2G6 TCR transgenic T cells show *in vivo* efficacy. (A) Transgenic T cells were checked for phenotypic markers before application. Green = isotype control, Blue = antibody staining **(B)** Mice treated with PAPPA-2G6 TCR transgenic T cells showed significant tumor growth reduction in contrast to the controls.

5.5.7 Detection of TCR transgenic T cells in blood, bone marrow and tumor samples

Next to *in vivo* treatment efficacy we analyzed the mice for engraftment of TCR transgenic T cells in blood and bone marrow and for T cell infiltration into the tumor. Samples from blood, bone marrow and tumors were collected and stained for CD8, CD4, and specific multimer. In mice that had received unspecific T cells we were able to detect $CD4^+$ and $CD8^+$ cells in all tissues (Fig 30). T cell populations of mice that were treated with the PAPPA-2G6 transgenic T cells also showed multimer positivity in blood, bone marrow and tumors samples (Fig 31 A).

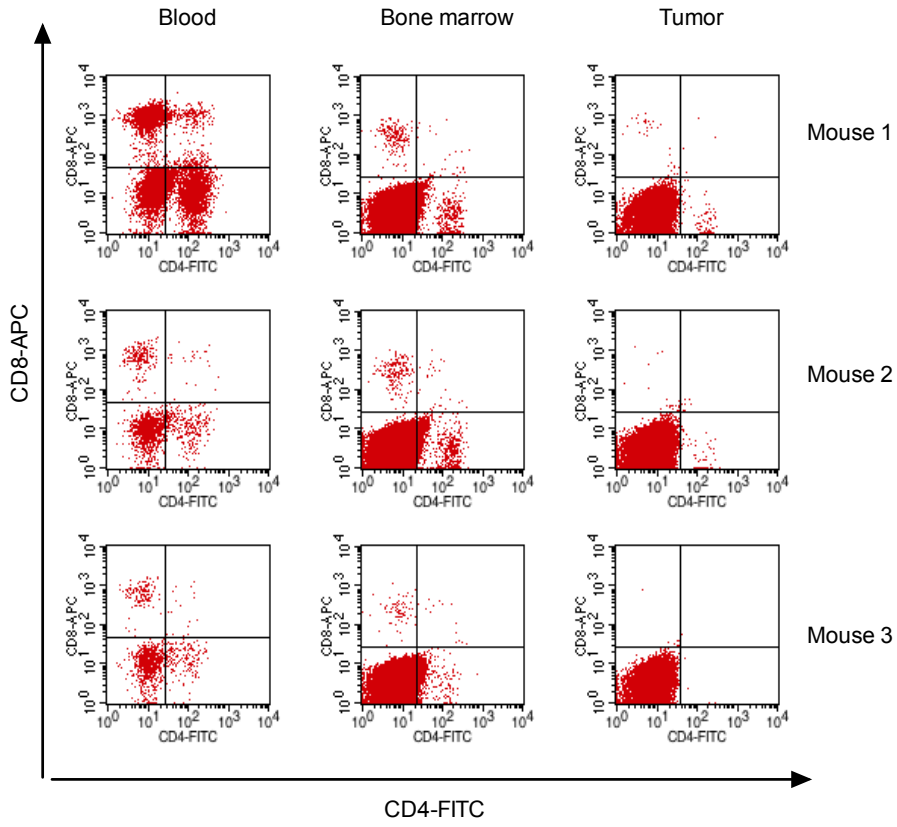

Figure 30: FACS staining shows persistence of unspecific T cell *in vivo*. Different samples were stained for CD8-APC and CD4-FITC to control engraftment of unspecific T cells in the control groups. Blood and bone marrow showed higher numbers of T cells engraftment than tumor samples.

Next to FACS analysis tumor-infiltrating T cells were additionally identified in immunohistochemistry slides (Fig. 31 B). In the control groups, unspecific T cells could be found at the tumor side, however, these unspecific T cells less frequently showed infiltration of the tumor site. This fact further highlights the potential of the PAPPA-2G6 TCR transgenic T cells. Furthermore, PAPPA expression was detected in A673 xenografts in contrast to adjacent normal murine tissue (Fig. 31 C right). Placental tissue served as a positive control (Fig. 31 C left).

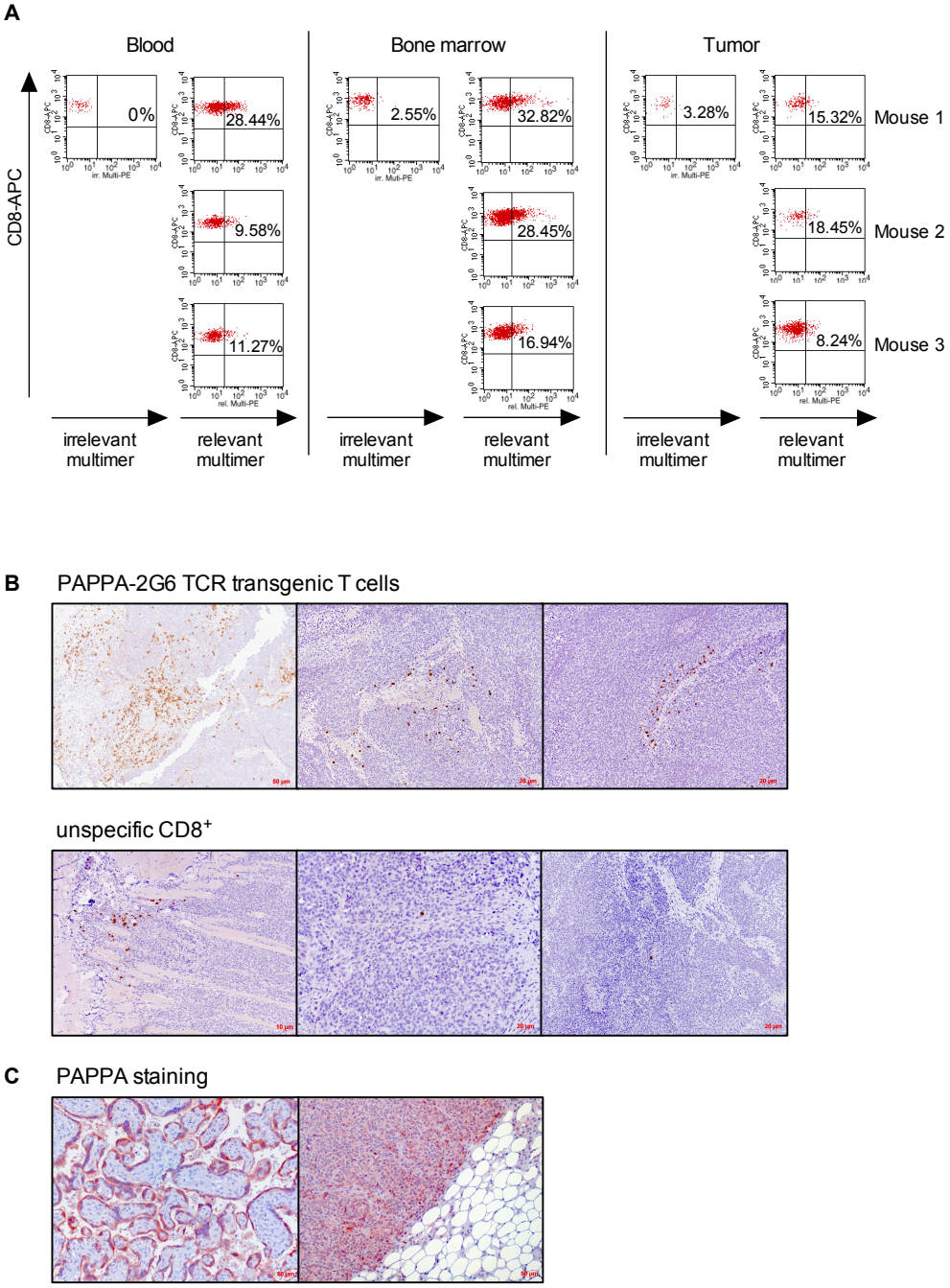

Figure 31: Detection of engraftment and infiltration of PAPPA-2G6 TCR transgenic T cells treated mice via FACS and immunohistochemistry. (A) FACS staining for CD8 and specific multimer shows transgenic T cells circulating in blood (left). Furthermore, T cells were detected in bone marrow (middle) and infiltrating into the A673 tumors (right). An irrelevant multimer served as a control **(B)** Tumor slides were stained with a specific antibody against CD8 in immunohistochemistry. Infiltration by T cells could be shown in PAPPA-2G6 treated mice (top). CD8 positivity upon mice treated with unspecific T cells was less frequent**. (C)** Immunohistochemistry further showed strong immunoreactivity in trophoblast layers of placental villi (left; positive control) and xenografted A673.

6. Discussion

6.1 Cancer immunotherapy

Allogeneic stem cell transplantation is an established treatment option for hematologic malignancies. Donor T cells induce a GvT effect beneficial in eradication of malignancies (Kolb et al. 1995). This treatment option, however, may be accompanied by a GvHD disease, which can result in a life-threatening situation for the patient (Baird et al. 2010). The identification and isolation of tumor specific T cells represents an option to specifically direct the potential of T cells towards the tumor rather than the host tissue (Thiel et al. 2011). Two different types of T cell therapies have emerged in the last decade: T cells expressing the classical TCR and, by contrast, T cells expressing an artificial chimeric antigen receptor (CAR) (Gross et al. 1989, Gross et al. 1989). Whereas the mode of action for the TCR relies on the identification of pMHC, the CAR T cell is independent of the MHC I expression of patients as this approach depends on the ability of antibodies recognizing peptide structures of cell surface molecules. Due to its MHC independent target recognition this approach is available for a broader range of patients. However, CAR T cells can only address surface molecules whereas the classical TCRs are not restricted in their target choice (Kershaw et al. 2013). Furthermore, down regulation of tumor surface molecules during CAR T cell treatment was observed resulting in CAR resistant cancer cells (Maude et al. 2014). However, both approaches show the risk of off target reactivity and GvHD when the target protein is expressed in healthy tissue. Yet only for CAR T cells the cytokine release syndrome (CRS) was reported (Morgan et al. 2010).

An obstacle for cellular T cell therapy is the high cost and time-consuming generation of wild type T cell populations against tumors in terms of an individualized cancer therapy. Furthermore, T cells may be exhausted due to extended division cycles and therefore less effective in persistence and *in vivo* efficacy. The retroviral insertion into random T cells of a certain subtype and optimized culture conditions represent a possibility to improve cellular immunotherapy in the future (Thiel et al. 2011, Blaeschke et al. 2016).

For AES patients allo-SCT represents an treatment option (Burdach et al. 2000). However, survival rates in patients that received reduced- versus high-intensity conditioning before allo-SCT did not differ, implicating an absence of a graft vs Ewing sarcoma (GvES) effect (Thiel et al.

2011). Yet, a recent study identified a new subgroup of AES patients. These patients with bone marrow (BM) involvement had a fatal outcome despite high dose therapy and allo-SCT, whereas patients with no BM involvement may be cured (Thiel et al. 2016). These findings underline the requirement for additional therapeutic strategies to direct T cell reactivity towards ES (Thiel et al. 2011).

6.2 Selection of potential targets for T cell mediated immunotherapy

The selection of a suitable antigen is of great importance for the generation of specific T cells as a therapy form against a certain type of cancer. Potential T cell antigens can be viral antigens expressed in malignant transformations, tumor specific antigens (such as EWS-FLI1 or BCR-ABL), cancer testis antigens, or TAAs (Cheever et al. 2009). As the ES is typically characterized by the EWS-FLI1 translocation a tumor specific antigen derived from EWS-FLI1 would be an ideal target for T cell mediated therapy (Delattre et al. 1992). However, both EWS and FLI1 are highly expressed in various cell types of healthy tissue. The fusion region of both proteins would represent an ideal target for T cell mediated immunotherapy. Yet, only for MHC II the EWS-FLI1 fusion region proofed to be capable of initiating an immune response whereas for MHC I no such peptide derived from the fusion region has been reported (Meyer-Wentrup et al. 2005). Evans et. al used peptides with modified anchor regions to improve the MHC I binding to generate specific T cells against this fusion region. Although they were able to isolate specific T cells still their EWS-FLI1 specificity is questionable as the wild type peptide is not able to stabilize HLA-A*02:01 MHC I (Evans et al. 2012). The presentation of the specific peptide on MHC I is crucial for the reactivity of T cells. The group of Hans-Georg Rammensee introduced high performance liquid chromatography mass spectrometry (HPLC-MS)-based approach was used to elude and analyze peptides bound to MHC I (Schirle et al. 2000, Singh-Jasuja et al. 2004). Identified tumor associated peptides can be used for T cell priming or cancer immunization. With the improvements in exome sequencing it is now even possible to synthesize minigenes consisting of mutated peptides specifically identified for each patient. These minigenes are introduced in autologous APCs, where they are processed. Co-culture of the APCs with the patients autologous T cells can stimulate an immune response and may be re-infused into the patient (Robbins et al. 2013). However, sequencing data implied that childhood sarcomas are

much less frequently mutated rendering this approach less attractive (Lawrence et al. 2013, Agelopoulos et al. 2015). Approaches, targeting EWS-FLI1 with conventional drugs have not gained the desired success (Uren et al. 2005). Therefore we considered targeting TAAs in Ewing sarcoma. Using DNA microarray we have previously identified 37 genes that are up-regulated in ES in comparison to normal body tissue (Staege et al. 2004). For three of these antigens we were already able to isolate tumor specific T cells showing the general feasibility of our approach (Thiel et al. 2011, Schirmer et al. 2016). To effectively kill the tumor via multiple targets we also attempted to generate additional TCR transgenic T cells directed against ADRB3 and PAPPA.

The ADRB3 receptor belongs to the family of transmembrane receptors with seven transmembrane segments (Coman et al. 2009). It is mainly located in the adipose tissue and involved in the regulation of lipolysis and thermogenesis. A gene mutation resulting in the replacement of tryptophan by arginine at position 64 (Trp64Arg) is linked an increased risk for obesity (Clement et al. 1995). This single nucleotide polymorphism (SNP) has been implicated for an increased risk for colon cancer and gall bladder cancer risk (Takezaki et al. 2001, Rai et al. 2015). However, a SNP in ADRB3 for Ewing sarcoma has not been reported so far.

PAPPA was first described as a circulating protein that emerges during pregnancy (Lin et al. 1974). PAPPA exists in two major forms. During pregnancy two PAPPA molecules are covalently linked with two eosinophil major basic protein (proMPB) molecules. In this form it is functionally inactive (Oxvig et al. 1993). In its active form PAPPA can be circulating as a dimer without bound proMPB (Lawrence et al. 1999). Furthermore, PAPPA can be tightly bound via glycosaminoglycans to the cell surface (Conover 2012). PAPPA functions thereby as a zinc metalloproteinase cleaving IGF binding protein-4 (IGFBP-4) when IGF is bound to IGFBP-4 and reducing its affinity to IGF towards its binding partner. Thereby IGF is released and accessible for interacting with the IGF receptor (IGFR) on the cell surface. With PAPPA directly linked to the cell surface the concentration of IGF at the receptor site is even further increased locally (Lawrence et al. 1999, Conover 2012). PAPPA expression is important in normal healing responses and tissue regeneration, as IGFs have shown to be important for normal growth, maintenance, and regeneration of essentially all tissues (Miller et al. 2007, Rehage et al. 2007, Conover 2012). IGF is one of the most prominent growth factors deposited in the bone matrix, bound to IGFBP4 it represents a key substance in bone modeling (Canalis et al. 1993, Mohan et al. 1995,

Pfeilschifter et al. 1995). PAPPA knock out mice are reduced in size by 40 % as IGFBP4 effectively inhibits IGF-stimulated mitogenesis (Conover et al. 2004). It has been reported that PAPPA is associated with breast, ovarian, renal, gastric, and lung cancer, as well as pleural mesothelioma (Dalgin et al. 2007, Bulut et al. 2009, Boldt et al. 2011, Nagarajan et al. 2012, Huang et al. 2013, Loddo et al. 2014). Furthermore, it was shown that proteolytic activity of PAPPA enhances tumorigenic potential supporting tumor growth (Alexiadis et al. 2006, Bulut et al. 2009, Boldt et al. 2011). The IGF-1 pathway is crucial in the ES metabolism (Scotlandi et al. 1996, Kim et al. 2009). EWS-FLI1 induces the expression of IGF and simultaneously represses the expression of IGFBP-3 (Prieur et al. 2004, Cironi et al. 2008, Herrero-Martin et al. 2009). As previously reported by our group PAPPA is overexpressed in ES and may therefore further contribute to this autocrine loop with its IGFB4 cleaving abilities (Staege et al. 2004). PAPPA is an important factor for growth of ES as shown in PAPPA knock out assays. Here, *in vitro* growth is hampered. In an *in vivo* study prolonged survival in mice was recently reported after PAPPA knock out (Heitzeneder S 2016). These finding further highlight the importance of PAPPA expression for tumor progression not only for ES but also for other types of cancer.

6.3 Cross reactive potential of allogeneic TCRs

An emerging draw-back in TCR immunotherapy is the potential risk of cross reactivity and the resulting GvHD. For a long time the paradigm of “one clonotype - one specificity” was widely accepted believing that a single specific TCR exits for every foreign peptide. Yet cross reactivity studies revealed that a single TCR may be able to recognize up to 10^6-10^7 different peptides. This insight highlights the potency of TCRs to distinguish non-self from self rather than different non-self peptides from another (Mason 1998, Sewell 2012). The theoretical TCR diversity is approximately 10^{18} in humans. However, the individual TCR repertoire is only about 10^8 due to negative selection during T cell development leading to holes in the T cell repertoire (Arstila et al. 1999, Frankild et al. 2008, Robins et al. 2009). At the same time the number of peptides presented by self-MHC is about 10^{15}. Thus T cells need to recognize more than 10^6 peptides for an effective immune response (Mason 1998, Wooldridge et al. 2012).

In this work we addressed cross reactivity due to the fact that especially off-target/off-site reactivity can cause major side effects. MHC I recognition was determined using IFNγ Elispot

assays against various LCL cell lines covering a broad spectrum of HLA types. Furthermore, these cells were tested after pulsing them with the specific peptide. However, in the case of the ADRB3-1F4 this assay was not able to detect cross reactivity that we observed for this TCR. Only LCLs expressing the HLA-A2 super-family were recognized by the TCR. Yet for PAPPA-2G6 putative restrictions for patient/donor MHC I combinations could be identified.

As a second approach we used alanine/serine/threonine amino acid substituted peptides to identify essential amino acids for TCR/pMHC recognition and to further identify 9-mer peptides with a similar sequence pattern that can represent putative cross reactive targets. This assay was previously used to investigate titin cross reactivity of MAGE-A3 specific TCRs and proofed to be suited for the here investigated TCRs to indicate putative cross-reactive peptides (Cameron et al. 2013, Linette et al. 2013). Yet, although for CHM1-4B4 the INFγ ELISpot assay was comparable to ADRB3-1F4, the results differed substantially. This assay only predicted three essential amino acids for ADRB3-1F4 and four for CHM1-4B4, respectively. Although this may indicate nonspecific peptide recognition for both TCRs, the amount of possible peptides carrying the core motive was significantly less for CHM1-4B4 in contrast to ADRB3-1F4. Further, also the SYFPEITHY binding affinities towards HLA-A1, -A2, and -A3 were significantly weaker. These results are congruent with our finding that the selection of possible donors for CHM1-4B4 transductions is not impaired by cross reactivity. The combination of the large amount of peptides carrying the ADRB3-1F4 core peptide sequence and the increased affinity of these peptides towards different HLAs is a possible reason for the impeded cell growth after TCR transduction as for nearly every MHC I several binders/TCR targets can be found within the 5068 identified peptides. Annexin positivity has already been proven to be associated with TCR transgenic mediated fratricide (Leisegang et al. 2010). But in our studies we could not observe annexin positivity with impeded cell growth for every donor. Therefore we aimed to measure T cell reactivity directly. Also we wanted to be able to show transgenic TCR mediated cross reactivity. The Lysosome-associated membrane protein 1 (LAMP1/CD107a) is a transmembrane protein that has shown to be a specific marker for degranulation of active T cells upon target recognition (Betts et al. 2003). Using this marker for T cell activity transgenic TCR mediated cross-reactivity could be shown directly after transduction. Further we were able to demonstrate an association

between T cell reactivity of our transduced T cells with impeded cell growth and to predict the outcome future transductions.

Next to overall peptide reactivity for the ADRB3-1F4 TCR this assay was also used for the PAPPA-2G6 TCR. Among 7 putative off-target peptides, which were further investigated, only the OAT peptide was recognized on peptide pulsed T2 cells. Among the identified peptides OAT had the most similarities (kvLPMNtgV) towards $PAPPA^{1434}$ (IILPMNVTV). Within the identified peptides, a PM pattern in the sequence was commonly identified in 5 out of 7 9-mer peptides. Yet, OAT showed the highest similarity and constitutes the only peptide that shares 4 amino acids in a row with $PAPPA^{1434}$. We assessed OAT cross reactivity and identified the osteosarcoma cell line SaOS and $CD8^+$ T cells as OAT expressing and at the same time PAPPA negative cell lines. However, the SaOs cell line was recognized by PAPPA-2G6 TCR transgenic T cells in IFNγ ELISpot assays. Further, when we tried to generate HLA-A*02:01^+/PAPPA-2G6 TCR transgenic T cells we observed CD107a positivity and impeded cell expansion rates. Both assays indicated cross reactivity potential.

6.4 Improvements in T cell immunotherapy and potency for Ewing sarcoma treatment

The ground for TCR transgenic T cell therapy was paved by Dembić in 1986 by showing that the functional activity of a certain T cell can be transferred to another T cell via its TCR (Dembic et al. 1986, Dembic et al. 1986). This method allows the production of large populations of T cells directed against a specific target. Feasibility of this approach in humans was first shown with TCR transgenic T cells directed against MART-1 in melanoma patients (Morgan et al. 2006).

Many studies use retro- or lentiviruses to introduce the transgenic TCR into donor T cells (Morgan et al. 2013). As the usage of viruses under GMP conditions is not without concern new methods are arising. The usage of transposons for the introduction of the T cell receptor DNA shows great potential. This method is rapid and cost effective without the need to generate viruses for transduction (Field et al. 2014, Deniger et al. 2016).

Still, when the new TCR is introduced into the donor T cells it competes with the endogenous TCR for its presentation on the cell surface. A potential risk arises in the generation of new combinations of the endogenous and the introduced α- and β-chains. This process is known as

mispairing and can give rise to a TCR with unpredictable specificity (Bendle et al. 2010, Thomas et al. 2010). Yet it was observed that murine constant chains exhibit a higher affinity towards one another than the human counterparts. Exchanging the human constant chain for the murine one improved pairing of the introduced TCR and its presentation on the cell surface (Cohen et al. 2006). However, introduction of foreign structures can result in immunological response (Davis et al. 2010). Sommermeyer et. al demonstrated that substituting specific AA in the constant chain with the murine counterpart is sufficient to increase the affinity of the introduced TCRs towards another and simultaneously reduce the risk for TCR mispairing (Sommermeyer et al. 2010). In our work we use a GMP approved vector system for the introduction of the TCR sequences that shows very good expression rates in lymphocytes (Engels et al. 2003). Moreover, potential mispairing is reduced via exchanging specific AA in the human constant chain for its murine counterparts (Sommermeyer et al. 2010). Using these methods we observed good albeit slightly varying transduction rates that however varied regarding the different TCRs constructs.

Although immunotherapy as a tool to treat cancer shows great potential, off-target and off-tumor reactivity has increased cautiousness. Former safe but less effective TCRs caused after affinity maturation GvHD reactions in patients after affinity maturation (Cameron et al. 2013, Linette et al. 2013, Morgan et al. 2013). Introduction of safety switches to shut down cross-reactive T cells represents a possibility. These safety features are supposed to eliminate TCR transgenic T cells in case of a GvHD and different concepts concerning this matter are being investigated. One of the first approaches was the introduction of the herpes simplex virus thymidine kinase (HSV-TK) (Tiberghien et al. 1994). Although it has shown promise as a safety feature it is of viral origin and can cause immunogenic reactions. Furthermore, T cell killing can take several days and may be incomplete which made this not the ideal method (Riddell et al. 1996, Tiberghien et al. 2001, Ciceri et al. 2009). Other studies use co-transduced surface molecules with approved therapeutic antibodies to eradicate cross-reactive T cells, e.g rituximab (Griffioen et al. 2009). A different approach relies upon the implementation of an inducible caspase 9 (iCasp9) system that is activated after administering a small molecule. A single application can eradicate up to 90 % of modified T cells within 30 min when causing a GvHD (Straathof et al. 2005, Di Stasi et al. 2011). However, to be efficient all introduced safety mechanisms require a reliable expression as long as the cells are active.

In vivo efficacy of ES immunotherapy treatment was shown in Rag2$^{-/-}$γc$^{-/-}$ mice. This immunodeficient mouse model is suited to study immunotherapeutic approaches as it lacks development of functional B-, and T-, and NK cell populations (Goldman et al. 1998). Yet, as parts of the lymphatic system such as thymus and lymph nodes are missing in this mouse strand several adjustments have been necessary to improve survival and engraftment of the applied TCR transgenic T cells. To prepare the mice for the graft they received a full body irradiation 24 h before T cell injection (Traggiai et al. 2004). Moreover, to increase engraftment efficiency CD8^{+} depleted PBMCs were applied in addition to the TCR transgenic T cells. Additionally, IL-15 secreting NSO cells were injected twice per week (Klebanoff et al. 2004, Wang et al. 2011). All these amendments were applied to facilitate T cell engraftment and tumor rejection.

In our mouse experiments we chose 3 control groups to study the effects of the additionally applied NSO cells, T cell depleted PBMCs, or unspecific T cells on the tumor growth. In the controls no difference in tumor growth was observed after 17 d. By contrast, we did observe a significant reduced tumor weight in the mice treated with the PAPPA-2G6 TCR transgenic T cells. When we further controlled for T cell engraftment we saw CD8^{+}/multimer^{+} T cells in the bone marrow. Furthermore, circulating T cells were found in blood from treated mice. These findings were of importance as it showed the potency of the transgenic T cells to engraft, proliferate, and circulate *in vivo*, which symbolizes the potency of immunotherapy, as these cells are capable to proliferate and sustain themselves. Yet the multimer staining was not as strong as in *in vitro* cultures. This effect might be due to the different *in vivo* environment. Nevertheless, expression of the transgenic TCR could be shown. T cell infiltration into the tumor site was observed for the TCR transgenic T cells as well as for the unspecific T cells. However, the amount of infiltrating T cells in the study group was larger than for the control group receiving unspecific T cells. In summary we were able to show *in vivo* efficacy of PAPPA2-2G6 TCR transgenic T cells in s.c. inoculated A673 ES tumor cell line. Of great importance was the confirmation of engrafting, circulating and tumor infiltration. Especially the bone marrow engraftment proved to be of great value. As we reported recently bone marrow involvement correlates with a fatal outcome in patients with AES (Uwe Thiel 2016). The finding of infiltrating PAPPA specific T cells into the bone marrow opens new treatment options, in particular for patients with marrow involvement.

7. Summary

In this study we could generate TCR transgenic T cells after allogeneic T cell priming directed against the TAAs ADRB3 and PAPPA. Both TCRs were tested *in vitro* for their reactivity and killing towards HLA-A*02:01^{+} ES cell lines. After identification of the specific TCR sequence via PCR and additional Vβ chain FACS analysis the modified sequences were cloned into the MP71 vector. Both TCRs were successfully introduced into donor T cells and TCR transgenic T cells were isolated using magnetic PE beads after staining the TCR transgenic T cells with its specific multimer. In IFNγ ELISpot assays both TCRs functionality was comparably to the wild type T cells. Effective killing of ES cells A673 was either shown in grB ELISpot assays or via detachment after addition of the T cells in xCELLigence system.

The significance of cross reactivity of TCRs became increasingly evident. Therefore different test systems for cross reactivity were introduced and tested on the TCR transgenic T cells. Unfortunately, for the ADRB3-1F4 TCR a major cross reactivity revealed upon transduction, which resulted in impeded cell growth. Cross reactivity of transgenic T cells was shown via annexin V and CD107a. Furthermore, the cross-reactive potential of the TCR was confirmed in amino acid exchange scans. This cross reactivity made further experiments challenging due to a limited number of suited donors. Due to this fact, this TCR was considered not suitable for the clinical application and no further *in vivo* experiments were conducted. As for the PAPPA directed T cell clone 2G6 the level of potential cross reactivity we observed was much lower. Reactivity of the TCR transgenic T cells was assessed in Rag2$^{-/-}$γc$^{-/-}$ mice. Mice treated with PAPPA specific TCR transgenic T cells had reduced tumor growth in subcutaneously inoculated A673 tumors. Furthermore, engraftment and tumor infiltration of the transgenic T cells could be confirmed.

Zusammenfassung

In dieser Studie konnten wir T-Zellen mit transgenen T-Zellrezeptoren (TZR) gerichtet gegen PAPPA und ADRB3 nach allogener T-Zellstimulation herstellen. Beide TZR wurden *in vitro* bezüglich ihrer Reaktivität gegenüber ES Zellen und ihrer Fähigkeit diese zu lysieren getestet. Nach der Identifizierung der TZR mittels PCR und zusätzlicher Vβ-Analyse wurden die modifizierten TZR-Sequenzen in den MP71 Vektor kloniert. Beide TZR konnten erfolgreich in Spender T-Zellen eingebracht werden. Diese transgenen T-Zellen wurden mittels Anti-PE Magnetischer Beads nach Multimer-PE Färbung über Säulen aufgereinigt. In IFNγ ELISpot Tests zeigten beide TZR vergleichbare Werte wie ihre Wildtypzellen. Die Lyse der ES Zellen A673 wurde im xCELLigence System mittels Messung der Ablösung der Zellen von ihrer Kulturfläche nach Zugabe der T-Zellen gemessen.

Eine mögliche Kreuzreaktivität der TZR gewann im Laufe der Arbeit immer mehr an Bedeutung. Daher wurden unterschiedliche Testsysteme zum Nachweis von Kreuzreaktivität etabliert und an den transgenen TZRs ausgetestet. Leider zeigte der transgene TZR ADRB3-1F4 ein ausgeprägtes Kreuzreaktivitäsniveau welches sich in vermindertem Wachstum und erhöhten Apoptosewerten nach Transduktion niederschlug. Dies wurde unter anderem Mittels CD107a nach Transduktion nachgewiesen. Weiter wurde das Kreuzreaktivitätspotential durch einen Aminosäureaustausch im spezifischen Peptid bestätigt. Für den PAPPA spezifischen TZR erwies sich das Kreuzreaktivitätspotential im Aminosäureaustausch als deutlich geringer. Die *in vivo* Effektivität der transgenen T-Zellen konnte in $Rag2^{-/-}\gamma c^{-/-}$ Mäusen nachgewiesen werden. Mäuse die mit den transgenen T-Zellen behandelt wurden wiesen ein verringertes Tumorwachstum auf. Zusätzlich konnte die Persistenz der T-Zellen in der Maus und eine Infiltration der T-Zellen in den Tumor nachgewiesen werden.

8. References

Agelopoulos, K., G. H. Richter, E. Schmidt, U. Dirksen, K. von Heyking, B. Moser, H. U. Klein, U. Kontny, M. Dugas, K. Poos, E. Korsching, T. Buch, M. Weckesser, I. Schulze, R. Besoke, A. Witten, M. Stoll, G. Kohler, W. Hartmann, E. Wardelmann, C. Rossig, D. Baumhoer, H. Jurgens, S. Burdach, W. E. Berdel and C. Muller-Tidow (2015). "Deep Sequencing in Conjunction with Expression and Functional Analyses Reveals Activation of FGFR1 in Ewing Sarcoma." Clin Cancer Res **21**(21): 4935-4946.

Aleksic, M., N. Liddy, P. E. Molloy, N. Pumphrey, A. Vuidepot, K. M. Chang and B. K. Jakobsen (2012). "Different affinity windows for virus and cancer-specific T-cell receptors: implications for therapeutic strategies." Eur J Immunol **42**(12): 3174-3179.

Alexiadis, M., P. Mamers, S. Chu and P. J. Fuller (2006). "Insulin-like growth factor, insulin-like growth factor-binding protein-4, and pregnancy-associated plasma protein-A gene expression in human granulosa cell tumors." Int J Gynecol Cancer **16**(6): 1973-1979.

Alimonti, J. B., L. Shi, P. K. Baijal and A. H. Greenberg (2001). "Granzyme B induces BID-mediated cytochrome c release and mitochondrial permeability transition." J Biol Chem **276**(10): 6974-6982.

Amrolia, P. J., S. D. Reid, L. Gao, B. Schultheis, G. Dotti, M. K. Brenner, J. V. Melo, J. M. Goldman and H. J. Stauss (2003). "Allorestricted cytotoxic T cells specific for human CD45 show potent antileukemic activity." Blood **101**(3): 1007-1014.

Arden, B., S. P. Clark, D. Kabelitz and T. W. Mak (1995). "Human T-cell receptor variable gene segment families." Immunogenetics **42**(6): 455-500.

Arstila, T. P., A. Casrouge, V. Baron, J. Even, J. Kanellopoulos and P. Kourilsky (1999). "A direct estimate of the human alphabeta T cell receptor diversity." Science **286**(5441): 958-961.

Baird, K., K. Cooke and K. R. Schultz (2010). "Chronic graft-versus-host disease (GVHD) in children." Pediatr Clin North Am **57**(1): 297-322.

Baker, K. S. and C. J. Fraser (2008). "Quality of life and recovery after graft-versus-host disease." Best Pract Res Clin Haematol **21**(2): 333-341.

Bendle, G. M., C. Linnemann, A. I. Hooijkaas, L. Bies, M. A. de Witte, A. Jorritsma, A. D. Kaiser, N. Pouw, R. Debets, E. Kieback, W. Uckert, J. Y. Song, J. B. Haanen and T. N. Schumacher (2010). "Lethal graft-versus-host disease in mouse models of T cell receptor gene therapy." Nat Med **16**(5): 565-570, 561p following 570.

Bernstein, M., H. Kovar, M. Paulussen, R. L. Randall, A. Schuck, L. A. Teot and H. Juergens (2006). "Ewing's sarcoma family of tumors: current management." Oncologist **11**(5): 503-519.

Betts, M. R., J. M. Brenchley, D. A. Price, S. C. De Rosa, D. C. Douek, M. Roederer and R. A. Koup (2003). "Sensitive and viable identification of antigen-specific CD8+ T cells by a flow cytometric assay for degranulation." J Immunol Methods **281**(1-2): 65-78.

Blaeschke, F., U. Thiel, A. Kirschner, M. Thiede, R. A. Rubio, D. Schirmer, T. Kirchner, G. H. Richter, S. Mall, R. Klar, S. Riddell, D. H. Busch, A. Krackhardt, T. G. Grunewald and S. Burdach (2016). "Human HLA-A*02:01/CHM1+ allo-restricted T cell receptor transgenic CD8+ T Cells specifically inhibit Ewing sarcoma growth in vitro and in vivo." Oncotarget.

Boldt, H. B. and C. A. Conover (2011). "Overexpression of pregnancy-associated plasma protein-A in ovarian cancer cells promotes tumor growth in vivo." Endocrinology **152**(4): 1470-1478.

Brochet, X., M. P. Lefranc and V. Giudicelli (2008). "IMGT/V-QUEST: the highly customized and integrated system for IG and TR standardized V-J and V-D-J sequence analysis." Nucleic Acids Res **36**(Web Server issue): W503-508.

Bulut, I., A. Coskun, A. Ciftci, E. Cetinkaya, G. Altiay, T. Caglar and E. Gulcan (2009). "Relationship between pregnancy-associated plasma protein-A and lung cancer." Am J Med Sci **337**(4): 241-244.

Burchill, S. A. (2003). "Ewing's sarcoma: diagnostic, prognostic, and therapeutic implications of molecular abnormalities." J Clin Pathol **56**(2): 96-102.

Burdach, S. and H. J. Kolb (2013). "The vigor of defense against non-self: potential superiority of allorestricted T cells in immunotherapy of cancer?" Front Oncol **3**: 100.

Burdach, S., U. Thiel, M. Schoniger, R. Haase, A. Wawer, M. Nathrath, H. Kabisch, C. Urban, H. J. Laws, U. Dirksen, M. Steinborn, J. Dunst, H. Jurgens and E. S. G. Meta (2010). "Total body MRI-governed involved compartment irradiation combined with high-dose chemotherapy and stem cell rescue improves long-term survival in Ewing tumor patients with multiple primary bone metastases." Bone Marrow Transplant **45**(3): 483-489.

Burdach, S., B. van Kaick, H. J. Laws, S. Ahrens, R. Haase, D. Korholz, H. Pape, J. Dunst, T. Kahn, R. Willers, B. Engel, U. Dirksen, C. Kramm, W. Nurnberger, A. Heyll, R. Ladenstein, H. Gadner, H. Jurgens and U. Go el (2000). "Allogeneic and autologous stem-cell transplantation in advanced Ewing tumors. An update after long-term follow-up from two centers of the European Intergroup study EICESS. Stem-Cell Transplant Programs at Dusseldorf University Medical Center, Germany and St. Anna Kinderspital, Vienna, Austria." Ann Oncol **11**(11): 1451-1462.

Cameron, B. J., A. B. Gerry, J. Dukes, J. V. Harper, V. Kannan, F. C. Bianchi, F. Grand, J. E. Brewer, M. Gupta, G. Plesa, G. Bossi, A. Vuidepot, A. S. Powlesland, A. Legg, K. J. Adams, A. D. Bennett, N. J. Pumphrey, D. D. Williams, G. Binder-Scholl, I. Kulikovskaya, B. L. Levine, J. L. Riley, A. Varela-Rohena, E. A. Stadtmauer, A. P. Rapoport, G. P. Linette, C. H. June, N. J. Hassan, M. Kalos and B. K. Jakobsen (2013). "Identification of a Titin-derived HLA-A1-presented peptide as a cross-reactive target for engineered MAGE A3-directed T cells." Sci Transl Med **5**(197): 197ra103.

Canalis, E., J. Pash, B. Gabbitas, S. Rydziel and S. Varghese (1993). "Growth factors regulate the synthesis of insulin-like growth factor-I in bone cell cultures." Endocrinology **133**(1): 33-38.

Cancer.org (2016). "Cancer.org." from http://www.cancer.org.

cancerresearchuk.org (2016). "cancerresearchuk.org." from http://www.cancerresearchuk.org.

Catalfamo, M. and P. A. Henkart (2003). "Perforin and the granule exocytosis cytotoxicity pathway." Curr Opin Immunol **15**(5): 522-527.

Cheever, M. A., J. P. Allison, A. S. Ferris, O. J. Finn, B. M. Hastings, T. T. Hecht, I. Mellman, S. A. Prindiville, J. L. Viner, L. M. Weiner and L. M. Matrisian (2009). "The prioritization of cancer antigens: a national cancer institute pilot project for the acceleration of translational research." Clin Cancer Res **15**(17): 5323-5337.

Ciceri, F., C. Bonini, M. T. Stanghellini, A. Bondanza, C. Traversari, M. Salomoni, L. Turchetto, S. Colombi, M. Bernardi, J. Peccatori, A. Pescarollo, P. Servida, Z. Magnani, S. K. Perna, V. Valtolina, F. Crippa, L. Callegaro, E. Spoldi, R. Crocchiolo, K. Fleischhauer, M. Ponzoni, L. Vago, S. Rossini, A. Santoro, E. Todisco, J. Apperley, E. Olavarria, S. Slavin, E. M. Weissinger, A. Ganser, M. Stadler, E. Yannaki, A. Fassas, A. Anagnostopoulos, M. Bregni, C. G. Stampino, P. Bruzzi and C. Bordignon (2009). "Infusion of suicide-gene-engineered donor lymphocytes after family haploidentical haemopoietic stem-cell transplantation for leukaemia (the TK007 trial): a non-randomised phase I-II study." Lancet Oncol **10**(5): 489-500.

Cieri, N., S. Mastaglio, G. Oliveira, M. Casucci, A. Bondanza and C. Bonini (2014). "Adoptive immunotherapy with genetically modified lymphocytes in allogeneic stem cell transplantation." Immunol Rev **257**(1): 165-180.

Cironi, L., N. Riggi, P. Provero, N. Wolf, M. L. Suva, D. Suva, V. Kindler and I. Stamenkovic (2008). "IGF1 is a common target gene of Ewing's sarcoma fusion proteins in mesenchymal progenitor cells." PLoS One **3**(7): e2634.

Clay, T. M., M. C. Custer, J. Sachs, P. Hwu, S. A. Rosenberg and M. I. Nishimura (1999). "Efficient transfer of a tumor antigen-reactive TCR to human peripheral blood lymphocytes confers anti-tumor reactivity." J Immunol **163**(1): 507-513.

Clement, K., C. Vaisse, B. S. Manning, A. Basdevant, B. Guy-Grand, J. Ruiz, K. D. Silver, A. R. Shuldiner, P. Froguel and A. D. Strosberg (1995). "Genetic variation in the beta 3-adrenergic receptor and an increased capacity to gain weight in patients with morbid obesity." N Engl J Med **333**(6): 352-354.

Cohen, C. J., Y. Zhao, Z. Zheng, S. A. Rosenberg and R. A. Morgan (2006). "Enhanced antitumor activity of murine-human hybrid T-cell receptor (TCR) in human lymphocytes is associated with improved pairing and TCR/CD3 stability." Cancer Res **66**(17): 8878-8886.

Cole, D. K., N. J. Pumphrey, J. M. Boulter, M. Sami, J. I. Bell, E. Gostick, D. A. Price, G. F. Gao, A. K. Sewell and B. K. Jakobsen (2007). "Human TCR-binding affinity is governed by MHC class restriction." J Immunol **178**(9): 5727-5734.

Coman, O. A., H. Paunescu, I. Ghita, L. Coman, A. Badararu and I. Fulga (2009). "Beta 3 adrenergic receptors: molecular, histological, functional and pharmacological approaches." Rom J Morphol Embryol **50**(2): 169-179.

Conover, C. A. (2012). "Key questions and answers about pregnancy-associated plasma protein-A." Trends Endocrinol Metab **23**(5): 242-249.

Conover, C. A., L. K. Bale, M. T. Overgaard, E. W. Johnstone, U. H. Laursen, E. M. Fuchtbauer, C. Oxvig and J. van Deursen (2004). "Metalloproteinase pregnancy-associated plasma protein A is a critical growth regulatory factor during fetal development." Development **131**(5): 1187-1194.

Dalgin, G. S., D. T. Holloway, L. S. Liou and C. DeLisi (2007). "Identification and characterization of renal cell carcinoma gene markers." Cancer Inform **3**: 65-92.

Darmon, A. J., D. W. Nicholson and R. C. Bleackley (1995). "Activation of the apoptotic protease CPP32 by cytotoxic T-cell-derived granzyme B." Nature **377**(6548): 446-448.

Davis, J. L., M. R. Theoret, Z. Zheng, C. H. Lamers, S. A. Rosenberg and R. A. Morgan (2010). "Development of human anti-murine T-cell receptor antibodies in both responding and nonresponding patients enrolled in TCR gene therapy trials." Clin Cancer Res **16**(23): 5852-5861.

Davis, M. M. (1990). "T cell receptor gene diversity and selection." Annu Rev Biochem **59**: 475-496.

Davis, M. M. and P. J. Bjorkman (1988). "T-cell antigen receptor genes and T-cell recognition." Nature **334**(6181): 395-402.

Delattre, O., J. Zucman, B. Plougastel, C. Desmaze, T. Melot, M. Peter, H. Kovar, I. Joubert, P. de Jong, G. Rouleau and et al. (1992). "Gene fusion with an ETS DNA-binding domain caused by chromosome translocation in human tumours." Nature **359**(6391): 162-165.

Dembic, Z., W. Haas, S. Weiss, J. McCubrey, H. Kiefer, H. von Boehmer and M. Steinmetz (1986). "Transfer of specificity by murine alpha and beta T-cell receptor genes." Nature **320**(6059): 232-238.

Dembic, Z., H. von Boehmer and M. Steinmetz (1986). "The role of T-cell receptor alpha and beta genes in MHC-restricted antigen recognition." Immunol Today **7**(10): 308-311.

Deniger, D. C., A. Pasetto, E. Tran, M. R. Parkhurst, C. J. Cohen, P. F. Robbins, L. J. Cooper and S. A. Rosenberg (2016). "Stable, Nonviral Expression of Mutated Tumor Neoantigen-specific T-cell Receptors Using the Sleeping Beauty Transposon/Transposase System." Mol Ther **24**(6): 1078-1089.

Di Stasi, A., S. K. Tey, G. Dotti, Y. Fujita, A. Kennedy-Nasser, C. Martinez, K. Straathof, E. Liu, A. G. Durett, B. Grilley, H. Liu, C. R. Cruz, B. Savoldo, A. P. Gee, J. Schindler, R. A. Krance, H. E. Heslop, D. M. Spencer, C. M. Rooney and M. K. Brenner (2011). "Inducible apoptosis as a safety switch for adoptive cell therapy." N Engl J Med **365**(18): 1673-1683.

Dutoit, V., P. Guillaume, P. Romero, J. C. Cerottini and D. Valmori (2002). "Functional analysis of HLA-A*0201/Melan-A peptide multimer+ CD8+ T cells isolated from an HLA-A*0201- donor: exploring tumor antigen allorestricted recognition." Cancer Immun **2**: 7.

Eggensperger, S. and R. Tampe (2015). "The transporter associated with antigen processing: a key player in adaptive immunity." Biol Chem **396**(9-10): 1059-1072.

Engels, B., H. Cam, T. Schuler, S. Indraccolo, M. Gladow, C. Baum, T. Blankenstein and W. Uckert (2003). "Retroviral vectors for high-level transgene expression in T lymphocytes." Hum Gene Ther **14**(12): 1155-1168.

Evans, C. H., F. Liu, R. M. Porter, R. P. O'Sullivan, T. Merghoub, E. P. Lunsford, K. Robichaud, F. Van Valen, S. L. Lessnick, M. C. Gebhardt and J. W. Wells (2012). "EWS-FLI-1-targeted cytotoxic T-cell killing of multiple tumor types belonging to the Ewing sarcoma family of tumors." Clin Cancer Res **18**(19): 5341-5351.

Ewing, J. (1972). "Classics in oncology. Diffuse endothelioma of bone. James Ewing. Proceedings of the New York Pathological Society, 1921." CA Cancer J Clin **22**(2): 95-98.

Falkenburg, J. H., A. R. Wafelman, P. Joosten, W. M. Smit, C. A. van Bergen, R. Bongaerts, E. Lurvink, M. van der Hoorn, P. Kluck, J. E. Landegent, H. C. Kluin-Nelemans, W. E. Fibbe and R. Willemze (1999). "Complete remission of accelerated phase chronic myeloid leukemia by treatment with leukemia-reactive cytotoxic T lymphocytes." Blood **94**(4): 1201-1208.

Felix, N. J. and P. M. Allen (2007). "Specificity of T-cell alloreactivity." Nat Rev Immunol **7**(12): 942-953.

Ferrara, J. L., J. E. Levine, P. Reddy and E. Holler (2009). "Graft-versus-host disease." Lancet **373**(9674): 1550-1561.

Field, K. M., M. A. Rosenthal, M. Yilmaz, M. Tacey and K. Drummond (2014). "Comparison between poor and long-term survivors with glioblastoma: review of an Australian dataset." Asia Pac J Clin Oncol **10**(2): 153-161.

Frankild, S., R. J. de Boer, O. Lund, M. Nielsen and C. Kesmir (2008). "Amino acid similarity accounts for T cell cross-reactivity and for "holes" in the T cell repertoire." PLoS One **3**(3): e1831.

Gasparini, M., S. Barni, A. Lattuada, R. Musumeci, G. Bonadonna and F. Fossati-Bellani (1977). "Ten years experience with Ewing's sarcoma." Tumori **63**(1): 77-90.

Gattinoni, L., C. A. Klebanoff, D. C. Palmer, C. Wrzesinski, K. Kerstann, Z. Yu, S. E. Finkelstein, M. R. Theoret, S. A. Rosenberg and N. P. Restifo (2005). "Acquisition of full effector function in vitro paradoxically impairs the in vivo antitumor efficacy of adoptively transferred CD8+ T cells." J Clin Invest **115**(6): 1616-1626.

Gattinoni, L., C. A. Klebanoff and N. P. Restifo (2012). "Paths to stemness: building the ultimate antitumour T cell." Nat Rev Cancer **12**(10): 671-684.

Giudicelli, V., X. Brochet and M. P. Lefranc (2011). "IMGT/V-QUEST: IMGT standardized analysis of the immunoglobulin (IG) and T cell receptor (TR) nucleotide sequences." Cold Spring Harb Protoc **2011**(6): 695-715.

Glass, A. G. and J. F. Fraumeni, Jr. (1970). "Epidemiology of bone cancer in children." J Natl Cancer Inst **44**(1): 187-199.

Goldman, J. M., R. P. Gale, M. M. Horowitz, J. C. Biggs, R. E. Champlin, E. Gluckman, R. G. Hoffmann, S. J. Jacobsen, A. M. Marmont, P. B. McGlave and et al. (1988). "Bone marrow transplantation for chronic myelogenous leukemia in chronic phase. Increased risk for relapse associated with T-cell depletion." Ann Intern Med **108**(6): 806-814.

Goldman, J. P., M. P. Blundell, L. Lopes, C. Kinnon, J. P. Di Santo and A. J. Thrasher (1998). "Enhanced human cell engraftment in mice deficient in RAG2 and the common cytokine receptor gamma chain." Br J Haematol **103**(2): 335-342.

Goldrath, A. W. and M. J. Bevan (1999). "Selecting and maintaining a diverse T-cell repertoire." Nature **402**(6759): 255-262.

Griffioen, M., E. H. van Egmond, M. G. Kester, R. Willemze, J. H. Falkenburg and M. H. Heemskerk (2009). "Retroviral transfer of human CD20 as a suicide gene for adoptive T-cell therapy." Haematologica **94**(9): 1316-1320.

Gross, G., G. Gorochov, T. Waks and Z. Eshhar (1989). "Generation of effector T cells expressing chimeric T cell receptor with antibody type-specificity." Transplant Proc **21**(1 Pt 1): 127-130.

Gross, G., T. Waks and Z. Eshhar (1989). "Expression of immunoglobulin-T-cell receptor chimeric molecules as functional receptors with antibody-type specificity." Proc Natl Acad Sci U S A **86**(24): 10024-10028.

Grunewald, T. G., V. Bernard, P. Gilardi-Hebenstreit, V. Raynal, D. Surdez, M. M. Aynaud, O. Mirabeau, F. Cidre-Aranaz, F. Tirode, S. Zaidi, G. Perot, A. H. Jonker, C. Lucchesi, M. C. Le Deley, O. Oberlin, P. Marec-Berard, A. S. Veron, S. Reynaud, E. Lapouble, V. Boeva, T. Rio Frio, J. Alonso, S. Bhatia, G. Pierron, G. Cancel-Tassin, O. Cussenot, D. G. Cox, L. M. Morton, M. J. Machiela, S. J. Chanock, P. Charnay and O. Delattre (2015). "Chimeric EWSR1-FLI1 regulates the Ewing sarcoma susceptibility gene EGR2 via a GGAA microsatellite." Nat Genet **47**(9): 1073-1078.

Heitzeneder S, S. J., Khan J, Mackall C. (2016). Pregnancy associated plasma protein A (PAPP-A) is a potential novel therapeutic target in Ewing sarcoma. Proceedings of the 107th Annual Meeting of the American Association for Cancer Research. New Orleans, LA. Philadelphia (PA). **Abstract nr 571**.

Herrero-Martin, D., D. Osuna, J. L. Ordonez, V. Sevillano, A. S. Martins, C. Mackintosh, M. Campos, J. Madoz-Gurpide, A. P. Otero-Motta, G. Caballero, A. T. Amaral, D. H. Wai, Y. Braun, M. Eisenacher, K. L. Schaefer, C. Poremba and E. de Alava (2009). "Stable interference of EWS-FLI1 in an Ewing sarcoma cell line impairs IGF-1/IGF-1R signalling and reveals TOPK as a new target." Br J Cancer **101**(1): 80-90.

Horowitz, M. M., R. P. Gale, P. M. Sondel, J. M. Goldman, J. Kersey, H. J. Kolb, A. A. Rimm, O. Ringden, C. Rozman, B. Speck and et al. (1990). "Graft-versus-leukemia reactions after bone marrow transplantation." Blood **75**(3): 555-562.

Huang, J., H. T. Khong, M. E. Dudley, M. El-Gamil, Y. F. Li, S. A. Rosenberg and P. F. Robbins (2005). "Survival, persistence, and progressive differentiation of adoptively transferred tumor-reactive T cells associated with tumor regression." J Immunother **28**(3): 258-267.

Huang, J., S. Tabata, S. Kakiuchi, T. The Van, H. Goto, M. Hanibuchi and Y. Nishioka (2013). "Identification of pregnancy-associated plasma protein A as a migration-promoting gene in malignant pleural mesothelioma cells: a potential therapeutic target." Oncotarget **4**(8): 1172-1184.

Janknecht, R. (2005). "EWS-ETS oncoproteins: the linchpins of Ewing tumors." Gene **363**: 1-14.

Jurgens, H., U. Exner, H. Gadner, D. Harms, J. Michaelis, R. Sauer, J. Treuner, T. Voute, W. Winkelmann, K. Winkler and et al. (1988). "Multidisciplinary treatment of primary Ewing's sarcoma of bone. A 6-year experience of a European Cooperative Trial." Cancer **61**(1): 23-32.

Kershaw, M. H., J. A. Westwood and P. K. Darcy (2013). "Gene-engineered T cells for cancer therapy." Nat Rev Cancer **13**(8): 525-541.

Kim, S. Y., J. A. Toretsky, D. Scher and L. J. Helman (2009). "The role of IGF-1R in pediatric malignancies." Oncologist **14**(1): 83-91.

Klebanoff, C. A., S. E. Finkelstein, D. R. Surman, M. K. Lichtman, L. Gattinoni, M. R. Theoret, N. Grewal, P. J. Spiess, P. A. Antony, D. C. Palmer, Y. Tagaya, S. A. Rosenberg, T. A. Waldmann and N. P. Restifo (2004). "IL-15 enhances the in vivo antitumor activity of tumor-reactive CD8+ T cells." Proc Natl Acad Sci U S A **101**(7): 1969-1974.

Knabel, M., T. J. Franz, M. Schiemann, A. Wulf, B. Villmow, B. Schmidt, H. Bernhard, H. Wagner and D. H. Busch (2002). "Reversible MHC multimer staining for functional isolation of T-cell populations and effective adoptive transfer." Nat Med **8**(6): 631-637.

Kolb, H. J. (2008). "Graft-versus-leukemia effects of transplantation and donor lymphocytes." Blood **112**(12): 4371-4383.

Kolb, H. J., A. Schattenberg, J. M. Goldman, B. Hertenstein, N. Jacobsen, W. Arcese, P. Ljungman, A. Ferrant, L. Verdonck, D. Niederwieser, F. van Rhee, J. Mittermueller, T. de Witte, E. Holler, H. Ansari, B. European Group for and L. Marrow Transplantation Working Party Chronic (1995). "Graft-versus-leukemia effect of donor lymphocyte transfusions in marrow grafted patients." Blood **86**(5): 2041-2050.

Koscielniak, E., U. Gross-Wieltsch, J. Treuner, P. Winkler, T. Klingebiel, P. Lang, P. Bader, D. Niethammer and R. Handgretinger (2005). "Graft-versus-Ewing sarcoma effect and long-term remission induced by haploidentical stem-cell transplantation in a patient with relapse of metastatic disease." J Clin Oncol **23**(1): 242-244.

Lawrence, J. B., C. Oxvig, M. T. Overgaard, L. Sottrup-Jensen, G. J. Gleich, L. G. Hays, J. R. Yates, 3rd and C. A. Conover (1999). "The insulin-like growth factor (IGF)-dependent IGF binding protein-4 protease secreted by human fibroblasts is pregnancy-associated plasma protein-A." Proc Natl Acad Sci U S A **96**(6): 3149-3153.

Lawrence, M. S., P. Stojanov, P. Polak, G. V. Kryukov, K. Cibulskis, A. Sivachenko, S. L. Carter, C. Stewart, C. H. Mermel, S. A. Roberts, A. Kiezun, P. S. Hammerman, A. McKenna, Y. Drier, L. Zou, A. H. Ramos, T. J. Pugh, N. Stransky, E. Helman, J. Kim, C. Sougnez, L. Ambrogio, E. Nickerson, E. Shefler, M. L. Cortes, D. Auclair, G. Saksena, D. Voet, M. Noble, D. DiCara, P. Lin, L. Lichtenstein, D. I. Heiman, T. Fennell, M. Imielinski, B. Hernandez, E. Hodis, S. Baca, A. M. Dulak, J. Lohr, D. A. Landau, C. J. Wu, J. Melendez-Zajgla, A. Hidalgo-Miranda, A. Koren, S. A. McCarroll, J. Mora, R. S. Lee, B. Crompton, R. Onofrio, M. Parkin, W. Winckler, K. Ardlie, S. B. Gabriel, C. W. Roberts, J. A. Biegel, K. Stegmaier, A. J. Bass, L. A. Garraway, M. Meyerson, T. R. Golub, D. A. Gordenin, S. Sunyaev, E. S. Lander and G. Getz (2013). "Mutational heterogeneity in cancer and the search for new cancer-associated genes." Nature **499**(7457): 214-218.

Laws, H. J., S. Burdach, B. van Kaick, B. Engel, U. Dirksen, D. Korholz, H. Pape, T. Kahn, H. Merck, M. Schmitz, A. Heyll, B. Dockhorn-Dworniczak, H. Jurgens and U. Gobel (1999). "Multimodality diagnostics and megatherapy in poor prognosis Ewing's tumor patients. A single-center report." Strahlenther Onkol **175**(10): 488-494.

Leisegang, M., B. Engels, P. Meyerhuber, E. Kieback, D. Sommermeyer, S. A. Xue, S. Reuss, H. Stauss and W. Uckert (2008). "Enhanced functionality of T cell receptor-redirected T cells is defined by the transgene cassette." J Mol Med (Berl) **86**(5): 573-583.

Leisegang, M., S. Wilde, S. Spranger, S. Milosevic, B. Frankenberger, W. Uckert and D. J. Schendel (2010). "MHC-restricted fratricide of human lymphocytes expressing survivin-specific transgenic T cell receptors." J Clin Invest **120**(11): 3869-3877.

Lessnick, S. L., C. S. Dacwag and T. R. Golub (2002). "The Ewing's sarcoma oncoprotein EWS/FLI induces a p53-dependent growth arrest in primary human fibroblasts." Cancer Cell **1**(4): 393-401.

Lin, T. M., S. P. Galbert, D. Kiefer, W. N. Spellacy and S. Gall (1974). "Characterization of four human pregnancy-associated plasma proteins." Am J Obstet Gynecol **118**(2): 223-236.

Linette, G. P., E. A. Stadtmauer, M. V. Maus, A. P. Rapoport, B. L. Levine, L. Emery, L. Litzky, A. Bagg, B. M. Carreno, P. J. Cimino, G. K. Binder-Scholl, D. P. Smethurst, A. B. Gerry, N. J. Pumphrey, A. D. Bennett, J. E. Brewer, J. Dukes, J. Harper, H. K. Tayton-Martin, B. K. Jakobsen, N. J. Hassan, M. Kalos and C. H. June (2013). "Cardiovascular toxicity and titin cross-reactivity of affinity-enhanced T cells in myeloma and melanoma." Blood **122**(6): 863-871.

Loddo, M., J. Andryszkiewicz, S. Rodriguez-Acebes, K. Stoeber, A. Jones, D. Dafou, S. Apostolidou, A. Wollenschlaeger, M. Widschwendter, R. Sainsbury, S. Tudzarova and G. H. Williams (2014). "Pregnancy-associated plasma protein A regulates mitosis and is epigenetically silenced in breast cancer." J Pathol **233**(4): 344-356.

Lucas, K. G., C. Schwartz and J. Kaplan (2008). "Allogeneic stem cell transplantation in a patient with relapsed Ewing sarcoma." Pediatr Blood Cancer **51**(1): 142-144.

Luo, W., K. Gangwal, S. Sankar, K. M. Boucher, D. Thomas and S. L. Lessnick (2009). "GSTM4 is a microsatellite-containing EWS/FLI target involved in Ewing's sarcoma oncogenesis and therapeutic resistance." Oncogene **28**(46): 4126-4132.

Marmont, A. M., M. M. Horowitz, R. P. Gale, K. Sobocinski, R. C. Ash, D. W. van Bekkum, R. E. Champlin, K. A. Dicke, J. M. Goldman, R. A. Good and et al. (1991). "T-cell depletion of HLA-identical transplants in leukemia." Blood **78**(8): 2120-2130.

Mason, D. (1998). "A very high level of crossreactivity is an essential feature of the T-cell receptor." Immunol Today **19**(9): 395-404.

Mathe, G., J. L. Amiel, L. Schwarzenberg, A. Cattan, M. Schneider, M. J. Devries, M. Tubiana, C. Lalanne, J. L. Binet, M. Papiernik, G. Seman, M. Matsukura, A. M. Mery, V. Schwarzmann and A. Flaisler (1965). "Successful Allogenic Bone Marrow Transplantation in Man: Chimerism, Induced Specific Tolerance and Possible Anti-Leukemic Effects." Blood **25**: 179-196.

Maude, S. L., N. Frey, P. A. Shaw, R. Aplenc, D. M. Barrett, N. J. Bunin, A. Chew, V. E. Gonzalez, Z. Zheng, S. F. Lacey, Y. D. Mahnke, J. J. Melenhorst, S. R. Rheingold, A. Shen, D. T. Teachey, B. L. Levine, C. H. June, D. L. Porter and S. A. Grupp (2014). "Chimeric antigen receptor T cells for sustained remissions in leukemia." N Engl J Med **371**(16): 1507-1517.

Mellman, I., G. Coukos and G. Dranoff (2011). "Cancer immunotherapy comes of age." Nature **480**(7378): 480-489.

Meyer-Wentrup, F., G. Richter and S. Burdach (2005). "Identification of an immunogenic EWS-FLI1-derived HLA-DR-restricted T helper cell epitope." Pediatr Hematol Oncol **22**(4): 297-308.

Miller, B. S., J. T. Bronk, T. Nishiyama, H. Yamagiwa, A. Srivastava, M. E. Bolander and C. A. Conover (2007). "Pregnancy associated plasma protein-A is necessary for expeditious fracture healing in mice." J Endocrinol **192**(3): 505-513.

Miyagawa, Y., H. Okita, H. Nakaijima, Y. Horiuchi, B. Sato, T. Taguchi, M. Toyoda, Y. U. Katagiri, J. Fujimoto, J. Hata, A. Umezawa and N. Kiyokawa (2008). "Inducible expression of chimeric EWS/ETS proteins confers Ewing's family tumor-like phenotypes to human mesenchymal progenitor cells." Mol Cell Biol **28**(7): 2125-2137.

Mohan, S., Y. Nakao, Y. Honda, E. Landale, U. Leser, C. Dony, K. Lang and D. J. Baylink (1995). "Studies on the mechanisms by which insulin-like growth factor (IGF) binding protein-4 (IGFBP-4) and IGFBP-5 modulate IGF actions in bone cells." J Biol Chem **270**(35): 20424-20431.

Morgan, R. A., N. Chinnasamy, D. Abate-Daga, A. Gros, P. F. Robbins, Z. Zheng, M. E. Dudley, S. A. Feldman, J. C. Yang, R. M. Sherry, G. Q. Phan, M. S. Hughes, U. S. Kammula, A. D. Miller, C. J. Hessman, A. A. Stewart, N. P. Restifo, M. M. Quezado, M. Alimchandani, A. Z. Rosenberg, A. Nath, T. Wang, B. Bielekova, S. C. Wuest, N. Akula, F. J. McMahon, S. Wilde, B. Mosetter, D. J. Schendel, C. M. Laurencot and S. A. Rosenberg (2013). "Cancer regression and neurological toxicity following anti-MAGE-A3 TCR gene therapy." J Immunother **36**(2): 133-151.

Morgan, R. A., M. E. Dudley, J. R. Wunderlich, M. S. Hughes, J. C. Yang, R. M. Sherry, R. E. Royal, S. L. Topalian, U. S. Kammula, N. P. Restifo, Z. Zheng, A. Nahvi, C. R. de Vries, L. J. Rogers-Freezer, S. A. Mavroukakis and S. A. Rosenberg (2006). "Cancer regression in patients after transfer of genetically engineered lymphocytes." Science **314**(5796): 126-129.

Morgan, R. A., J. C. Yang, M. Kitano, M. E. Dudley, C. M. Laurencot and S. A. Rosenberg (2010). "Case report of a serious adverse event following the administration of T cells transduced with a chimeric antigen receptor recognizing ERBB2." Mol Ther **18**(4): 843-851.

Moris, A., V. Teichgraber, L. Gauthier, H. J. Buhring and H. G. Rammensee (2001). "Cutting edge: characterization of allorestricted and peptide-selective alloreactive T cells using HLA-tetramer selection." J Immunol **166**(8): 4818-4821.

Mutis, T., E. Blokland, M. Kester, E. Schrama and E. Goulmy (2002). "Generation of minor histocompatibility antigen HA-1-specific cytotoxic T cells restricted by nonself HLA molecules: a potential strategy to treat relapsed leukemia after HLA-mismatched stem cell transplantation." Blood **100**(2): 547-552.

Nagarajan, N., D. Bertrand, A. M. Hillmer, Z. J. Zang, F. Yao, P. E. Jacques, A. S. Teo, I. Cutcutache, Z. Zhang, W. H. Lee, Y. Y. Sia, S. Gao, P. N. Ariyaratne, A. Ho, X. Y. Woo, L. Veeravali, C. K. Ong, N. Deng, K. V. Desai, C. C. Khor, M. L. Hibberd, A. Shahab, J. Rao, M. Wu, M. Teh, F. Zhu, S. Y. Chin, B. Pang, J. B. So, G. Bourque, R. Soong, W. K. Sung, B. Tean Teh, S. Rozen, X. Ruan, K. G. Yeoh, P. B. Tan and Y. Ruan (2012). "Whole-genome reconstruction and mutational signatures in gastric cancer." Genome Biol **13**(12): R115.

Negrin, R. S. (2015). "Graft-versus-host disease versus graft-versus-leukemia." Hematology Am Soc Hematol Educ Program **2015**: 225-230.

Neilsen, P. M., K. I. Pishas, D. F. Callen and D. M. Thomas (2011). "Targeting the p53 Pathway in Ewing Sarcoma." Sarcoma **2011**: 746939.

Nicholson, E., S. Ghorashian and H. Stauss (2012). "Improving TCR Gene Therapy for Treatment of Haematological Malignancies." Adv Hematol **2012**: 404081.

Oxvig, C., O. Sand, T. Kristensen, G. J. Gleich and L. Sottrup-Jensen (1993). "Circulating human pregnancy-associated plasma protein-A is disulfide-bridged to the proform of eosinophil major basic protein." J Biol Chem **268**(17): 12243-12246.

Pfeilschifter, J., F. Laukhuf, B. Muller-Beckmann, W. F. Blum, T. Pfister and R. Ziegler (1995). "Parathyroid hormone increases the concentration of insulin-like growth factor-I and transforming growth factor beta 1 in rat bone." J Clin Invest **96**(2): 767-774.

Potikyan, G., K. A. France, M. R. Carlson, J. Dong, S. F. Nelson and C. T. Denny (2008). "Genetically defined EWS/FLI1 model system suggests mesenchymal origin of Ewing's family tumors." Lab Invest **88**(12): 1291-1302.

Powell, D. J., Jr., M. E. Dudley, P. F. Robbins and S. A. Rosenberg (2005). "Transition of late-stage effector T cells to CD27+ CD28+ tumor-reactive effector memory T cells in humans after adoptive cell transfer therapy." Blood **105**(1): 241-250.

Prieur, A., F. Tirode, P. Cohen and O. Delattre (2004). "EWS/FLI-1 silencing and gene profiling of Ewing cells reveal downstream oncogenic pathways and a crucial role for repression of insulin-like growth factor binding protein 3." Mol Cell Biol **24**(16): 7275-7283.

Rai, R., J. J. Kim, S. Misra, A. Kumar and B. Mittal (2015). "A Multiple Interaction Analysis Reveals ADRB3 as a Potential Candidate for Gallbladder Cancer Predisposition via a Complex Interaction with Other Candidate Gene Variations." Int J Mol Sci **16**(12): 28038-28049.

Rammensee, H., J. Bachmann, N. P. Emmerich, O. A. Bachor and S. Stevanovic (1999). "SYFPEITHI: database for MHC ligands and peptide motifs." Immunogenetics **50**(3-4): 213-219.

Rehage, M., S. Mohan, J. E. Wergedal, B. Bonafede, K. Tran, D. Hou, D. Phang, A. Kumar and X. Qin (2007). "Transgenic overexpression of pregnancy-associated plasma protein-A increases the somatic growth and skeletal muscle mass in mice." Endocrinology **148**(12): 6176-6185.

Restifo, N. P., M. E. Dudley and S. A. Rosenberg (2012). "Adoptive immunotherapy for cancer: harnessing the T cell response." Nat Rev Immunol **12**(4): 269-281.

Richter, G. H., S. Plehm, A. Fasan, S. Rossler, R. Unland, I. M. Bennani-Baiti, M. Hotfilder, D. Lowel, I. von Luettichau, I. Mossbrugger, L. Quintanilla-Martinez, H. Kovar, M. S. Staege, C. Muller-Tidow and S. Burdach (2009). "EZH2 is a mediator of EWS/FLI1 driven tumor growth and metastasis blocking endothelial and neuro-ectodermal differentiation." Proc Natl Acad Sci U S A **106**(13): 5324-5329.

Riddell, S. R., M. Elliott, D. A. Lewinsohn, M. J. Gilbert, L. Wilson, S. A. Manley, S. D. Lupton, R. W. Overell, T. C. Reynolds, L. Corey and P. D. Greenberg (1996). "T-cell mediated rejection of gene-modified HIV-specific cytotoxic T lymphocytes in HIV-infected patients." Nat Med **2**(2): 216-223.

Riggi, N., L. Cironi, P. Provero, M. L. Suva, K. Kaloulis, C. Garcia-Echeverria, F. Hoffmann, A. Trumpp and I. Stamenkovic (2005). "Development of Ewing's sarcoma from primary bone marrow-derived mesenchymal progenitor cells." Cancer Res **65**(24): 11459-11468.

Riggi, N., B. Knoechel, S. M. Gillespie, E. Rheinbay, G. Boulay, M. L. Suva, N. E. Rossetti, W. E. Boonseng, O. Oksuz, E. B. Cook, A. Formey, A. Patel, M. Gymrek, V. Thapar, V. Deshpande, D. T. Ting, F. J. Hornicek, G. P. Nielsen, I. Stamenkovic, M. J. Aryee, B. E. Bernstein and M. N. Rivera (2014). "EWS-FLI1 utilizes divergent chromatin remodeling mechanisms to directly activate or repress enhancer elements in Ewing sarcoma." Cancer Cell **26**(5): 668-681.

Ringden, O., H. Karlsson, R. Olsson, B. Omazic and M. Uhlin (2009). "The allogeneic graft-versus-cancer effect." Br J Haematol **147**(5): 614-633.

Robbins, P. F., M. El-Gamil, Y. F. Li, Y. Kawakami, D. Loftus, E. Appella and S. A. Rosenberg (1996). "A mutated beta-catenin gene encodes a melanoma-specific antigen recognized by tumor infiltrating lymphocytes." J Exp Med **183**(3): 1185-1192.

Robbins, P. F., Y. C. Lu, M. El-Gamil, Y. F. Li, C. Gross, J. Gartner, J. C. Lin, J. K. Teer, P. Cliften, E. Tycksen, Y. Samuels and S. A. Rosenberg (2013). "Mining exomic sequencing data to identify mutated antigens recognized by adoptively transferred tumor-reactive T cells." Nat Med **19**(6): 747-752.

Robins, H. S., P. V. Campregher, S. K. Srivastava, A. Wacher, C. J. Turtle, O. Kahsai, S. R. Riddell, E. H. Warren and C. S. Carlson (2009). "Comprehensive assessment of T-cell receptor beta-chain diversity in alphabeta T cells." Blood **114**(19): 4099-4107.

Rosenberg, S. A., J. C. Yang, R. M. Sherry, U. S. Kammula, M. S. Hughes, G. Q. Phan, D. E. Citrin, N. P. Restifo, P. F. Robbins, J. R. Wunderlich, K. E. Morton, C. M. Laurencot, S. M. Steinberg, D. E. White and M. E. Dudley (2011). "Durable complete responses in heavily pretreated patients with metastatic melanoma using T-cell transfer immunotherapy." Clin Cancer Res **17**(13): 4550-4557.

Rudolph, M. G., R. L. Stanfield and I. A. Wilson (2006). "How TCRs bind MHCs, peptides, and coreceptors." Annu Rev Immunol **24**: 419-466.

Ruella, M. and M. Kalos (2014). "Adoptive immunotherapy for cancer." Immunol Rev **257**(1): 14-38.

Sadovnikova, E., L. A. Jopling, K. S. Soo and H. J. Stauss (1998). "Generation of human tumor-reactive cytotoxic T cells against peptides presented by non-self HLA class I molecules." Eur J Immunol **28**(1): 193-200.

Sadovnikova, E. and H. J. Stauss (1996). "Peptide-specific cytotoxic T lymphocytes restricted by nonself major histocompatibility complex class I molecules: reagents for tumor immunotherapy." Proc Natl Acad Sci U S A **93**(23): 13114-13118.

Saillard, C., R. Crocchiolo, S. Furst, J. El-Cheikh, L. Castagna, A. Signori, C. Oudin, C. Faucher, C. Lemarie, C. Chabannon, A. Granata and D. Blaise (2014). "National Institutes of Health classification for chronic graft-versus-host disease predicts outcome of allo-hematopoietic stem cell transplant after fludarabine-busulfan-antithymocyte globulin conditioning regimen." Leuk Lymphoma **55**(5): 1106-1112.

Schirle, M., W. Keilholz, B. Weber, C. Gouttefangeas, T. Dumrese, H. D. Becker, S. Stevanovic and H. G. Rammensee (2000). "Identification of tumor-associated MHC class I ligands by a novel T cell-independent approach." Eur J Immunol **30**(8): 2216-2225.

Schirmer, D., T. G. Grunewald, R. Klar, O. Schmidt, D. Wohlleber, R. A. Rubio, W. Uckert, U. Thiel, F. Bohne, D. H. Busch, A. M. Krackhardt, S. Burdach and G. H. Richter (2016). "Transgenic antigen-specific, HLA-A*02:01-allo-restricted cytotoxic T cells recognize tumor-associated target antigen STEAP1 with high specificity." Oncoimmunology **5**(6): e1175795.

Schleiermacher, G., M. Peter, O. Oberlin, T. Philip, H. Rubie, F. Mechinaud, D. Sommelet-Olive, J. Landman-Parker, D. Bours, J. Michon, O. Delattre and P. Societe Francaise d'Oncologie (2003). "Increased risk of systemic relapses associated with bone marrow micrometastasis and circulating tumor cells in localized ewing tumor." J Clin Oncol **21**(1): 85-91.

Schmidt, D., D. Harms and S. Burdach (1985). "Malignant peripheral neuroectodermal tumours of childhood and adolescence." Virchows Arch A Pathol Anat Histopathol **406**(3): 351-365.

Schuster, I. G., D. H. Busch, E. Eppinger, E. Kremmer, S. Milosevic, C. Hennard, C. Kuttler, J. W. Ellwart, B. Frankenberger, E. Nossner, C. Salat, C. Bogner, A. Borkhardt, H. J. Kolb and A. M. Krackhardt (2007). "Allorestricted T cells with specificity for the FMNL1-derived peptide PP2 have potent antitumor activity against hematologic and other malignancies." Blood **110**(8): 2931-2939.

Scotlandi, K., S. Benini, M. Sarti, M. Serra, P. L. Lollini, D. Maurici, P. Picci, M. C. Manara and N. Baldini (1996). "Insulin-like growth factor I receptor-mediated circuit in Ewing's sarcoma/peripheral neuroectodermal tumor: a possible therapeutic target." Cancer Res **56**(20): 4570-4574.

Sewell, A. K. (2012). "Why must T cells be cross-reactive?" Nat Rev Immunol **12**(9): 669-677.

Shresta, S., C. T. Pham, D. A. Thomas, T. A. Graubert and T. J. Ley (1998). "How do cytotoxic lymphocytes kill their targets?" Curr Opin Immunol **10**(5): 581-587.

Singh-Jasuja, H., N. P. Emmerich and H. G. Rammensee (2004). "The Tubingen approach: identification, selection, and validation of tumor-associated HLA peptides for cancer therapy." Cancer Immunol Immunother **53**(3): 187-195.

Sommermeyer, D. and W. Uckert (2010). "Minimal amino acid exchange in human TCR constant regions fosters improved function of TCR gene-modified T cells." J Immunol **184**(11): 6223-6231.

Staege, M. S., C. Hutter, I. Neumann, S. Foja, U. E. Hattenhorst, G. Hansen, D. Afar and S. E. Burdach (2004). "DNA microarrays reveal relationship of Ewing family tumors to both endothelial and fetal neural crest-derived cells and define novel targets." Cancer Res **64**(22): 8213-8221.

Steinle, A., C. Reinhardt, P. Jantzer and D. J. Schendel (1995). "In vivo expansion of HLA-B35 alloreactive T cells sharing homologous T cell receptors: evidence for maintenance of an oligoclonally dominated allospecificity by persistent stimulation with an autologous MHC/peptide complex." J Exp Med **181**(2): 503-513.

Straathof, K. C., M. A. Pule, P. Yotnda, G. Dotti, E. F. Vanin, M. K. Brenner, H. E. Heslop, D. M. Spencer and C. M. Rooney (2005). "An inducible caspase 9 safety switch for T-cell therapy." Blood **105**(11): 4247-4254.

Takashima, Y., T. Era, K. Nakao, S. Kondo, M. Kasuga, A. G. Smith and S. Nishikawa (2007). "Neuroepithelial cells supply an initial transient wave of MSC differentiation." Cell **129**(7): 1377-1388.

Takezaki, T., N. Hamajima, K. Matsuo, R. Tanaka, T. Hirai, T. Kato, K. Ohashi and K. Tajima (2001). "Association of polymorphisms in the beta-2 and beta-3 adrenoceptor genes with risk of colorectal cancer in Japanese." Int J Clin Oncol **6**(3): 117-122.

Thiel, U., S. Pirson, C. Muller-Spahn, H. Conrad, D. H. Busch, H. Bernhard, S. Burdach and G. H. Richter (2011). "Specific recognition and inhibition of Ewing tumour growth by antigen-specific allo-restricted cytotoxic T cells." Br J Cancer **104**(6): 948-956.

Thiel, U., A. Wawer, I. von Luettichau, H. U. Bender, F. Blaeschke, T. G. Grunewald, M. Steinborn, B. Roper, H. Bonig, T. Klingebiel, P. Bader, E. Koscielniak, M. Paulussen, U. Dirksen, H. Juergens, H. J. Kolb and S. E. Burdach (2016). "Bone marrow involvement identifies a subgroup of advanced Ewing sarcoma patients with fatal outcome irrespective of therapy in contrast to curable patients with multiple bone metastases but unaffected marrow." Oncotarget.

Thiel, U., A. Wawer, P. Wolf, M. Badoglio, A. Santucci, T. Klingebiel, O. Basu, A. Borkhardt, H. J. Laws, Y. Kodera, A. Yoshimi, C. Peters, R. Ladenstein, A. Pession, A. Prete, E. C. Urban, W. Schwinger, P. Bordigoni, A. Salmon, M. A. Diaz, B. Afanasyev, I. Lisukov, E. Morozova, A. Toren, B. Bielorai, J. Korsakas, F. Fagioli, D. Caselli, G. Ehninger, B. Gruhn, U. Dirksen, F. Abdel-Rahman, M. Aglietta, E. Mastrodicasa, M. Torrent, P. Corradini, F. Demeocq, G. Dini, P. Dreger, M. Eyrich, J. Gozdzik, F. Guilhot, E. Holler, E. Koscielniak, C. Messina, D. Nachbaur, R. Sabbatini, E. Oldani, H. Ottinger, H. Ozsahin, R. Schots, S. Siena, J. Stein, S. Sufliarska, A. Unal, M. Ussowicz, P. Schneider, W. Woessmann, H. Jurgens, M. Bregni, S. Burdach, P. Solid Tumor Working, B. the Pediatric DiseaseWorking Party of the European Group for, T. Marrow, B. Asia Pacific, T. Marrow, T. Pediatric Registry for Stem Cell and E. S. G. Meta (2011). "No improvement of survival with reduced- versus high-intensity conditioning for allogeneic stem cell transplants in Ewing tumor patients." Ann Oncol **22**(7): 1614-1621.

Thomas, S., H. J. Stauss and E. C. Morris (2010). "Molecular immunology lessons from therapeutic T-cell receptor gene transfer." Immunology **129**(2): 170-177.

Tiberghien, P., C. Ferrand, B. Lioure, N. Milpied, R. Angonin, E. Deconinck, J. M. Certoux, E. Robinet, P. Saas, B. Petracca, C. Juttner, C. W. Reynolds, D. L. Longo, P. Herve and J. Y. Cahn (2001). "Administration of herpes simplex-thymidine kinase-expressing donor T cells with a T-cell-depleted allogeneic marrow graft." Blood **97**(1): 63-72.

Tiberghien, P., C. W. Reynolds, J. Keller, S. Spence, M. Deschaseaux, J. M. Certoux, E. Contassot, W. J. Murphy, R. Lyons, Y. Chiang and et al. (1994). "Ganciclovir treatment of herpes simplex thymidine kinase-transduced primary T lymphocytes: an approach for specific in vivo donor T-cell depletion after bone marrow transplantation?" Blood **84**(4): 1333-1341.

Tirode, F., K. Laud-Duval, A. Prieur, B. Delorme, P. Charbord and O. Delattre (2007). "Mesenchymal stem cell features of Ewing tumors." Cancer Cell **11**(5): 421-429.

Traggiai, E., L. Chicha, L. Mazzucchelli, L. Bronz, J. C. Piffaretti, A. Lanzavecchia and M. G. Manz (2004). "Development of a human adaptive immune system in cord blood cell-transplanted mice." Science **304**(5667): 104-107.

UniProt. "UniProt." from http://www.uniprot.org.

Uren, A. and J. A. Toretsky (2005). "Ewing's sarcoma oncoprotein EWS-FLI1: the perfect target without a therapeutic agent." Future Oncol **1**(4): 521-528.

Uwe Thiel, A. W., Irene von Luettichau, Hans-Ulrich Bender, Franziska Blaeschke,Thomas G.P. Grunewald, Marc Steinborn, Barbara Röper, Halvard Bonig, Thomas Klingebiel, Peter Bader, Ewa Koscielniak, Michael Paulussen, Uta Dirksen, Heribert Juergens, Hans-Jochem Kolb, Stefan E.G. Burdach (2016). "Bone marrow involvement identifies a subgroup of advanced Ewing sarcoma patients with fatal outcome irrespective of therapy in contrast to curable patients with multiple bone metastases but unaffected marrow." Oncotarget.

Voskoboinik, I., M. J. Smyth and J. A. Trapani (2006). "Perforin-mediated target-cell death and immune homeostasis." Nat Rev Immunol **6**(12): 940-952.

Walia, V., E. W. Mu, J. C. Lin and Y. Samuels (2012). "Delving into somatic variation in sporadic melanoma." Pigment Cell Melanoma Res **25**(2): 155-170.

Wang, X., C. Berger, C. W. Wong, S. J. Forman, S. R. Riddell and M. C. Jensen (2011). "Engraftment of human central memory-derived effector CD8+ T cells in immunodeficient mice." Blood **117**(6): 1888-1898.

Weiden, P. L., K. M. Sullivan, N. Flournoy, R. Storb and E. D. Thomas (1981). "Antileukemic effect of chronic graft-versus-host disease: contribution to improved survival after allogeneic marrow transplantation." N Engl J Med **304**(25): 1529-1533.

Whitelegg, A. M., L. E. Oosten, S. Jordan, M. Kester, A. G. van Halteren, J. A. Madrigal, E. Goulmy and L. D. Barber (2005). "Investigation of peptide involvement in T cell allorecognition using recombinant HLA class I multimers." J Immunol **175**(3): 1706-1714.

Wooldridge, L., J. Ekeruche-Makinde, H. A. van den Berg, A. Skowera, J. J. Miles, M. P. Tan, G. Dolton, M. Clement, S. Llewellyn-Lacey, D. A. Price, M. Peakman and A. K. Sewell (2012). "A single autoimmune T cell receptor recognizes more than a million different peptides." J Biol Chem **287**(2): 1168-1177.

9. Publications

Parts of this doctoral thesis have already been published:

Andreas Kirschner, Melanie Thiede, Franziska Blaeschke, Günther H.S. Richter, Julia S. Gerke, Michaela C. Baldauf, Thomas G.P. Grünewald, Dirk H. Busch, Stefan Burdach, Uwe Thiel (2016). *Lysosome-associated membrane glycoprotein 1 predicts fratricide amongst T cell receptor transgenic CD8+ T cells directed against tumor-associated antigens.*
Oncotarget. 2016 Jul 18. doi: 10.18632/oncotarget.10647. PMID: 27447745

Andreas Kirschner, Melanie Thiede, Rebecca Alba Rubio, Günther HS Richter, Thomas Kirchner, Thomas G.P. Grünewald, Dirk H. Busch, Stefan Burdach, Uwe Thiel.
Pappalysin T Cell Receptor Transgenic Allorestricted T Cells Specificlly Kill Ewing Sarcoma In Vitro and In Vivo.
Manuscript in preparation.

Franziska Blaeschke, Uwe Thiel, **Andreas Kirschner**, Melanie Thiede, Rebecca Alba Rubio, David Schirmer, Thomas Kirchner, Günther H.S. Richter, Sabine Mall, Richard Klar, Stanley Riddell, Dirk H. Busch, Angela Krackhardt, Thomas G.P. Grunewald, Stefan Burdach (2016). *Human HLA-A*02:01/CHM1+ allo-restricted T cell receptor transgenic CD8+ T Cells specifically inhibit Ewing sarcoma growth in vitro and in vivo.*
Oncotarget. 2016 May 7. doi: 10.18632/oncotarget.9218. PMID: 27281613

10. Appendices

10.1 Supplemental tables

Table 25: ADRB3-1F4wt TCR sequence

ADRB3-1F4wt	ATGAGCAACCAGGTGCTCTGCTGTGTGGTCCTTTGTTTCCTGGGAGCAAA CACCGTGGATGGTGGAATCACTCAGTCCCCAAAGTACCTGTTCAGAAAG GAAGGACAGAATGTGACCCTGAGTTGTGAACAGAATTTGAACCACGATGC CATGTACTGGTACCGACAGGACCCAGGGCAAGGGCTGAGATTGATCTAC TACTCACAGATAGTAAATGACTTTCAGAAAGGAGATATAGCTGAAGGGTA CAGCGTCTCTCGGGAGAAGAAGGAATCCTTTCCTCTCACTGTGACATCG GCCCAAAAGAACCCGACAGCTTTCTATCTCTGTGCCAGTACTACAACGGG GGTGAATGAGCAGTTCTTCGGGCCAGGGACACGGCTCACCGTGCTAGAA GATCTGCGGAACGTGACCCCCCCTAAGGTGTCCCTGTTCGAGCCCAGCA AGGCCGAGATCGCCAACAAGCAGAAAGCCACCCTGGTCTGCCTGGCTAG GGGCTTCTTCCCCGACCACGTGGAGCTGTCTTGGTGGGTGAACGGCAAA GAGGTGCACAGCGGCGTCAGCACCGACCCACAGGCCTACAAAGAGAGC AACTACAGCTACTGCCTGTCCTCTAGACTGCGGGTGTGCGCCACCTTCT GGCACAACCCCCGGAACCACTTCCGGTGCCAGGTGCAGTTCCACGGCCT GAGCGAAGAGGACAAGTGGCCCGAGGGCAGCCCCAAGCCCGTGACACA GAACATCAGCGCCGAGGCCTGGGGCAGAGCCGACTGCGGCATCACCAG CGCCAGCTACCACCAGGGCGTGCTGTCTGCCACCATCCTGTACGAGATC CTGCTGGGCAAGGCCACCCTGTACGCCGTGCTGGTGTCCGGCCTGGTG CTGATGGCCATGGTGAAGAAGAAGAACAGCGGCAGCGGCGCCACCAAC TTCAGCCTGCTGAAACAGGCCGGCGACGTGGAAGAGAACCCTGGCCCTA TGATGAAATCCTTGAGAGTTTTACTAGTGATCCTGTGGCTTCAGTTGAGCT GGGTTTGGAGCCAACAGAAGGAGGTGGAGCAGAATTCTGGACCCCTCAG TGTTCCAGAGGGAGCCATTGCCTCTCTCAACTGCACTTACAGTGACCGAG GTTCCCAGTCCTTCTTCTGGTACAGACAATATTCTGGGAAAAGCCCTGAG TTGATAATGTCCATATACTCCAATGGTGACAAAGAAGATGGAAGGTTTACA GCACAGCTCAATAAAGCCAGCCAGTATGTTTCTCTGCTCATCAGAGACTC CCAGCCCAGTGATTCAGCCACCTACCTCTGTGCCGTGGGTAACGACTAC AAGCTCAGCTTTGGAGCCGGAACCACAGTAACTGTAAGAGCAAATATCCA GAACCCCGAGCCCGCCGTGTACCAGCTGAAGGACCCCAGATCTCAGGA CTCTACACTGTGCCTGTTCACCGACTTCGACAGCCAGATCAACGTGCCCA AGACCATGGAAAGCGGCACCTTCATCACCGACAAGACCGTGCTGGACAT GAAGGCCATGGACAGCAAGAGCAACGGCGCCATTGCCTGGTCCAATCAG ACCAGCTTCACATGCCAGGACATCTTCAAAGAGACAAACGCCTGCTACCC CAGCTCCGACGTGCCCTGCGACGCCACCCTGACCGAGAAGAGCTTCGA GACAGACATGAACCTGAATTTCCAGAACCTGAGCGTGATGGGCCTGAGG ATCCTGCTGCTGAAGGTGGCCGGCTTCAATCTGCTGATGACCCTGCGGC TGTGGAGCAGCTGA

Table 26: ADRB3-1F4mm TCR sequence with modifications

ADRB3-1F4mm	ATGAGCAACCAGGTGCTCTGCTGTGTGGTCCTTTGTTTCCTGGGAGCAAA CACCGTGGATGGTGGAATCACTCAGTCCCCAAAGTACCTGTTCAGAAAG GAAGGACAGAATGTGACCCTGAGTTGTGAACAGAATTTGAACCACGATGC CATGTACTGGTACCGACAGGACCCAGGGCAAGGGCTGAGATTGATCTAC TACTCACAGATAGTAAATGACTTTCAGAAAGGAGATATAGCTGAAGGGTA CAGCGTCTCTCGGGAGAAGAAGGAATCCTTTCCTCTCACTGTGACATCG GCCCAAAAGAACCCGACAGCTTTCTATCTCTGTGCCAGTACTACAACGGG GGTGAATGAGCAGTTCTTCGGGCCAGGGACACGGCTCACCGTGCTAGAG GACCTGAAAAACGTGTTCCCACCCGAGGTCGCTGTGTTTGAGCCATCAAA GGCAGAGATCGCTCACACCCAAAAGGCCACACTGGTGTGCCTGGCCACA

	GGCTTCTACCCCGACCACGTGGAGCTGAGCTGGTGGGTGAATGGGAAG GAGGTGCACAGTGGGGTCAGCACAGACCCGCAGCCCCTCAAGGAGCAG CCCGCCCTCAATGACTCCAGATACTGCCTGAGCAGCCGCCTGAGGGTCT CGGCCACCTTCTGGCAGAACCCCCGCAACCACTTCCGCTGTCAAGTCCA GTTCTACGGGCTCTCGGAGAATGACGAGTGGACCCAGGATAGGGCCAAA CCTGTCACCCAGATCGTCAGCGCCGAGGCCTGGGGTAGAGCAGACTGT GGCATAACCTCCGCTTCTTACCATCAAGGGGTCCTGTCTGCCACCATCCT CTATGAGATCTTGCTAGGGAAGGCCACCTTGTATGCCGTGCTGGTCAGT GCCCTCGTGCTGATGGCCATGGTCAAGAGAAAGGATTCCAGAGGCGGCA GCGGCGCCACCAACTTCAGCCTGCTGAAACAGGCCGGCGACGTGGAAG AGAACCCTGGCCCTATGATGAAATCCTTGAGAGTTTTACTAGTGATCCTG TGGCTTCAGTTGAGCTGGGTTTGGAGCCAACAGAAGGAGGTGGAGCAGA ATTCTGGACCCCTCAGTGTTCCAGAGGGAGCCATTGCCTCTCTCAACTGC ACTTACAGTGACCGAGGTTCCCAGTCCTTCTTCTGGTACAGACAATATTC TGGGAAAAGCCCTGAGTTGATAATGTCCATATACTCCAATGGTGACAAAG AAGATGGAAGGTTTACAGCACAGCTCAATAAAGCCAGCCAGTATGTTTCT CTGCTCATCAGAGACTCCCAGCCCAGTGATTCAGCCACCTACCTCTGTGC CGTGGGTAACGACTACAAGCTCAGCTTTGGAGCCGGAACCACAGTAACT GTAAGAGCAAATATCCAGAACCCTGACCCTGCCGTGTACCAGCTGAGAG ACTCTAAATCCAGTGACAAGTCTGTCTGCCTATTCACCGATTTTGATTCTC AAACAAATGTGTCACAAAGTAAGGATTCTGATGTGTATATCACAGACAAAA CTGTGCTAGACATGAGGTCTATGGACTTCAAGAGCAACAGTGCTGTGGC CTGGAGCAACAAATCTGACTTTGCATGTGCAAACGCCTTCAACAACAGCA TTATTCCAGAAGACACCTTCTTCCCCAGTGACGTCCCTTCCTGTGATGTC AAGCTGGTCGAGAAAAGCTTTGAAACAGATACGAACCTAAACTTTCAAAA CCTGTCAGTGATTGGGTTCCGAATCCTCCTCCTGAAAGTGGCCGGGTTTA ATCTGCTCATGACGCTGCGGCTGTGGTCCAGCTGA

Table 27: PAPPA-2G6wt TCR sequence

PAPPA-2G6wt	ATGGGCTGCAGGCTGCTCTGCTGTGCGGTTCTCTGTCTCCTGGGAGCGG TCCCCATGGAAACGGGAGTTACGCAGACACCAAGACACCTGGTCATGGG AATGACAAATAAGAAGTCTTTGAAATGTGAACAACATCTGGGTCATAACG CTATGTATTGGTACAAGCAAAGTGCTAAGAAGCCACTGGAGCTCATGTTT GTCTACAGTCTTGAAGAACGGGTTGAAAACAACAGTGTGCCAAGTCGCTT CTCACCTGAATGCCCCAACAGCTCTCACTTATTCCTTCACCTACACACCC TGCAGCCAGAAGACTCGGCCCTGTATCTCTGCGCCAGCAGCCAAGTAGT AGCGGACAATGAGCAGTTCTTCGGGCCAGGGACACGGCTCACCGTGCTA GAGGACCTGAAAAACGTGTTCCCACCCGAGGTCGCTGTGTTTGAGCCAT CAGAAGCAGAGATCTCCCACACCCAAAAGGCCACACTGGTGTGCCTGGC CACAGGCTTCTACCCCGACCACGTGGAGCTGAGCTGGTGGGTGAATGG GAAGGAGGTGCACAGTGGGGTCAGCACAGACCCGCAGCCCCTCAAGGA GCAGCCCGCCCTCAATGACTCCAGATACTGCCTGAGCAGCCGCCTGAGG GTCTCGGCCACCTTCTGGCAGAACCCCCGCAACCACTTCCGCTGTCAAG TCCAGTTCTACGGGCTCTCGGAGAATGACGAGTGGACCCAGGATAGGGC CAAACCTGTCACCCAGATCGTCAGCGCCGAGGCCTGGGGTAGAGCAGA CTGTGGCTTCACCTCCGAGTCTTACCAGCAAGGGGTCCTGTCTGCCACC ATCCTCTATGAGATCTTGCTAGGGAAGGCCACCTTGTATGCCGTGCTGGT CAGTGCCCTCGTGCTGATGGCCATGGTCAAGAGAAAGGATTCCAGAGGC GGCAGCGGCGCCACCAACTTCAGCCTGCTGAAACAGGCCGGCGACGTG GAAGAGAACCCTGGCCCTATGAGGCAAGTGGCGAGAGTGATCGTGTTCC TGACCCTGAGTATGAGTAGAGGAGAGGATGTGGAGCAGAGTCTTTTCCT GAGTGTCCGAGAGGGAGACAGCTCCGTTATAAACTGCACTTACACAGAC AGCTCCTCCACCTACTTATACTGGTATAAGCAAGAACCTGGAGCAGGTCT CCAGTTGCTGACGTATATTTTTTCAAATATGGACATGAAACAAGACCAAAG ACTCACTGTTCTATTGAATAAAAAGGATAAACATCTGTCTCTGCGCATTGC AGACACCCAGACTGGGGACTCAGCTATCTACTTCTGTGCAGAGATTCGTC ACACAGGCAAACTAATCTTTGGGCAAGGGACAACTTTACAAGTAAAACCA GATATCCAGAACCCTGACCCTGCCGTGTACCAGCTGAGAGACTCTAAATC

	CAGTGACAAGTCTGTCTGCCTATTCACCGATTTTGATTCTCAAACAAATGT GTCACAAAGTAAGGATTCTGATGTGTATATCACAGACAAAACTGTGCTAG ACATGAGGTCTATGGACTTCAAGAGCAACAGTGCTGTGGCCTGGAGCAA CAAATCTGACTTTGCATGTGCAAACGCCTTCAACAACAGCATTATTCCAGA AGACACCTTCTTCCCCAGCCCAGAAAGTTCCTGTGATGTCAAGCTGGTCG AGAAAAGCTTTGAAACAGATACGAACCTAAACTTTCAAAACCTGTCAGTGA TTGGGTTCCGAATCCTCCTCCTGAAAGTGGCCGGGTTTAATCTGCTCATG ACGCTGCGGCTGTGGTCCAGCTGA

Table 28: PAPPA-2G6mm TCR sequence with modifications

PAPPA-2G6mm	ATGGGATGTAGACTGCTGTGTTGCGCCGTGCTGTGTCTGCTGGGAGCCG TGCCTATGGAAACCGGCGTGACCCAGACCCCCAGACACCTCGTGATGGG CATGACCAACAAGAAAAGCCTGAAGTGCGAGCAGCACCTGGGCCACAAC GCCATGTACTGGTACAAGCAGAGCGCCAAGAAACCCCTGGAACTGATGT TCGTGTACAGCCTGGAAGAGAGGGTGGAAAACAACAGCGTGCCCAGCC GGTTCAGCCCCGAGTGCCCTAATAGCAGCCACCTGTTTCTGCATCTGCA CACCCTGCAGCCCGAGGACAGCGCCCTGTATCTGTGTGCCAGCTCTCAG GTGGTGGCCGACAACGAGCAGTTCTTCGGCCCTGGCACCAGACTGACC GTGCTGGAAGATCTGAAGAACGTGTTCCCCCCAGAGGTGGCCGTGTTCG AGCCTAGCAAGGCCGAGATCGCCCACACCCAGAAAGCCACCCTCGTGTG TCTGGCCACAGGCTTCTACCCCGACCACGTGGAACTGTCTTGGTGGGTC AACGGCAAAGAGGTGCACAGCGGCGTGTCCACCGATCCCCAGCCTCTGA AAGAACAGCCCGCCCTGAACGACAGCCGGTACTGCCTGAGCAGCAGACT GAGAGTGTCCGCCACCTTCTGGCAGAACCCCCGGAACCACTTCAGATGC CAGGTGCAGTTTTACGGCCTGAGCGAGAACGACGAGTGGACCCAGGACA GAGCCAAGCCCGTGACACAGATCGTGTCTGCCGAAGCCTGGGGCAGAG CCGATTGTGGCATCACCAGCGCCAGCTACCATCAGGGCGTGCTGAGCGC CACAATCCTGTACGAGATCCTGCTGGGCAAGGCCACCCTGTATGCAGTG CTGGTGTCAGCCCTGGTGCTGATGGCCATGGTCAAGCGGAAGGACAGCA GAGGCGGAAGCGGCGCCACCAACTTCAGCCTGCTGAAACAGGCCGGCG ACGTGGAAGAGAACCCTGGCCCTATGAGACAGGTGGCCAGAGTGATCGT GTTCCTGACCCTGAGCATGAGCAGGGGCGAGGACGTGGAACAGTCCCT GTTCCTGTCTGTGCGCGAGGGCGACAGCAGCGTGATCAATTGCACCTAC ACCGACAGCTCCAGCACCTACCTGTATTGGTATAAGCAGGAACCCGGCG CTGGCCTGCAGCTGCTGACCTACATCTTCAGCAACATGGACATGAAGCA GGACCAGCGGCTGACTGTGCTGCTGAACAAGAAGGACAAGCACCTGAGC CTGCGGATCGCCGATACCCAGACAGGCGACAGCGCCATCTACTTTTGCG CCGAGATCCGGCACACCGGCAAGCTGATCTTTGGCCAGGGCACCACACT GCAAGTGAAGCCCGACATCCAGAACCCCGACCCCGCCGTGTACCAGCTG AGAGACAGCAAGAGCAGCGACAAGAGCGTGTGCCTGTTCACCGACTTCG ACAGCCAGACCAACGTGTCCCAGAGCAAGGACAGCGACGTGTACATCAC CGACAAGACAGTGCTGGACATGCGGAGCATGGACTTCAAGAGCAACAGC GCCGTGGCCTGGTCCAACAAGAGCGATTTCGCCTGCGCCAACGCCTTCA ACAACAGCATTATCCCTGAGGACACATTCTTCCCCAGCTCCGACGTGCCC TGCGACGTGAAGCTGGTGGAAAAGAGCTTCGAGACAGACACCAACCTGA ACTTCCAGAACCTGAGCGTGATCGGCTTCAGAATCCTGCTGCTGAAGGT GGCCGGCTTCAACCTGCTGATGACCCTGAGACTGTGGTCCAGCTGA

10.2 List of figures

10.3 List of tables

11. Acknowledgements

Ich möchte mich zum Schluss bei allen bedanken die zum Gelingen dieser Doktorarbeit beigetragen haben.

Herrn Prof. Dr. Stefan Burdach und Herrn Dr. Uwe Thiel für die Möglichkeit meine Dissertation an diesem interessanten und anspruchsvollen Thema am Forschungszentrum für krebskranke Kinder der TU München durchführen zu können, für das mir entgegengebrachte Vertrauen sowie für ihre Unterstützung und Begleitung der Arbeit.

Dr. Uwe Thiel möchte ich nochmals extra für die kritische und hilfreiche Durchsicht dieser Arbeit und der Publikationen danken und vor allem für seinen Zuspruch und Rückhalt.

Ich möchte auch PD Dr. Günther Richter dafür danken, dass er bei Problemen immer ansprechbar war und stets konstruktive Anregungen hatte.

Mein Dank geht auch an Dr. Thomas Grünewald und seiner Arbeitsgruppe für ihre tatkräftige Unterstützung bei unseren Publikationen.

Meinen Arbeitskollegen möchte ich für die schöne Zeit und die Unterstützung im Labor bedanken. Besonderer Danke geht dabei an meine Kollegen David Schirmer, Tim Hensel, Kristina von Heyking, Oxana Schmidt und Melanie Thiede. Aber auch an unsere Medizinstudenten Esther Heid, Henrieke Gerdes, Isabell Storz und Fiona Becker-Dettling.

Zu Letzt geht mein Dank an meine Familie und an meine Partnerin die mich jederzeit unterstützt, an guten und in schweren Tagen, und die immer an mich geglaubt haben. Ohne euch wäre diese Arbeit nicht möglich gewesen wäre.

VIELEN DANK!